

**Editor-in-Chief B.E.Paton**

**Editorial board:**

Yu.S.Borisov V.F.Grabin  
Yu.Ya.Gretskii A.Ya.Ishchenko  
B.V.Khitrovskaya V.F.Khorunov  
I.V.Krivtsun  
S.I.Kuchuk-Yatsenko  
Yu.N.Lankin V.K.Lebedev  
V.N.Lipodaev L.M.Lobanov  
V.I.Makhnenko A.A.Mazur  
V.F.Moshkin O.K.Nazarenko  
I.K.Pokhodnya I.A.Ryabtsev  
Yu.A.Sterenbogen N.M.Voropai  
K.A.Yushchenko  
A.T.Zelnichenko

**International editorial council:**

N.P.Alyoshin (Russia)  
B.Braithwaite (UK)  
C.Boucher (France)  
Guan Qiao (China)  
U.Diltey (Germany)  
P.Seyffarth (Germany)  
A.S.Zubchenko (Russia)  
T.Eagar (USA)  
K.Inoue (Japan)  
N.I.Nikiforov (Russia)  
B.E.Paton (Ukraine)  
Ya.Pilarczyk (Poland)  
D.von Hofe (Germany)  
Zhang Yanmin (China)  
V.K.Sheleg (Belarus)

**Promotion group:**

V.N.Lipodaev, V.I.Lokteva  
A.T.Zelnichenko (exec. director)

**Translators:**

I.N.Kutianova, V.N.Mironenko,  
T.K.Vasilenko, N.V.Yalanskaya

**Editor**

N.A.Dmitrieva

**Electron galley:**

I.S.Batasheva, T.Yu.Snegiryova

**Address:**

E.O. Paton Electric Welding Institute,  
International Association «Welding»,  
11, Bozhenko str., 03680, Kyiv, Ukraine

Tel.: (38044) 287 67 57

Fax: (38044) 528 04 86

E-mail: journal@paton.kiev.ua

http://www.nas.gov.ua/pwj

State Registration Certificate

KV 4790 of 09.01.2001

**Subscriptions:**

**\$324**, 12 issues per year,  
postage and packaging included.  
Back issues available.

All rights reserved.

This publication and each of the articles  
contained herein are protected by copyright.  
Permission to reproduce material contained in  
this journal must be obtained in writing from  
the Publisher.

Copies of individual articles may be obtained  
from the Publisher.

**CONTENTS**

SCIENTIFIC AND TECHNICAL

**Guan Q., Guo D.L., Zhang C.X. and Li J.** Low stress no  
distortion welding based on thermal tensioning effects for  
thin materials ..... 2

**Osin V.V., Ryabtsev I.A. and Kondratiev I.A.** Study of  
sulfur effect on properties of deposited metal of Kh51 FS  
type ..... 12

**Patyupkin A.V. and Bykovsky O.G.** Cavitation-corrosion  
resistance of surfaced parts of compressors of  
titanium-and-magnesium production process ..... 16

**Borisova A.L., Tunik A.Yu. and Adeeva L.I.** Structure  
and properties of powders of Al-Cu-Fe system alloy for  
thermal spraying of quasi-crystalline coatings ..... 19

INDUSTRIAL

**Bondarev A.A. and Ishchenko A.Ya.** Technology of EBW  
of the stainless steel-aluminium alloy welded joints ..... 27

**Murashov A.P., Demianov I.A., Borisov Yu.S.,  
Zhadkevich M.L. and Golnik V.F.** Anticorrosion  
protection of base metal structures by metallised coatings  
(Review) ..... 30

**Levchenko O.G. and Pavlyk A.O.** Problems of welders'  
labour safety ..... 34

BRIEF INFORMATION

**Gedrovich A.I., Tkachenko A.N. and Tkachenko S.A.**  
Structure and properties of a joint of 10Kh13G18D +  
09G2S steels ..... 37

Theses for scientific degree ..... 40

Developed at PWI ..... 11

Index of articles for TPWJ'2006, Nos. 1-12 ..... 42

List of authors ..... 51



# LOW STRESS NO DISTORTION WELDING BASED ON THERMAL TENSIONING EFFECTS FOR THIN MATERIALS

Q. GUAN, D.L. GUO, C.X. ZHANG and J. LI

Beijing Aeronautical Manufacturing Technology Research Institute, Beijing, China

To prevent welding buckling especially in manufacturing aerospace structures with material thickness less than 4 mm low stress no distortion (LSND) welding techniques have been pioneered and developed at the Beijing Aeronautical Manufacturing Technology Research Institute (BAMTRI). The mechanisms of LSND welding techniques using either the whole cross-section thermal tensioning effect or the localized thermal tensioning effect are described in this paper. The basic idea of LSND welding techniques is to perform active in-process control of inherent plastic (incompatible) strain and stress formation during welding to achieve distortion-free results so that no costly postweld reworking operations for distortion correction is required. Emphasis is given to the finite element analysis to predict and optimize the thermal tensioning techniques for engineering application.

*Keywords:* welding residual stress, low stress no distortion (LSND) welding, buckling distortion, distortion-free result, thermal tensioning, temperature gradient stretching, heat source-heat sink, finite element analysis

Buckling distortions are more pronounced than any other form of welding distortion in manufacturing thin-walled structures, and they are the main troublesome problem in sheet metal fabrication where fusion welding is applied, especially for aerospace structures such as sheet metal airframe panels, fuel tanks, shells of engine cases, etc., where thin-sheet materials of less than 4 mm thickness are widely used. Buckling distortions affect the performance of welded structures in a great many ways. During the past decades efforts have been made and progress has been achieved in solving buckling problems by experts in the welding science and technology field world-wide. Many effective methods for removal, mitigation and prevention of welding distortions adopted before welding, during or after welding have been successfully developed and widely applied in industries [1–10]. Over the past 25 years, the present authors have devoted their efforts to achieve distortion-free results in manufacturing thin-walled aerospace structural components by implementing active in-process control of inherent residual plastic strain formation during welding without having to undertake costly reworking operations for distortion correction after welding [11]. Extensive research and development studies to explore LSND welding techniques were carried out at BAMTRI.

Two innovative methods of LSND welding have been developed for industrial application: one is based on the whole cross-section thermal tensioning effect [12], the other is based on the localized thermal tensioning effect [13].

**Buckling distortions.** The nature of buckling is mostly a phenomenon of loss of stability of thin elements under compressive stresses. Buckling distortions caused by longitudinal welds either in plates, panels or shells are mainly dominated by longitudinal compressive residual stresses induced in areas away

from the weld. Figure 1, a, b show the typical patterns of buckled components. The mechanism of buckling in weldments lies in the action of inherent residual plastic (incompatible) strains formed during welding.

Losing stability, the buckled plate (see Figure 1, a) is released from an unstable flat position of high potential energy with the maximum level of residual stress distribution after conventional welding (Figure 1, c) and takes a stable warped shape. Losing stability, the buckled plate reaches a state of minimum potential energy. In other words, any forced change of the stable curvature of the buckled plate will cause increase in potential energy and once the force is removed, the buckled plate will be restored to its stable position minimizing the potential energy.

For plates of thickness less than 4 mm as widely used in aerospace and modern vehicle welded structures, the value of  $\sigma_{cr}$  is much lower than the peak value of compressive stress  $\sigma_{comp\ max}$  after conventional gas tungsten arc welding (GTAW) (see Figure 1, c). However, the actual  $\sigma_{cr}$  value for a welded element is difficult to be solely determined either by the linear stability theory of small deformations or by the non-linear theory of large deformations in theory of plates and shells. These problems are very complex [14].

In principle, all efforts either «passive» postweld correction measures or «active» in-process control methods of LSND welding to eliminating buckling aim at adjusting the compressive residual stresses to achieve  $\sigma_{comp\ max} < \sigma_{cr}$  at which buckling occurs (see Figure 1, c) by means of reduction and redistribution of the inherent residual plastic strains.

In the past decade, welding simulation and prediction by computational method have been increasingly applied in addition to classic analytical and conventional empirical procedures. Finite element method was adopted by Michaleris, Deo et al. [15–19] for analyzing buckling distortions of stiffened rectangular welded plates for shipbuilding. Shrinkage forces were obtained from a thermal elastic-plastic cross-sectional model analysis. Based on the finite element analysis for large displacements, and using an inherent

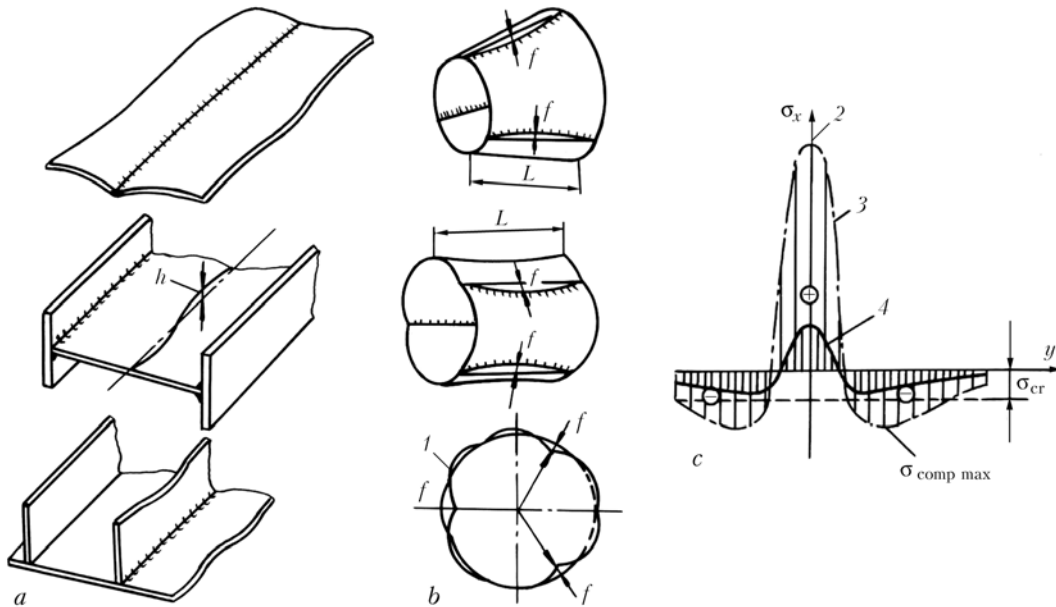


**Figure 1.** Typical buckling patterns of plates, panels (a) and shells (b) with longitudinal welds (to prevent buckling,  $\sigma_{comp\ max}$  reduction to a value lower than  $\sigma_{cr}$ , (c) provides the low stress no distortion result): 1 — cross section; 2 — residual stress  $\sigma_x$ ; 3 — conventional GTAW; 4 — LSND welding;  $h, f$  — buckling distortion;  $L$  — length of weld

shrinkage strain method, Tsai et al. [20] investigate the buckling phenomena of a rectangular plate of aluminum alloy with longitudinal T-stiffeners.

Buckling can be controlled by a variety of methods applied before, during and after welding for its removal, mitigation or prevention.

Pre-tensioning can be classified in either the category of methods applied before or during welding [21–23]. For each particular structural design of panels, a device for mechanical tensile loading is required.

LSND results could be achieved during the welding process based on the thermal tensioning (temperature gradient stretching) effect which is produced by establishing a specific temperature gradient either in whole cross section of the plate to be welded or in a localized area in the near-arc zone. Simultaneously, restraining transient out-of-plane warpage movements of the workpiece is necessary. Differing from the «passive» methods which have to be applied after welding once buckling is in existence, LSND welding techniques can be classified as «active» methods for in-process control of buckling distortions with no need of reworking operations after welding.

**Thermal tensioning effects.** The method for low temperature stress relieving [24] is well-known in shipbuilding and vessel manufacturing industries. This technique is practiced with flame heating combined with water cooling of thicker plate sections of thickness 20–40 mm for mitigation of longitudinal residual stresses after welding. It is based on temperature gradient stretching effect induced by local linear heating and cooling parallel to the weld-line on plates. This technique is not applicable for either stress relieving or buckling removal after welding of thin-walled elements of less than 4 mm thickness where the metal sheets are not stiff enough to resist the transient out-of-plane displacement during local heat-

ing and forced cooling. But the idea of the temperature gradient stretching effect (or commonly termed thermal tensioning effect) is logically feasible for avoiding buckling of plates and shells during welding. Efforts in this direction were made during last decades [4, 11, 12, 25–30].

The basic principle of the whole cross-section thermal tensioning effect is shown in Figure 2. Two curves ( $\sigma_{x1}$  and  $\sigma_{x2}$ ) of thermal stress distributions are created by a preset heating with the temperature profiles ( $T_1$  and  $T_2$  correspondingly) on the thin plate. In this case, the thermal tensioning effect is defined as the value of  $\sigma_x^*$  in the plate edge of  $y = 0$  where the weld bead will be applied. For a given  $\sigma_x^*$ , the greater temperature gradient ( $\partial T_1 / \partial y > \partial T_2 / \partial y$ ), the higher will be the induced maximum value of compressive stress  $-\sigma_{1x\ max}$ . An optimized temperature curve can be calculated mathematically for an estimated value  $\sigma_x^*$  while the value  $-\sigma_{1x\ max}$  is kept below the yield stress.

Based on the results of mathematical analysis for the thermal tensioning effect, Burak et al. [27, 28]

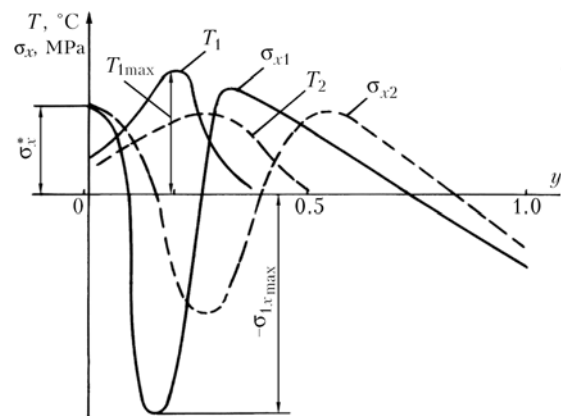


**Figure 2.** Basic principle of whole cross-section thermal tensioning effect (for designations see the text)

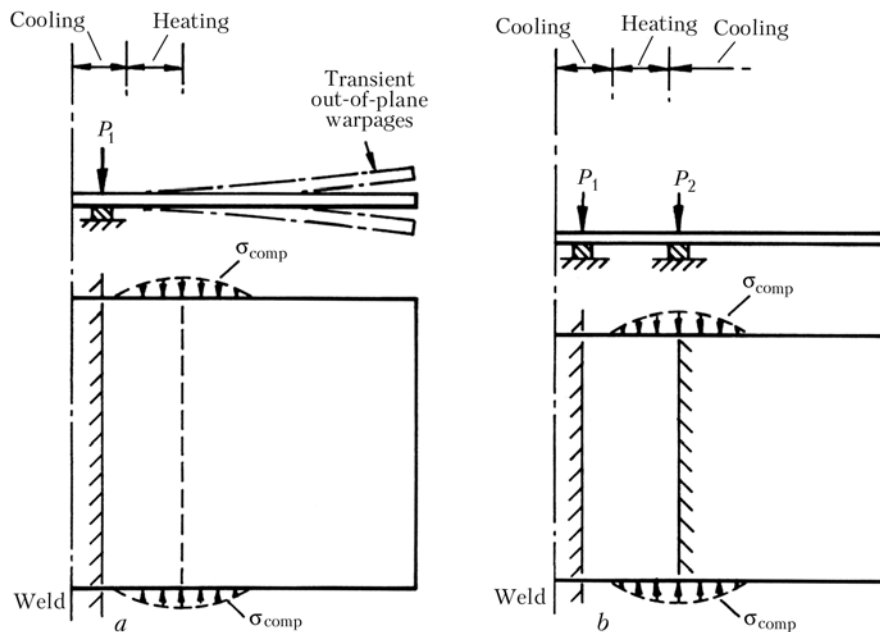


**Figure 3.** Transient out-of-plane warpage displacement of workpiece in conventional clamping system (a) and its prevention in the newly improved «two-point» finger clamping system (b) [12]

conducted an experiment to control longitudinal plastic strains in weld on aluminum plate of thickness 4 mm.

Early in the 1980's, to apply the thermal tensioning effect to avoid buckling in aerospace structures of thickness less than 4 mm, a series of experiment was carried out by Guan et al. [12, 25, 26]. It has been proved by the results of repeated experiments that the Burak's scheme for the plates thicker than 4 mm is not applicable to eliminating buckling in elements of less than 4 mm thickness. The reason is that owing to the susceptibility to losing stability of the thinner elements, transient out-of-plane displacements occur in areas away from the weld zone (Figure 3, a). The transient out-of-plane displacements outside the clamping fingers (indicated by  $P_1$  in Figure 3, a) release the potential energy of the preset plane thermal stresses distribution. In the lost stability position, the expected preset thermal tensioning stress  $\sigma_x^*$  (see Figure 2) ceases to exist.

Progress was made in solving the above mentioned problem to improve the thermal tensioning technique and make it applicable to elements of less than 4 mm thickness especially in manufacturing aerospace structures [12]. Figure 3, b shows the improvement in clamping systems. In conventional clamping system with «one-point» finger fixture ( $P_1$  in Figure 3, a), the transient out-of-plane warpings of the workpiece are inevitable, whereas, using the improved «two-point» finger clamping system ( $P_1$  and  $P_2$  in Figure 3, b) the desirable thermal tensioning effect in terms of  $\sigma_x^*$  (see Figure 2) can be established without transient out-of-plane warpage displacements. Only in the case of «two-point» finger clamping system while the plate keeps its flat position during welding the expected  $\sigma_x^*$  could be effective.

As an active in-process control method, this improved technique is more widely acknowledged as LSND welding method for thin materials [11, 12, 25]. It is worthwhile to note that the LSND welding technique as an active in-process control method is replacing the formerly adopted passive measures for buckling removal after welding in most cases in aerospace engineering in China.

To create the whole cross-section thermal tensioning effect along the plate edges to be welded, the temperature profile can be built up either statically as a preset temperature field by stationary linear heaters arranged underneath the workpiece parallel to the weld direction or as a transient temperature field built up by two movable heating devices on both sides of the weld and synchronously traveling with the welding torch [25, 31]. The LSND welding techniques can be implemented in either of the two ways.

In a broad sense of the term «thermal tensioning», the effect can be created not only in the longitudinal direction of the weld to control the longitudinal plastic strains in weld zone, but the effect in mitigating the transverse shrinkage of the weld could also be utilized for hot-cracking prevention [32]. Furthermore, manipulating the combination of heat sources and heat sinks, the thermal tensioning effect as well as the thermal compressing effect could also be established properly for specific purposes. Mitigating residual stresses in Al-Li repair welds [33] is an example in applying the alternative options of thermal tensioning effect.

The thermal tensioning effects can be classified into two categories: one is created in an entire cross-section of plate (whole cross-section thermal tensioning) using additional heating and cooling as mentioned above, the other is created in a localized zone limited to a near-arc high-temperature area within a certain isotherm induced solely by welding arc without any



additional heating (localized thermal tensioning). For the localized thermal tensioning a heat source–heat sink system (a heat sink coupled with welding heat source), could be utilized (Figure 4).

**Whole cross-section thermal tensioning** --- **LSND welding.** To satisfy the stringent geometrical integrity requirements and ensure dimensionally consistent fabrication of aerospace structures. LSND welding technique for thin materials, mainly for metal sheets of less than 4 mm thickness, was pioneered and developed early in 1980's at the BAMTRI [12, 25, 26]. This technique was aimed to provide an in-process active control method to avoid buckling distortions based on the whole cross-section thermal tensioning effect.

Figure 5 shows schematically the basic principle for practical implementation of LSND welding [12]. The thermal tensioning effect with the maximum tensile stress  $\sigma_{max}^*$  in the weld zone (Figure 5, a) is formed due to the cooling contraction of the zone I by water-cooling backing bar underneath the weld and the heating expansion of zone II on both sides adjacent to the weld by linear heaters. Both the curve  $T$  and curve  $\sigma$  are symmetrical to the weld centerline. The higher  $\sigma_{max}^*$ , the better will be the results of controlling buckling distortions.

It is proved by experiments and engineering applications that the thermal tensioning effect is the necessary condition for LSND welding of materials of thickness less than 4 mm, whereas the sufficient condition is the prevention of transient out-of-plane displacements by applying flattening forces in «two-point» finger clamping systems shown by  $P_1$  and  $P_2$  in Figure 5, a. The selected curve  $T$  is mainly determined by  $T_{max}$ ,  $T_0$  and  $H$  (here  $H$  is the distance of  $T_{max}$  to the weld centerline). The thermal tensioning effect  $\sigma_{max}^*$  becomes stronger as the temperature gradient ( $T_{max} - T_0$ ) increases while  $H$  decreases. The optimization of  $\sigma_{max}^*$  and technological parameters such as  $H$  etc. can be implemented computationally using FEM and verified experimentally.

The typical temperature field in GTAW of thin plate is shown schematically in Figure 6, a. Actually, in engineering practice, the GTAW of longitudinal

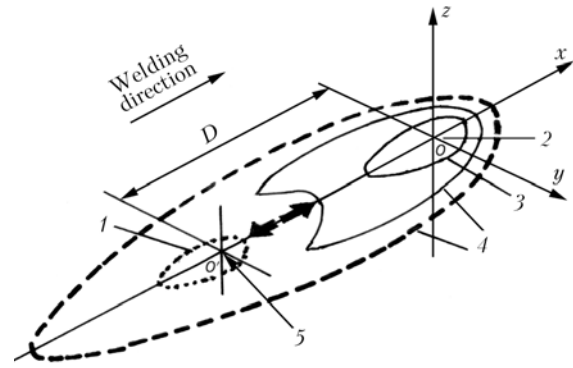


**Figure 4.** Localized thermal tensioning effect (heavy arrows) induced by a trailing spot heat sink coupled to the welding arc in a distance  $D$  behind: 1 — temperature valley; 2 — arc center (heat source); 3 — weld pool; 4 — isotherms; 5 — center of heat sink

weld on thin plate is performed in a longitudinal seam welder. Workpieces are rigidly fixed in a pneumatic finger-clamping system with copper backing bar on mandrel support. Owing to the intensive heat transfer from workpiece to copper backing bar, the temperature field is different from the normal shape and takes a narrowed distribution, as shown in Figure 6, b. To implement LSND welding, additional preset temperature field, as shown in Figure 6, c, is formed by heating and cooling. Therefore, the LSND welding temperature field, shown in Figure 6, d, results by superposition of the temperature fields of Figure 6, b and c.

For clearer quantitative assessment of LSND welding technique, a systematic investigation was carried out [11, 25, 26]. Figure 7 shows comparisons between the experimentally measured inherent strain  $\epsilon_x^p$  distributions (Figure 7, a) and residual stress  $\sigma_x$  distributions (Figure 7, b) after conventional GTAW (curve 1) and LSND welding (curve 2) of aluminum plate of 1.5 mm thick. Reductions of either  $\epsilon_x^p$  or  $\sigma_x$  are obvious as indicated by curve 2 in comparison with curve 1.

The photographs in Figure 8 show that the specimens of either stainless steel (Figure 8, a) or aluminum alloy (Figure 8, b) welded conventionally are severely buckled in all cases, but the LSND welded specimens are completely buckle-free and as flat as before welding.

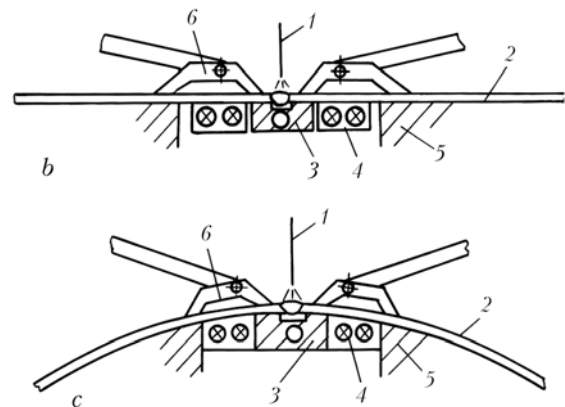
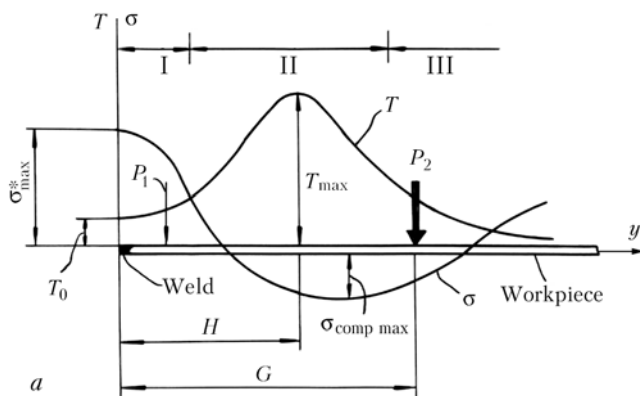


**Figure 5.** Basic principle for implementation of LSND welding (a), clamping jigs for longitudinal weld inplates (b) and cylindrical shells (c) [12]: 1 — arc; 2 — workpiece; 3 — water-cooling backing bar; 4 — linear heaters; 5 — supporting mandrel; 6 — «two-point» finger clamping system

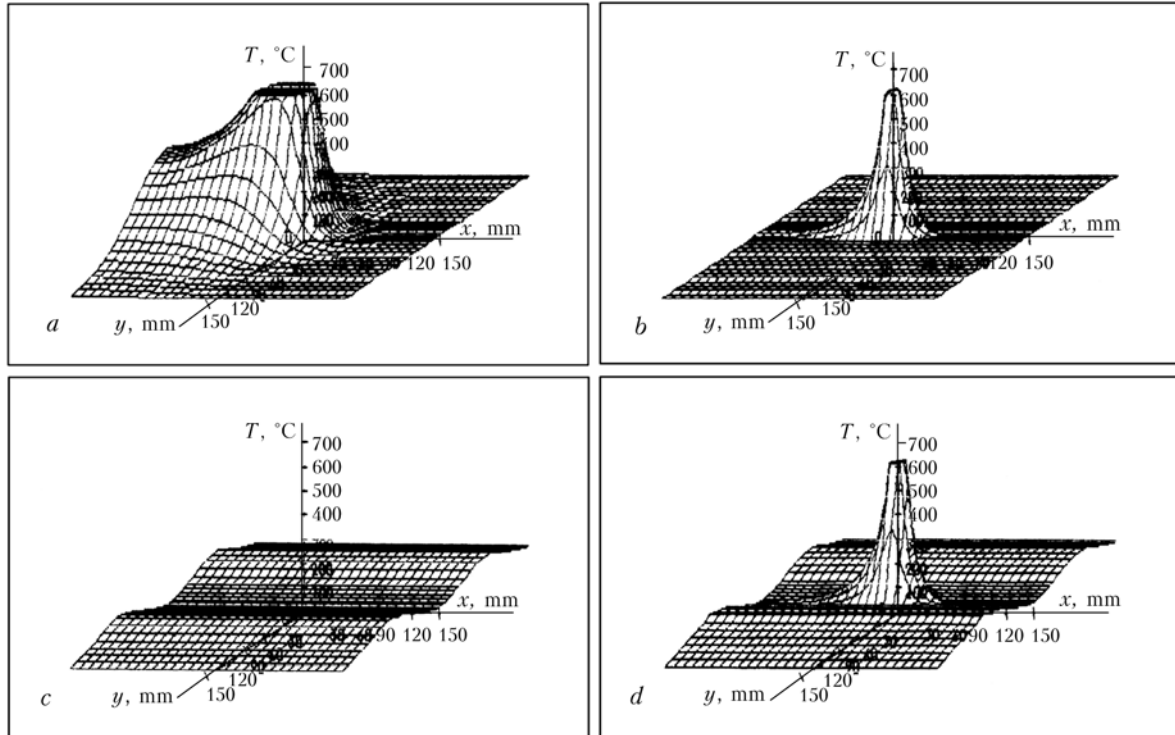


**Figure 6.** Temperature fields on thin plate in conventional GTAW (a), GTAW on copper backing bar with intensive heat transfer (b), preset temperature field (c) and temperature field for LSND welding (d)

Comparisons are also given between the results of measured deflections  $f$  on specimens 1.6 mm thick welded conventionally using GTAW and those welded using LSND welding technique for stainless steel (Figure 8, c) and aluminum alloy (Figure 8, d). Completely buckle-free ( $f = 0$ ) results were achieved when the optimized technological parameters for LSND welding techniques were selected.

As demonstrated above, designers and manufacturers who suffer from problems of buckling could now adopt a new idea that buckling is no longer inevitable with LSND welding technique. Buckling can be prevented completely and residual stresses can be reduced significantly or controlled to a level lower than  $\sigma_{cr}$  at which buckling occurs.

Successful results in preventing buckling distortions were achieved in manufacturing thin-walled jet

engine cases of nickel base alloys, stainless steels, as well as rocket fuel tanks of aluminum alloys, where the acceptable allowance of residual buckling deflections  $f$  at a weld length of  $L$  should be limited to the ratio of  $f/L < 0.001$  [34].

**Localized thermal tensioning --- DC-LSND welding with a trailing spot heat sink.** Over the past 15 years, progress has been made in seeking active in-process control of welding buckling to explore a localized thermal tensioning technique using a trailing spot heat sink. As shown above in Figure 4, the heat sink moving synchronously with the welding arc creates an extremely high temperature gradient along the weld bead within a limited area of high temperature zone close to the weld pool. This technique was entitled «Dynamically Controlled Low Stress No Distortion (DC-LSND) Welding Method» [13, 34–36]. In

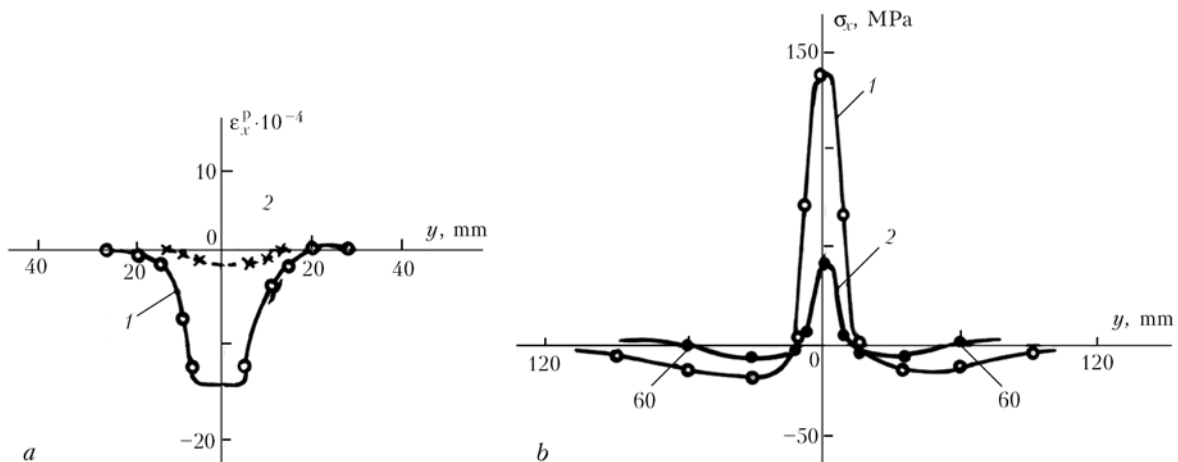


**Figure 7.** Comparisons between experimentally measured inherent strain  $\epsilon_x^p$  (a) and residual stress  $\sigma_x$  (b) distributions after conventional GTAW (1) and LSND welding (2) of aluminum plate 1.5 mm thick [11, 26]

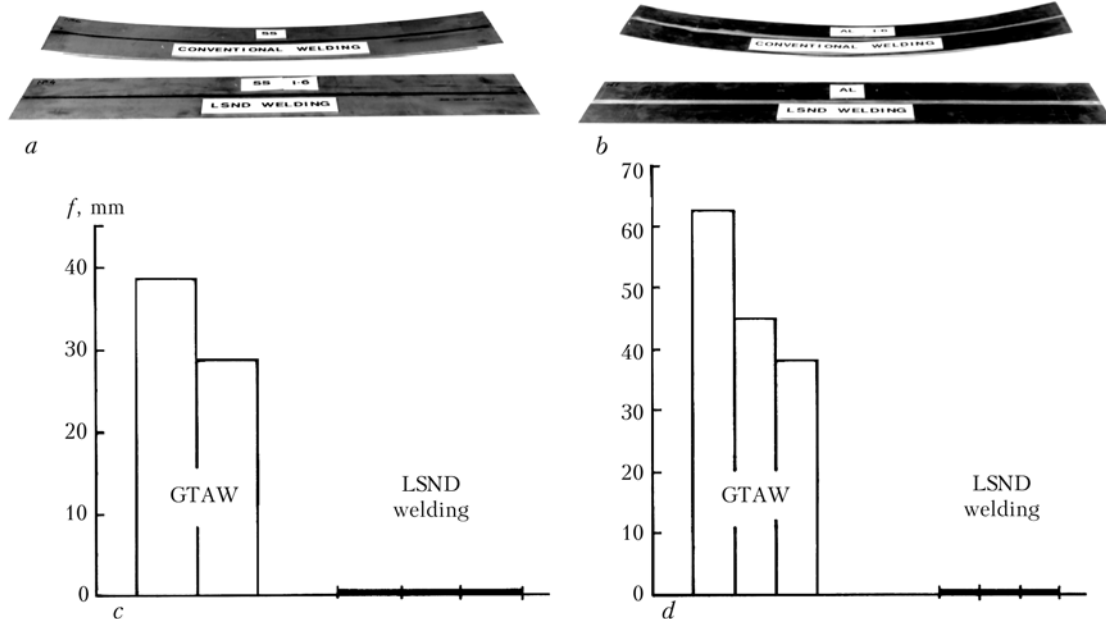


**Figure 8.** Specimens of stainless steel (a) and aluminum alloy (b) 1.6 mm thick, 1000 mm long welded by conventional GTAW with buckling distortion (upper) and by LSND welding without distortion (lower), and deflections  $f$  measured on these specimens (c, d) [25]

this innovative method, the preset heating (Figure 5, a) is no longer necessary. The formation of specific inverse plastically stretched inherent strains  $\epsilon_x^p$  in the near-arc zone behind the weld pool is dynamically controlled by a localized trailing thermal tensioning effect induced between the welding heat source and the spot heat sink along the weld bead (see Figure 4).

Device for engineering implementation of the DC-LSND welding technique was designed and further developed at BAMTRI as shown schematically in Figure 9 [13].

With this device attached to the welding torch, an atomized cooling jet of the trailing spot heat sink impinges directly on the just solidified weld bead surface. Liquid coolant, such as  $\text{CO}_2$ ,  $\text{N}_2$  or water, could be selected for atomized cooling jet. Atomizing the liquid coolant is essential to improve the efficiency of intensive cooling rather than using liquid jet directly impinging the weld bead. To protect the arc from the possible interference of the cooling media, there is a co-axial tube to draw the vaporized media out of the zone nearby the arc. The technological parameters for the trailing spot heat sink and all the welding procedures are automatically synchronously-controlled with the GTAW process. The dominating factors, namely the distance between the heat source and the heat sink and the intensity of the cooling jet, can be selected properly to reach a buckle-free result.

In systematic investigations, finite element analysis with a model of cooling jet impinging the weld bead surface is combined with a series of experimental studies [35, 37–40]. Comparisons between the temperature fields on conventional GTA-welded titanium plate and on plate welded using DC-LSND technique are given in Figure 10.

In this case, DC-LSND welding was carried out using the same parameters as in conventional GTAW.

The flow rate of cooling medium (atomized water) was selected at 2.5 ml/s. The distance between the arc and cooling jet were regulated from 80 to 25 mm. It can be seen clearly (Figure 10, b, d) that in DC-LSND welding there is a deep temperature valley formed by the cooling jet behind the weld pool. An extremely high temperature gradient from the peak to the valley is created. The 800 and 400 °C isotherms in front of the heat sink are severely distorted pushing forward closer to the weld pool (Figure 10, d).

The abnormal thermal cycles by DC-LSND welding (Figure 11, b) produce correspondingly the abnormal thermo-elastic-plastic stress and strain cycles (Figure 11, d) in comparison with the cycles formed by conventional GTAW (Figure 11, a, c). Obviously,

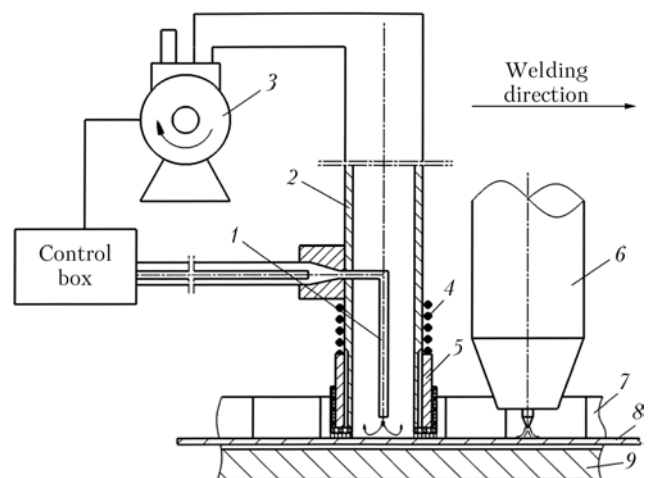


**Figure 9.** Specially designed device for buckle-free DC-LSND welding of thin-walled elements [13]: 1 — nozzle for atomized cooling jet of liquid media; 2 — co-axial tube to draw the vaporized coolant; 3 — vacuum pump; 4 — spring; 5 — axle over-sleeve tube; 6 — GTAW torch; 7 — clamping fingers; 8 — workpiece; 9 — beneath weld backing bar

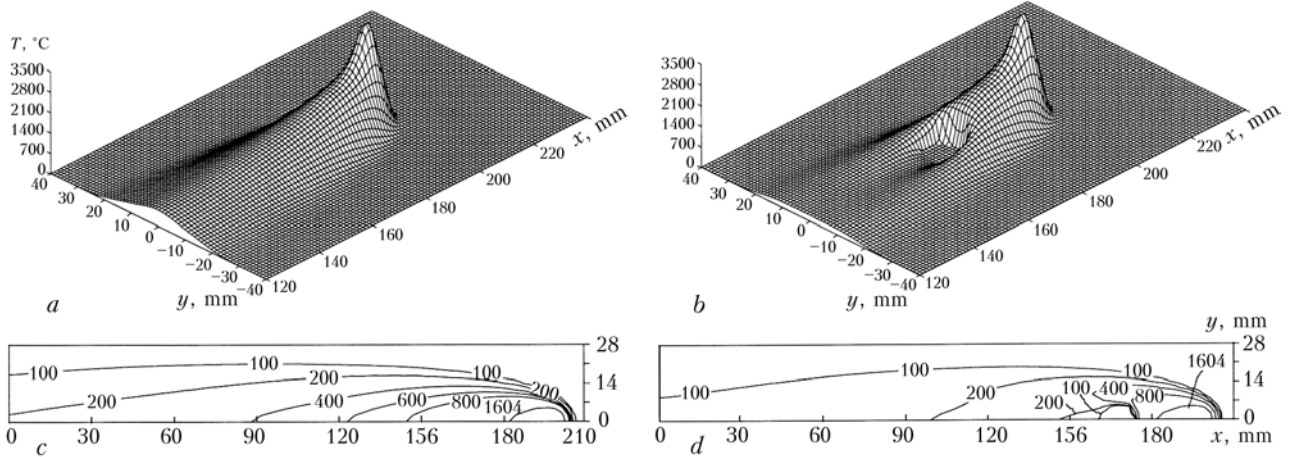


**Figure 10.** Temperature fields and isotherms on Ti-6Al-4V plate 2.5 mm thick [38] conventional GTA-welded on copper backing bar (a, c) and welded using DC-LSND method (b, d) at the same welding parameters:  $I_w = 200$  A,  $U_a = 12$  V,  $v_w = 12$  m/h

the localized thermal tensing effect is acting only within a limited zone behind the weld pool.

It can be seen also from Figure 11, d that behind the arc, the compressive plastic strains formed before in the just solidified weld zone can be compensated properly by the inherent tensile plastic strains in the area of temperature valley (Figure 11, d).

In DC-LSND welding, both the value of inherent plastic strains and the width of its distribution can be controlled quantitatively by selecting the proper technological parameters: the distance  $D$  between the

welding heat source and the heat sink (Figure 12) as well as the intensity of the heat sink.

Figure 13 shows the residual strain and stress distributions in cross-section of the weld on titanium plate. Comparisons are given between conventional GTAW (solid line) and DC-LSND welding with different distance  $D$  of 25, 50 and 80 mm (acc. to Figure 12). For a selected intensity of heat sink, the closer the heat sink to the heat source (the shorter the distance  $D$ ), the stronger is the localized thermal tensing effect. For example, at the distance  $D =$

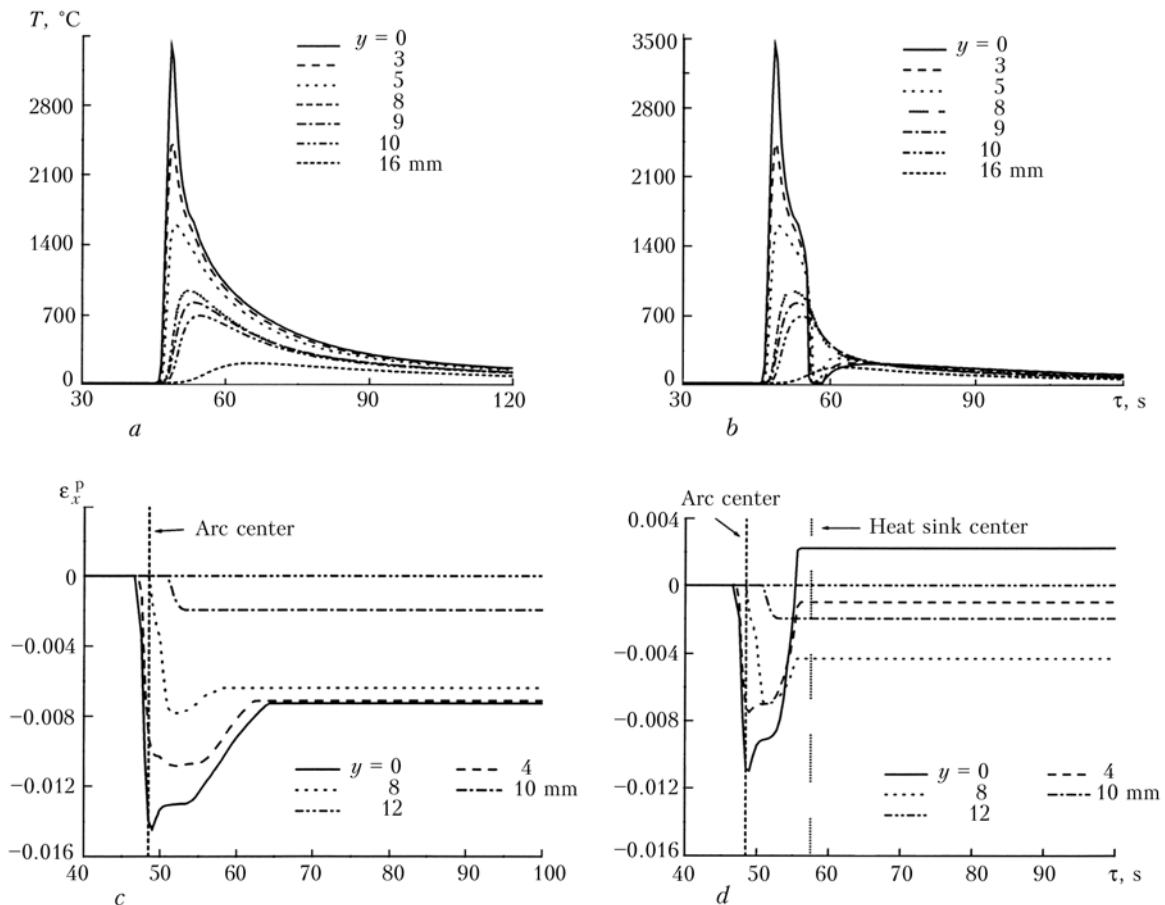


**Figure 11.** Comparisons of thermal cycles (a, b) and transient plastic strain cycles (c, d) between conventional GTAW (a, c) and DC-LSND welding (b, d) [38, 39]



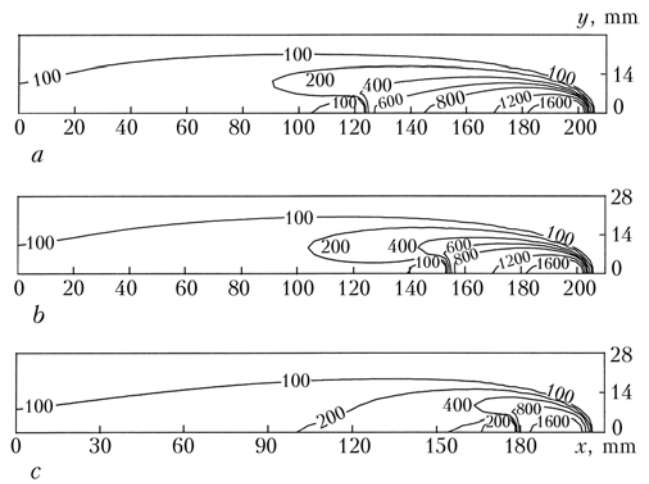
= 25 mm, the residual plastic inherent strain  $\epsilon_x^p$  on the weld centerline even changes its sign from negative to positive (Figure 13, a), and the residual stress on the weld centerline changes from tensile to compressive correspondingly (Figure 13, b).

Figure 14 gives some typical examples from the systematic experimental investigation program. As shown in Figure 14, a, the peak tensile stress measured in weld on mild steel plate welded using conventional GTA method reaches 300 MPa (curve 1) and the maximum compressive stress in the peripheral area is about 90 MPa which causes buckling with deflections more than 20 mm in the center of specimen of 500 mm long. In the case of DC-LSND welding the patterns of measured residual stress distribution (curves 2–4) alter dramatically with different technological parameters, even with the compressive residual stresses in the centerline of the weld. The reason is that the shrinkage induced by the great temperature gradient between the arc and the cooling jet tends not only to compensate the welding compressive plastic strains but also to alter the sign of residual strain to its opposite. Results show that the distance  $D$  has more significant influence on both  $\epsilon_x^p$  and  $\sigma_x$  in controlling buckling on thin materials. After DC-LSND welding, the specimens are completely buckle-free and as flat as original before welding. Similar results were obtained, as shown in Figure 14, b and c, on stainless steel and aluminum plates.

Based on the experimental investigations and FEM analysis results, the recommended parameters for engineering application of DC-LSND welding are given in Figure 15 (for the case of titanium plate examined according to Figure 10) to achieve buckle-free results.

Metallurgical and mechanical examinations show that the cooling jet medium gives no noticeable influence on the titanium joint properties. Actually the cooling jet is impinging directly on the solidified weld bead at a temperature less than 400 °C as shown by the distorted abnormal isotherm of 400 °C in front of the heat sink (see Figures 10, d and 12).

Recent progress in numerical simulation of welding phenomena offers researchers powerful tools for studying in more detail of welding thermal and mechanical



**Figure 12.** Isotherms on titanium plate with different distance  $D$  of 80 (a), 50 (b) and 25 (c) mm between the arc center and the cooling jet center [38, 39]

behaviors. These tools allow for the prediction of precise control of the abnormal temperature fields and therefore the abnormal thermal elastic-plastic cycles created by the possible variable combinations of the heat source–heat sink welding techniques. It is expected that a variety of coupled heat source–heat sink processes are feasible for not only welding distortion controlling but also defect-free welds. For example, the device for trailing spot heat sink can be attached not only to the GTAW torch but also could be coupled to other heat sources like the head of laser beam or the tool of friction stir welding to control distortion, and to improve joint performances as well.

**CONCLUSIONS**

1. LSND welding techniques for thin materials can be implemented using either the whole cross-section thermal tensioning effect or the localized thermal tensioning effect. Basic principles and mechanism of LSND welding techniques are clarified through experimental studies and theoretical analyses with FEM.

2. For LSND welding using the whole cross-section thermal tensioning, the necessary condition is to create an adequate temperature profile coupled to the welding temperature field, whereas its sufficient condition

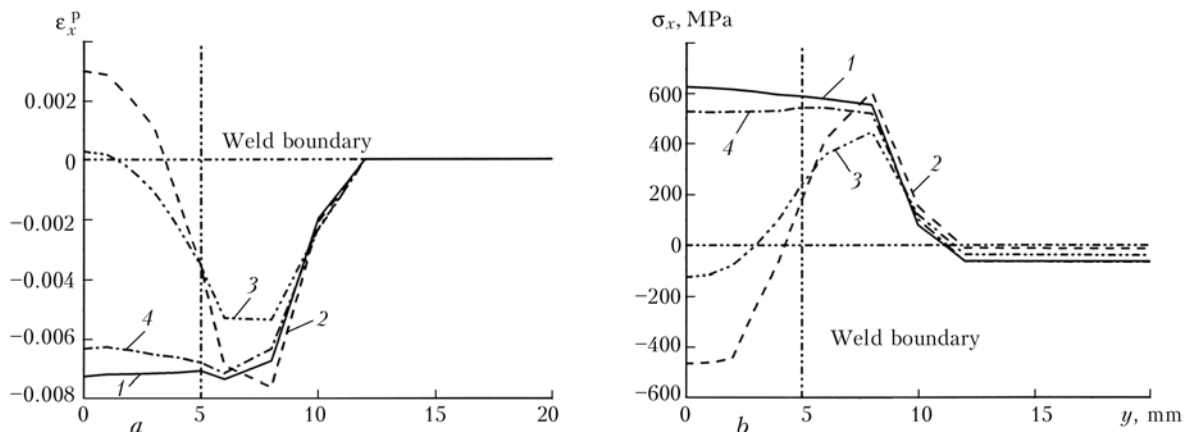


**Figure 13.** Residual strain  $\epsilon_x^p$  (a) and stress  $\sigma_x$  (b) distributions in cross-section of the weld on titanium plate GTA- (1) and DC-LSND-welded with  $D = 25$  (2), 50 (3) and 80 (4) mm [39, 40]

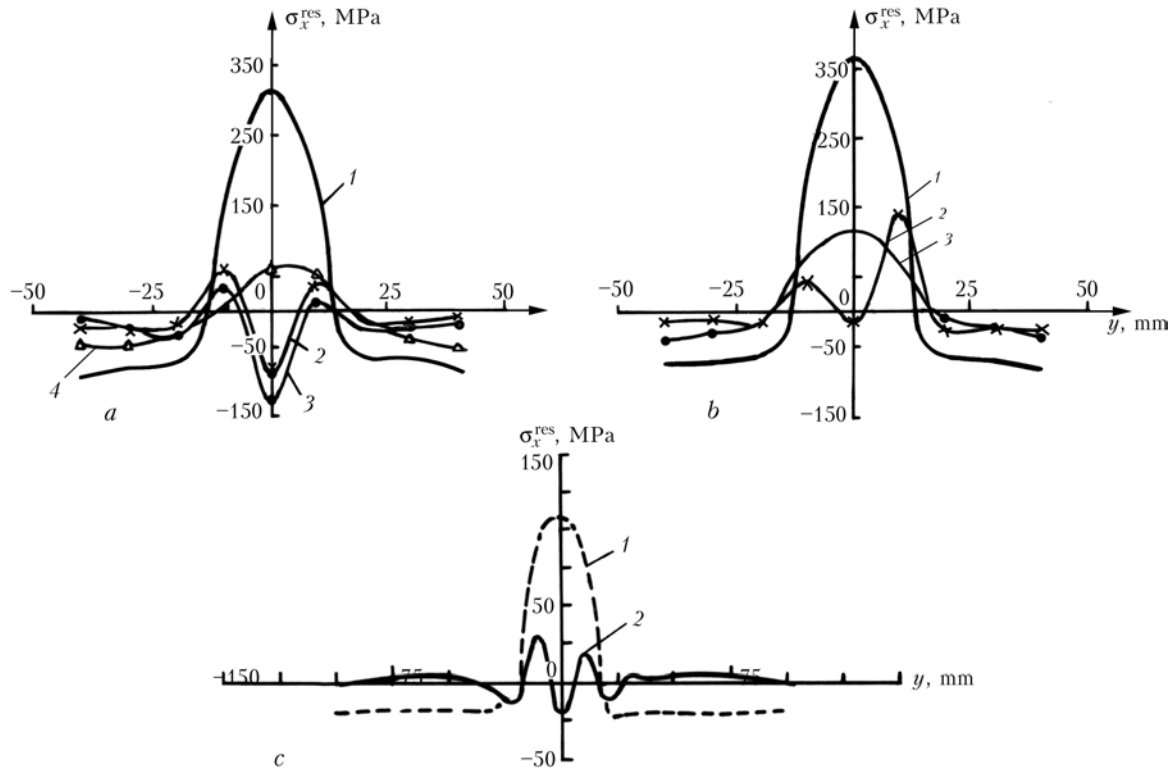


**Figure 14.** Measured residual stress distributions on plates 1 mm thick of mild (a) and stainless steel (b), and 2 mm thick aluminum alloy (c) GTA- (1) and DC-LSND-welded with different technological parameters (2-4) [35, 37]

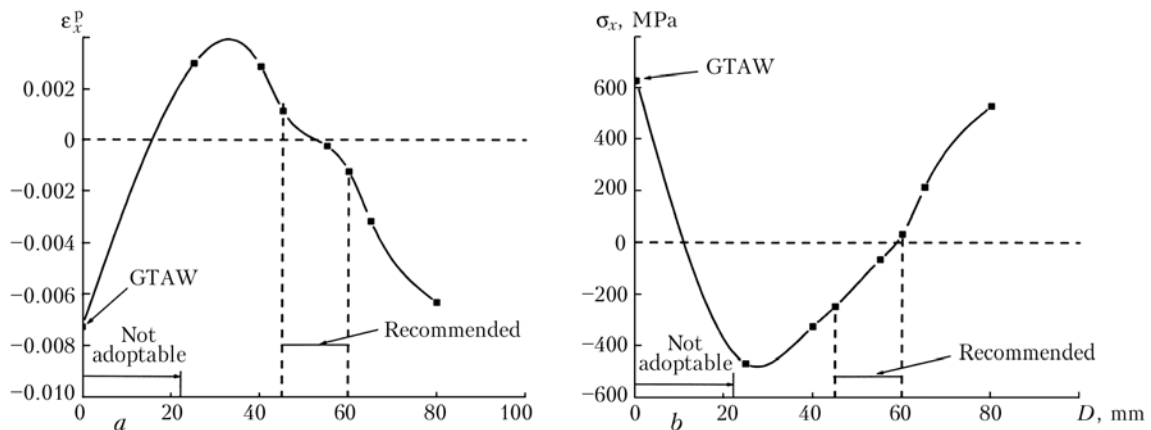


**Figure 15.** Peak value of residual plastic strain  $\epsilon_x^p$  (a) and residual stress  $\sigma_x$  in weld centerline (b) as function of distance  $D$  (acc. to Figure 13)

is to keep the thin plate elements in a plane position without any transient loss of stability during welding.

3. In executing DC-LSND welding technique using localized thermal tensioning, the dominating technological parameters are the distance between the heat source and the heat sink and the intensity of the heat sink. For engineering solution and industrial application, optimized technological parameters are recommended based on FEM analysis results.

4. Both LSND welding techniques have been applied successfully in sheet metal industries to satisfy the stringent geometrical integrity requirements especially to ensure dimensional consistent fabrication of aerospace components.

*Acknowledgments.* This paper summarizes the main results of a series of research projects supported

by the National Natural Science Foundation of China under Contract No. IX-85343 and the Foundation for Aerospace Science and Technology of China under Contracts Nos. 87625003 and 98H25002. The authors would like to express their gratitude to BAMTRI for the constant support to develop the LSND welding techniques and promote their industrial applications.

1. Paton, E.Ī . et al. (1936) Shrinkage stresses in welded cylindrical vessels. *Avtogen. Delo*, **5/6**.
2. Nikolaev, G.A., Kurkin, S.A., Vinokurov, V.A. (1982) *Welded structures, strength of welded joints and deformation of structures*. Moscow: Vysshaya Shkola.
3. Okerblom, N.O. (1950) *Welding stresses in metal structures*. Moscow.
4. Masubuchi, K. (1980) *Analysis of welded structures*. Oxford: Pergamon Press.
5. Lobanov, L.M. et al. (1993) *Welded structures*. Vol. 1. Kiev: Naukova Dumka.



6. Makhnenko, V.I. (1976) *Calculation methods for the investigation of kinetics of welding stresses and deformations*. Kiev: Naukova Dumka.
7. Nedoseka, A.Ya. (1998) *Fundamental of evaluation and diagnostics of welded structures*. Kiev: INDPROM.
8. Vinokurov, V.A. (1968) *Welding stress and distortion: determination and elimination*. Moscow: Mashinostroenie.
9. Sagalevich, V.M. (1974) *Methods for eliminating welding deformations and stresses*. Moscow: Mashinostroenie.
10. Watanabe, M., Satoh, K. (1958) Fundamental studies on buckling of thin steel plate due to bead welding. *J. JWS*, 27(6), 313–320.
11. Guan, Q. (1999) A survey of development in welding stress and distortion control in aerospace manufacturing engineering in China. *Welding in the World*, 43(1), 14–24.
12. Guan, Q., Guo, D.L. et al. *Method and apparatus for low stress no-distortion welding of thin-walled structural elements*. Pat. 87100959.5 China. Int. Cl. GB 88/00136. Publ. 1998.
13. Guan, Q., Zhanget, C.X. et al. *Dynamically controlled low stress no-distortion welding method and its facility*. Pat. 93101690.8 China. Publ. 1993.
14. Zhong, X.M., Murakawa, H., Ueda, Y. (1995) Buckling behavior of plates under idealized inherent strain. *Transact. of JWRI*, 24(2), 87–91.
15. Michaleris, P., DeBicari, A. (1997) Prediction of welding distortion. *Welding J.*, 76(4), 172–181.
16. Michaleris, P., Sun, X. (1997) Finite element analysis of thermal tensioning techniques mitigating weld buckling distortion. *Ibid.*, 76(11), 451–457.
17. Michaleris, P. et al. (1999) Minimization of welding residual stress and distortion in large structures. *Ibid.*, 78(11), 361–366.
18. Deo, M.V., Michaleris, P., Sun, J. (2003) Prediction of buckling distortion of welded structures. *Sci. and Techn. of Welding and Joining*, 8(1), 55–61.
19. Deo, M.V., Michaleris, P. (2003) Mitigating of welding induced buckling distortion using transient thermal tensioning. *Ibid.*, 8(1), 49–54.
20. Tsai, N.L. et al. (1999) Welding distortion of a thin-plate panel structure. *Welding J.*, 78(5), 156–165.
21. Stanhope, A. et al. (1972) Welding airframe structures in titanium alloys using tensile loading as a means of overcoming distortion. *Metal Constr. and British Welding J.*, 10.
22. Chertov, I.M. et al. (1980) Strains and stresses in welding of longitudinal joints in cylindrical shells of the AMg6 alloy with pre-tensioning. *Avtomatich. Svarka*, 5, 31–33.
23. Paton, A.A., Lobanov, L.M. et al. (1989) Fabrication of thin-walled welded large panels of high-strength aluminum alloys. *Ibid.*, 10.
24. Radaj, D. (1992) *Heat effects of welding: temperature field, residual stress, distortion*. Berlin: Springer.
25. Guan, Q., Leggatt, R.H., Brown, K.W. (1988) *Low stress non-distortion (LSND) TIG welding of thin-walled structural elements*: TWI Res. report 374. Abington, Cambridge: TWI.
26. Guan, Q. et al. (1990) Low stress no-distortion (LSND) welding — a new technique for thin materials. *Transact. of Chinese Welding Society*, 11(4), 231–237.
27. Burak, Ya.I. et al. (1977) Controlling the longitudinal plastic shrinkage of metal during welding. *Avtomatich. Svarka*, 3, 27–29.
28. Burak, Ya.I. et al. (1979) Selection of the optimum fields for preheating plates before welding. *Ibid.*, 5, 5–9.
29. Masubuchi, K. (1997) Prediction and control of residual stresses and distortion in welded structures. *Welding Res. Abroad*, 6/7, 2–16.
30. Takeno, S. et al. *Method for preventing welding distortion of sheet metals*. Pat. 4052079 Japan. Publ. 1992.
31. Mechaleris, P. et al. (1995) Analysis and optimization of weakly coupled thermo-elasto-plastic systems with application to weldment design. *Int. J. Numerical Methods in Eng.*, 38, 1259–1285.
32. Yang, Y.P., Dong, P., Zhang, J. et al. (2000) A hot-cracking mitigation technique for welding high-strength aluminum alloy. *Welding J.*, 79(1), 9–17.
33. Dong, P. et al. (1998) Analysis of residual stresses in Al–Li repair welds and mitigation techniques. *Ibid.*, 77(11), 439–445.
34. Guan, Q. et al. (1996) Low stress no-distortion welding for aerospace shell structures. *China Welding*, 5(1), 1–9.
35. Guan, Q., Zhang, C.X. et al. (1994) Dynamic control of welding distortion by moving spot heat sink. *Welding in the World*, 33(4), 308–313.
36. Guan, Q. (2001) Efforts to eliminating welding buckling distortions — from passive measures to active in-process control. In: *Proc. of 7th JWS Int. Symp. on Today and Tomorrow in Science and Technology of Welding and Joining* (Kobe, Nov., 2001), Vol. 2, 1045–1050.
37. Zhang, C.X., Guan, Q. et al. (1996) Study on application of dynamic control of welding stress and distortion in thin aluminum elements. In: *Proc. of 6th JWS Int. Welding Symp.* (Nagoya, Nov.), 593–544.
38. Li, J., Guan, Q., Shi, Y.W. et al. (2004) Studies on characteristics of temperature field during GTAW with a trailing heat sink for titanium sheet. *J. Materials Proc. Technology*, 147(3), 328–335.
39. Li, J. (2004) *Studies on the mechanism of low stress no distortion welding for titanium alloy*: PhD Dis. Beijing University of Technology.
40. Li, J., Guan, Q., Shi, Y.W. et al. (2004) Stress and distortion mitigation technique for welding titanium alloy thin sheet. *Sci. and Techn. of Welding and Joining*, 9(5), 451–458.

## PORTABLE LOW-VOLTAGE VENTILATION UNITS TEMP-NV AND TEMP-NV-M

Joint development of the E.O. Paton Electric Welding Institute  
and International R&D Centre TEMP

The units provide an efficient removal of harmful materials formed in welding from hard-to-reach places and closed volumes (holds of vessels, cisterns, tanks, etc.). Also, they are applied to feed pure air to a working zone when performing welding operations. They can operate under field conditions from carborne mains or other power supplies with a voltage of 14 to 24 V using no converter. The capacity of removal of air with TEMP-NV is not less than 1500 m<sup>3</sup>/h, and that with TEMP-NV-M is 3500 m<sup>3</sup>/h. Weight is 16 kg.

**Application.** Manual covered-electrode arc welding, semi-automatic welding and other related processes.

**Proposals for co-operation.** Manufacture and delivery on a contract base.



Contacts: Prof. Levchenko O.G.  
E-mail: levchenko.o@paton.kiev.ua



# STUDY OF SULFUR EFFECT ON PROPERTIES OF DEPOSITED METAL OF Kh51 FS TYPE

V.V. OSIN, I.A. RYABTSEV and I.A. KONDRATIEV  
E.O. Paton Electric Welding Institute, NASU, Kiev, Ukraine

The effect of sulfur alloying on wear and heat resistance of deposited metal of the type of chromium-molybdenum tool steel is considered. It is shown that formation of molybdenum sulphides in deposited metal prevents adhesion of metal surfaces of friction pair components, which leads to improvement of their wear resistance and cleanliness of the wear surface.

*Keywords:* surfacing, friction of metal on metal, wear resistance, heat resistance, sulfur alloying

As is shown in [1], sulfur in the limited amounts is used for alloying steels and iron-base alloys for improving the quality of treatment of parts surfaces. In the opinion of the authors of [2], the principal cause of such an effect of sulfur consists in that sulphides of some metals prevent adhesion at friction of metal on metal at normal and elevated temperatures and contact pressure.

It is well known [3] that sulfur is practically insoluble in solid iron, and forms sulphides with it or with alloying elements in steels and alloys. In terms of structure, shape and arrangement within the structure of metal, three types of sulphide inclusions can be distinguished [4, 5]: the first are globular, randomly distributed in the metal; the second are low-fusible of eutectic origin, forming films on grain boundaries; the third are crystal-form inclusions randomly distributed in the metal. From the point of view of reducing the probability of origination of cracks at solidification, preferable are globular sulphides uniformly distributed inside the grains. Thus it is desirable that the deposited metal were alloyed with high-melting sulphides. Table 1 shows the melting temperature of some sulphides [6]. The highest

melting point is with vanadium sulphides, while the lowest is with manganese sulphides. Its sulphides solidify last, at a rather low temperature, which can adversely affect crack resistance of the deposited metal in which sulfur is an alloying element. The contents of manganese in the deposited metal of this type should apparently be reduced to a minimum.

**Thermodynamic computations of the reactions of formation of sulphides of alloying elements.** The probability and sequence of sulphides formation at simultaneous alloying of the deposited metal with several alloying elements can be estimated proceeding from thermodynamic computations of the equilibrium of chemical reactions at their formation. For computation of isobar potentials of reactions of formation of alloying elements sulphides, an entropy method based on the well-known thermodynamic equation of computation of isobar potential of any chemical reaction, was used [7]:

$$\Delta Z_T = \Delta H_T - T\Delta S_T,$$

where  $\Delta H_T$  is the enthalpy of reaction products formation;  $\Delta S_T$  is the difference between values of absolute entropies of the reaction products and initial substances;  $T$  is the reaction temperature, K.

For the standard temperature of 298 K

**Table 1.** Main thermodynamic characteristics of sulphides under standard conditions

Chemical element	$S_{298}^0$ , J/(mol·K)	Sulphide	$T_{\text{melt}}$ , °N	$-\Delta H_{298}^0$ , kJ/mol	$S_{298}^0$ , kJ/(mol·K)
Si	18.90	SiS <sub>2</sub>	1090	163.8	--
Mn	31.92	MnS	--	186.48	78.54
		MnS <sub>2</sub>	700	193.2	--
Cr	23.85	Cr <sub>2</sub> S <sub>3</sub>	--	462.0	--
Mo	28.68	MoS <sub>2</sub>	1185	235.2	63.84
		MoS <sub>3</sub>	--	258.3	66.78
V	29.40	VS	1900	189.0	60.90
Fe	27.25	FeS	1190	96.18	67.62
		FeS <sub>2</sub>	697	174.3	52.50
S	32.00	--	--	--	--



**Table 2.** Isobar potentials of sulphide formation reactions

Chemical element	Sulphide formation reaction	$\Delta H_{298}$ , kJ/mol	$\Delta S_{298} \cdot 10^{-3}$ , kJ/(mol·K)	$\Delta Z_T$ , kJ/mol	
				298 K	2043 K
Si	$Si + 2S = SiS_2$	-163.80	--	--	--
Mn	$Mn + S = MnS$	-186.48	14.61	-190.80	-216.30
	$Mn + 2S = MnS_2$	-193.20	--	--	--
Cr	$2Cr + 3S = Cr_2S_3$	-462.00	--	--	--
Mo	$Mo + 2S = MoS_2$	-235.20	-28.85	-226.59	-176.23
	$Mo + 3S = MoS_3$	-258.30	-57.91	-241.03	-139.94
V	$V + S = VS$	-189.00	-0.50	-188.83	-187.95
Fe	$Fe + S = FeS$	-96.180	8.35	-98.65	-113.23
	$Fe + 2S = FeS_2$	-174.30	-38.76	-162.70	-95.08

$$\Delta Z_{298}^0 = \Delta H_{298}^0 - 298\Delta S_{298}^0,$$

for other temperatures

$$\Delta Z_T^0 = \Delta H_{298}^0 - T\Delta S_{298}^0.$$

Computations were conducted for standard and mean temperature of the welding pool of 2043 K (1770 °N) [8].

Table 1 shows the values of entropy of basic alloying elements, as well as enthalpy and entropy of their sulphides formation under standard conditions [6].

Results of computation of isobar potentials of sulphides formation reactions are summarized in Table 2 and Figure 1, which show that formation of molybdenum, magnesium and vanadium sulphides is the most probable. Absence of the data on entropy of chromium and silicon sulphides did not allow making computation of isobar potentials of their formation. However taking into account high enthalpy of chromium sulphide  $Cr_2S_3$ , formation of this sulphide is deemed possible. Formation of sulphide  $SiS_2$  is less probable, as enthalpy of its formation is among of the lowest ones.

**Choice of a surfacing material for the study.** As it was mentioned above, sulfur can be used for alloying materials at surfacing the parts operated under conditions of friction of metal on metal at normal and elevated temperatures and contact pressure. Nowadays for surfacing of such parts, the flux-cored wire for deposition of the metal type 25Kh5MFS tool steel [9] is widely used. As above thermodynamic computations show, basic alloying elements of this deposited metal form the most resistant sulphides featuring quite a high melting point. Therefore for our study we have chosen a deposited metal of this type.

Joint effect of sulfur, molybdenum and carbon on wear resistance of the deposited metal type 25Kh5MFS (Table 3) at wearing under conditions of sliding friction of metal on metal without greasing was investigated. Taking into account that many parts, for whose restoration and hardening the wire PP-Np-25Kh5MFS is used, are operated under condi-

tions of cyclic thermal loading, study of the effect of sulfur on heat resistance of the deposited metal was carried out. Heat resistance is known to be one of the major characteristics of the metal operated under conditions of cyclically changing temperatures.

Among the alloying elements our attention was mainly focused on molybdenum forming disulphide  $MoS_2$ . As reported in [2], this disulphide is the most effective when used as a greasing agent. It has a layered structure, the layers are quite strong but can be displaced relative to each other, owing to which the friction force decreases.

**Experimental procedure.** Deposition on test samples was carried out on automatic plant U-653 using 2 mm diameter test flux-cored wires and flux AN-26P under the following conditions: current 220–250A; voltage 28–30 V; deposition speed 15 m/h.

Wear resistance of the deposited metal at wear under conditions of sliding friction of metal on metal without greasing was determined on friction machine

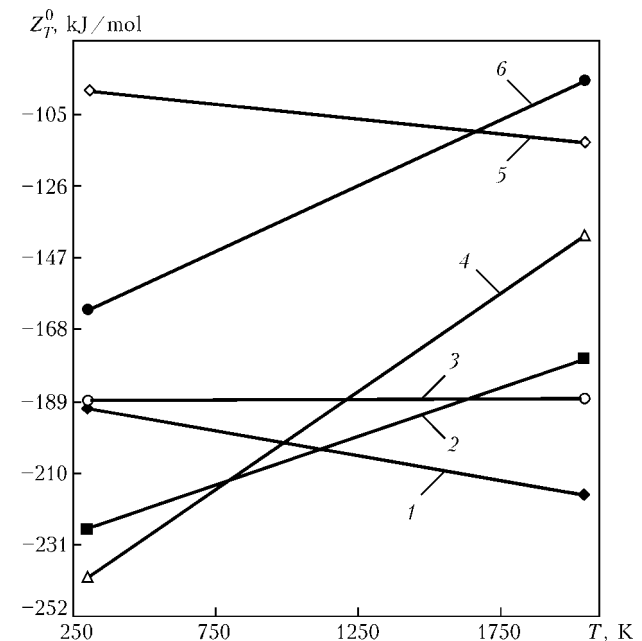


**Figure 1.** Temperature dependences of isobar potentials of sulphides of alloying elements formation reactions: 1 --- MnS; 2 ---  $MoS_2$ ; 3 --- VS; 4 ---  $MoS_3$ ; 5 --- FeS; 6 ---  $FeS_2$

**Table 3.** Chemical composition (wt.%) and HRC hardness of deposited metal

Type of deposited metal	C	Mn	Si	Cr	Mo	V	S	HRC
10Kh5MFS	0.13	0.65	0.90	5.10	0.93	0.45	0.02	30–33
	0.11	0.63	0.84	4.96	0.97	0.43	0.73	
10Kh5M3FS	0.10	0.59	0.80	4.95	3.15	0.52	0.02	18–23
	0.20	0.57	0.87	4.85	3.16	0.56	0.43	
20Kh5M3FS	0.15	0.62	0.92	5.20	3.02	0.45	0.02	34–35
	0.19	0.63	0.92	5.13	2.98	0.48	0.50	
30Kh5M3FS	0.31	0.56	0.82	4.60	2.90	0.50	0.02	44–46
	0.29	0.54	0.83	4.72	3.05	0.54	0.78	

[10] additionally equipped with the system of positioning specimens with respect to rotating shaft being a counter-body. The tests were conducted under the shaft–plane scheme, without feeding of grease into the friction zone. The upper layers of the deposited metal cut out and used as samples for tribotechnical testing had  $3 \times 17 \times 20$  mm dimensions. The wearing process took place on a  $3 \times 20$  mm area. The counter-body had diameter 40 mm and height 12 mm, was made of the hardened steel 45 having HRC 45–50 hardness.

While testing, the wear of the deposited metal sample was determined based on the volume of the wear crater, which was computed by the well-known formulas based on mean value of the crater width, using the measuring microscope (error not exceeding 0.01 mm). The total error at determining the wear of the sample did not exceed 1 %.

Based on the results of preliminary study, the mode of testing was chosen (sliding speed 1 m/s, loading 30 N, duration of test 600 s), which provided repetitiveness of wear resistance parameters of all studied steels. Use of the positioning system has allowed repeating tests of each sample not less than 3 times on a new area of the friction surface of the sample and a new friction track of the same counter-body.

Study of heat resistance of the deposited metal was conducted on a laboratory plant for complex evaluation of its properties [11]. Heat resistance of the deposited metal is defined based on the quantity of heating–cooling cycles to occurrence of erosion lattice on the ground surface of the  $40 \times 40 \times 30$  mm sample. The sample was fixed with a special holder, and its

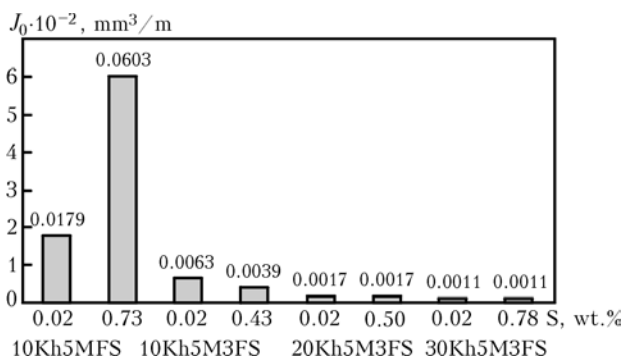
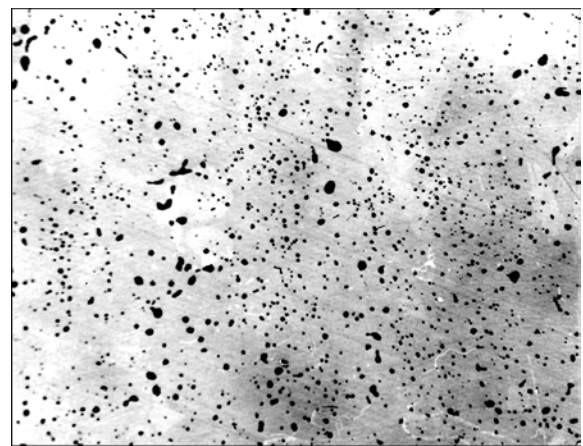
ground deposited surface was heated up using a gas-flame cutting torch, the heating spot was 15–20 mm in diameter. In 11 s the sample was heated up to 670–690 °N, then during 8 s it was cooled with a water jet down to 70–80 °N. Heating and cooling of the test sample was automatic.

**Results of the study.** Study of wear resistance at wear under conditions of sliding friction of metal on metal without greasing at room temperature revealed that influence of sulfur on this parameter of the deposited metal is closely linked with the contents of carbon and molybdenum (Figure 2).

At 0.1 wt.% C and about 1.0 wt.% S in the deposited metal, sulfur alloying sharply reduces its wear resistance. Evidently because of the low contents of molybdenum in the deposited metal, sulphide  $\text{MoS}_3$  (or another) reducing wear resistance is formed.

The increase in the contents of molybdenum up to 3 wt.% in the deposited metal type 10Kh5M3FS, results in substantial growth of wear resistance of the latter, thus sulfur alloying (0.68 wt.%) raises this parameter approximately 2 times. In the deposited metal molybdenum sulphide  $\text{MoS}_2$  is evidently formed, which, as it was shown above, owing to its greasing effect, improves wear resistance. Investigation of the deposited metal structure has confirmed presence in it of the sulphide inclusions (Figure 3).

In the case of the increase of carbon contents first to 0.2 wt.%, and then to 0.3 wt.%, wear resistance of

**Figure 2.** Effect of carbon, sulfur and molybdenum alloying on wear resistance  $J_0$  of deposited metal type Kh5MFS**Figure 3.** Microstructure of deposited metal 10Kh5M3FS (not etched) ( $\times 500$ )

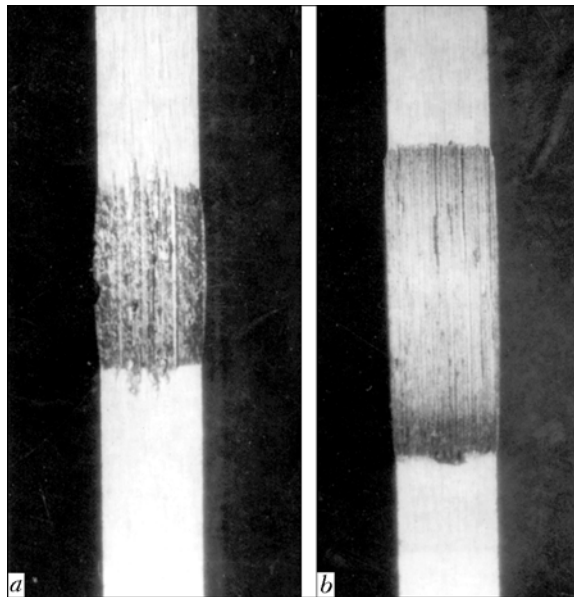


**Figure 4.** Appearance of worn out surface of deposited 20Kh5 $\bar{I}$  3FS metal sample without (a) and with (b) addition of sulfur

the deposited metal types 20Kh5 $\bar{I}$  3FS and 30Kh5 $\bar{I}$  3FS continues to grow, thus sulfur alloying practically has not influence on this parameter. Obviously this influence is neutralized by carbon partially binding molybdenum to produce carbides which considerably raises hardness of the deposited metal.

It should be noted that despite such an ambiguous influence of sulfur on wear resistance of the deposited metal type Kh5 $\bar{I}$  FS, cleanliness of the worn out surfaces of samples of the sulfur-alloyed deposited metal is always higher than with samples without sulfur. In the deposited metal alloyed with sulfur, no traces of scoring, adhesion, etc. were observed (Figure 4).

With regard for the designation of the surfaced parts, for the study of heat resistance, two types of deposited metal 10Kh5 $\bar{I}$  3FS and 20Kh5 $\bar{I}$  3FS alloyed with sulfur were chosen. Figure 5 shows the results of that study. For comparison also shown is heat resistance of hardened steel 45 and the metal deposited using standard flux-cored wires PP-Np-25Kh5MFS and PP-Np-35V9Kh3SF without sulfur, used for restoration and hardening of tools for hot deformation of metal.

Samples from deposited metal 10Kh5 $\bar{I}$  3FS and 20Kh5 $\bar{I}$  3FS had rather high heat resistance, thus with the latter it was much higher. Heat resistance of the tested deposited metal of both types is higher than that of the deposited metal type 35V9Kh3SF tool steel, but lower than with steel 25Kh5M3FS containing no sulfur.

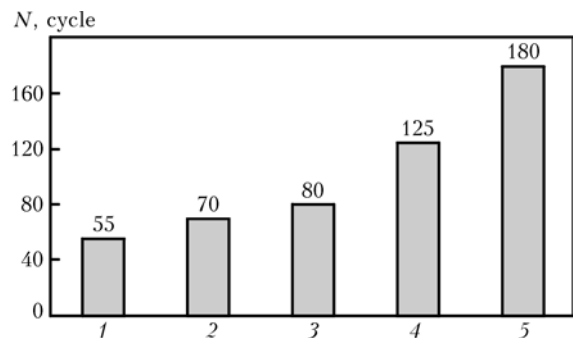


**Figure 5.** Heat resistance of hardened steel 45 (1) and deposited metal 35V9Kh3FS (2), 10Kh5 $\bar{I}$  3FS (3) (0.43 wt.% S), 20Kh5 $\bar{I}$  3FS (4) (0.50 wt.% S) and 25Kh5MFS (5); N --- number of cycles

Thus it was established that sulfur can successfully be applied for alloying the deposited metal of the type of chromium-molybdenum tool steel used for restoration and hardening of tools for hot deformation of metals. Wear resistance of the deposited metal is in the first place determined by the ratio of molybdenum and sulfur, which should exceed 1.5, i.e. to be such that molybdenum disulphide MoS<sub>2</sub> was formed in deposited metal. The latter plays the role of grease, prevents adhesion at friction of metal on metal, thus promoting increase in wear resistance of the deposited metal and improves cleanliness of the friction surfaces.

Sulfur alloying of chromium-molybdenum surfacing metal somewhat reduces its heat resistance, nevertheless this characteristic remains quite high, higher than with the deposited metal type tool steel 35V9Kh3SF.

1. Osin, V.V., Ryabtsev, I.A. (2004) Effect of sulphur on properties of iron-base alloys and prospects of its application in surfacing materials. *The Paton Welding J.*, **10**, 18–21.
2. Samsonov, G.V., Barsegyan, Sh.E., Tkachenko, Yu.G. (1973) About mechanism of lubricating action of refractory metal sulfides and selenides. *Fiz.-Khimich. Mekhanika Materialov*, **9**(1), 58–61.
3. Lunev, V.V., Averin, V.V. (1988) *Sulfur and phosphorus in steel*. Moscow: Metallurgiya.
4. Sime, K., Forgen, W. (1965) Nonmetallic inclusions. In: *Transact. on Steelmaking in Electric Furnaces*. Moscow: Metallurgiya.
5. Shulte, Yu.A. (1970) *Electrometallurgy of steel casting*. Moscow: Metallurgiya.
6. Kubashevsky, O., Evans, E. (1954) *Thermochemistry in metallurgy*. Moscow: Inostr. Literatura.
7. Vladimirov, L.P. (1970) *Thermodynamical calculations of metallurgical reaction equilibrium*. Moscow: Metallurgiya.
8. Frumin, I.I. (1961) *Automatic electric arc surfacing*. Kharkov: Metallurgizdat.
9. Kondratiev, I.A., Ryabtsev, I.A. (1999) *Mechanized electric arc surfacing of metallurgical equipment parts*. Kiev: Ekotekhnologiya.
10. Polotaj, V.V. (1970) Friction and wear testing machine. *Tekhnologiya i Organiz. Proizvodstva*, **6**, 96–98.
11. Ryabtsev, I.I., Chernyak, Ya., I., Osin, V.V. (2004) Modular machine of deposited metal testing. *Svarshchik*, **1**, 18–20.



# CAVITATION-CORROSION RESISTANCE OF SURFACED PARTS OF COMPRESSORS OF TITANIUM-AND-MAGNESIUM PRODUCTION PROCESS

À.V. PATYUPKIN and O.G. BYKOVSKY  
Zaporozhie National Technical University, Zaporozhie, Ukraine

Results are presented of metallographic and petrographic study of the deposited metal type 08Kh23N18İ 5 characterized by the improved cavitation-corrosion resistance, not inferior to that of alloy 06Kh23N28İ 3D30.

*Keywords:* arc surfacing, high-alloy steels and alloys, chlorine compressor, cavitation-corrosion resistance, phase composition

Nowadays the prevailing method of producing magnesium at titanium-and-magnesium works is based on the electrolysis of magnesium chloride, thus the end products of the process are magnesium, chlorine and the waste electrolyte. Chlorine is used for the production of  $TiCl_4$ , while magnesium for reduction of this compound to titanium. The waste magnesium chloride is returned to the magnesium division, to be used for production of magnesium and chlorine [1].

One of the basic elements of the anodic chlorine pump-out system is the chlorine compressor, in which rotor rotating the working liquid forms in the oval casing a liquid ring playing the role of a piston. At present for the removal of anodic chlorine from electrolyzers and its further feeding under the pressure of up to 0.1 MPa, in the production process are used compressors RZhK-1800/1.5. For forming a circular hydraulic seal in compressors, 98 % sulfuric acid is used (temperature of the liquid is 55 °Ñ) [2]. After filtration, 5–13 % of sublimation products (anodic chlorine with HCl fumes) are fed into the compressor, in so doing  $H_2SO_4$  concentration in the system drops from 98 to 92 %. Service life of the chlorine compressor of a magnesium production facility does not exceed 2000 h. Main compressor parts determining duration of its service life and reliability, are motionless cones, rotating rotor and covers of the casing (steel 12Kh18N100). Surfaces of these parts at assembling are very carefully seated, as exceeding operating tolerances between the parts drastically reduces productivity of the chlorine compressor.

Analysis of the condition of chlorine compressors after 2000-hour operation shows selective character of failure of cones partitions, rotor surfaces, compressor covers (Figure 1). Depth of cavities on parts reaches 15–20 mm. High wear is due to joint cavitation-corrosive attack of the working liquid on parts surfaces (it is well known that in 98 % solution of  $H_2SO_4$  the corrosion rate of steel 12Kh18N100 does not exceed 1 mm/year [3]). Even at low magnification ( $\times 30$ ) are visible damaged areas in the form of various-depth pittings with indistinct edges (Figure 2, a). At higher magnifications (Figure 2, b, c) it is clearly seen that corrosion failure arises mainly along the boundaries of grains yet at the initial stages of cavitation effect and develops in depth nonuniformly. Damage to parts of the process equipment in 92 % solution of  $H_2SO_4$  is due to the reduction of adhesion of the oxide layer formed on the metal surface and shear spalling of its individual fragments under avalanche-like microshock effect of the solution. The passive condition of the metal is perturbed, areas with the ruptured film acquire a stationary potential of the given steel (alloy), and become anodes, while the surfaces protected by

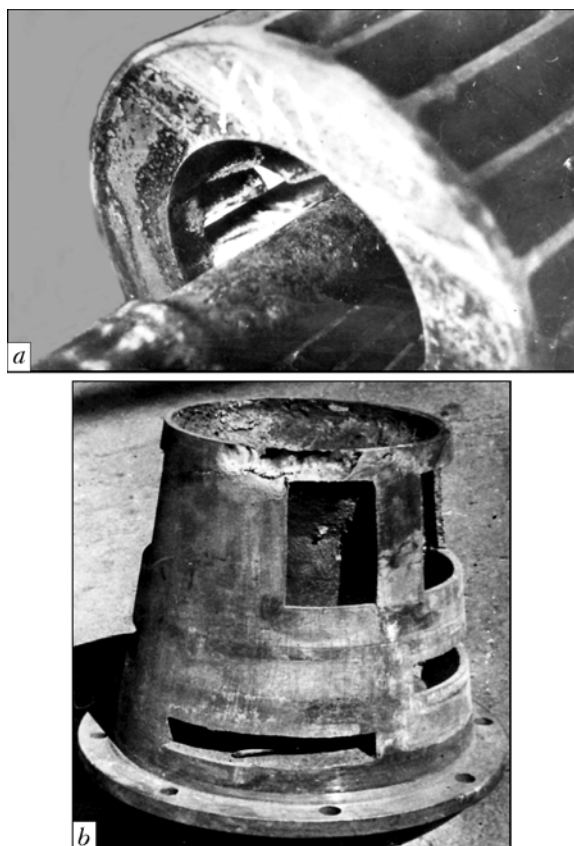


**Figure 1.** Appearance of worn out surface of rotor (a) and cone (b) of chlorine compressor

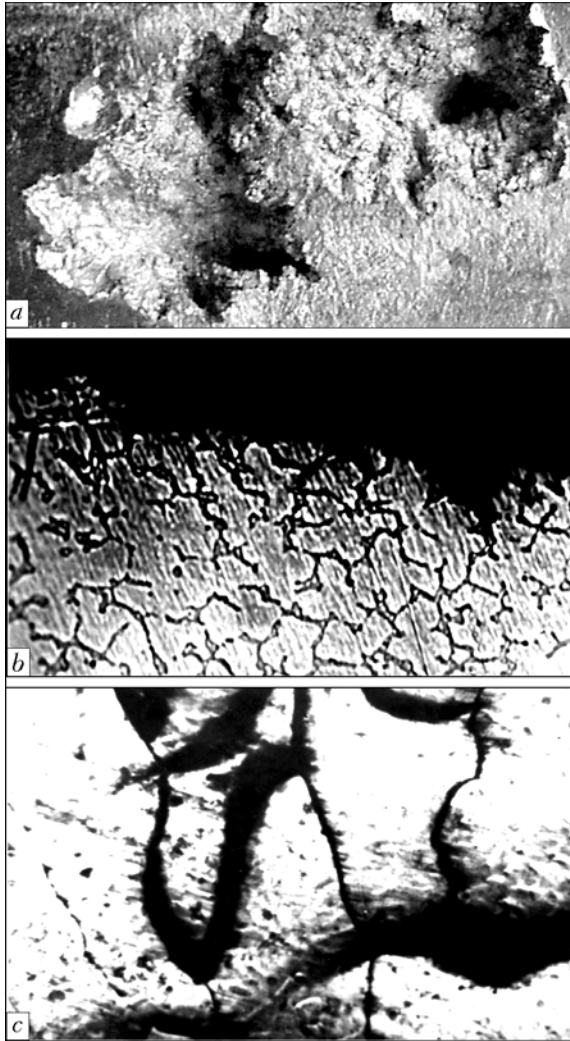
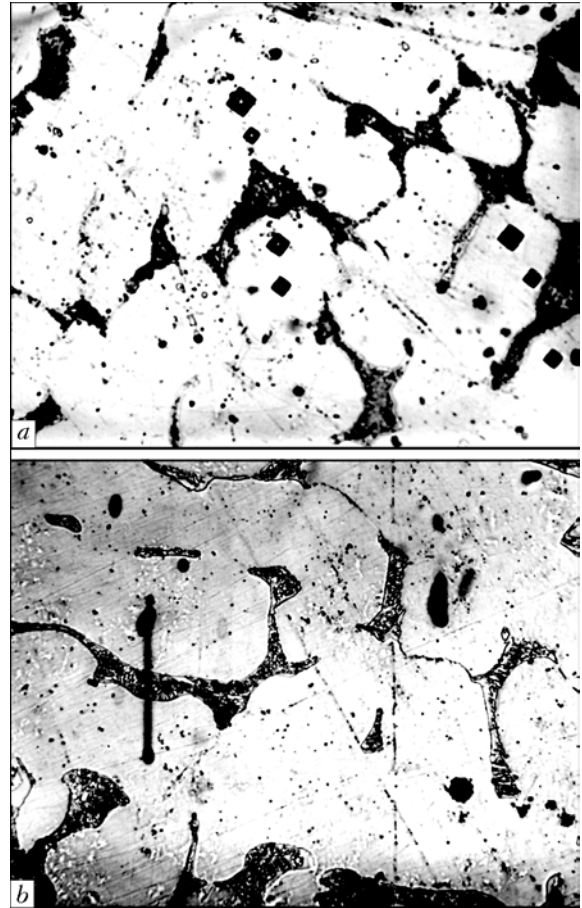


**Figure 2.** Appearance of pittings (*a* —  $\times 30$ ) and microstructure of metal of worn out area of surface of cone of chlorine compressor (*b* —  $\times 500$ ; *c* —  $\times 800$ )

the oxide film become cathodes. As a result, local current of galvanic corrosion grows. The subsequent cavitation effect on this weakened by corrosion surface results in essential change of the geometry of parts [4].

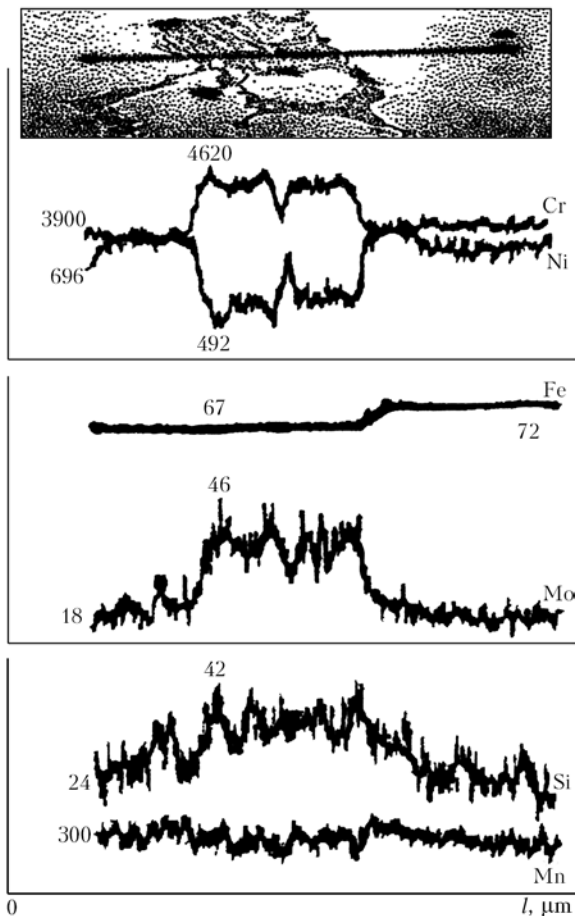
Decisive in ensuring cavitation-corrosion resistance of the process equipment is the correct choice of the chemical composition and structure of the metal. For estimation of cavitation-corrosion resistance of a series of stainless steels and alloys, testing of samples in 92 % solution of  $H_2SO_4$  on the shock-erosion stand by the technique of [5], was conducted. According to the results of statistical processing of the laboratory research data on cavitation-corrosion resistance of steels and alloys, optimum ranges of chromium, nickel and molybdenum content as basic alloying components of the tested samples were determined. This range includes steel 08Kh23N18I 5 and alloy 06Kh23N28I 3D30. During a 10-hour tests loss of mass of samples were of the same order for steel 08Kh23N18I 5 (0.50 g) and alloy 06Kh23N28I 3D30 (0.46 g), in spite of the high degree of alloying of the latter [5].

In order to obtain more accurate information of the mechanism of increasing cavitation-corrosion re-



**Figure 3.** Microstructure of metal of sample from steel 08Kh23N18I 5: *a* —  $\times 420$ ; *b* —  $\times 800$

sistance of steel 08Kh23N18I 5, metallographic and petrographic studies, as well as X-ray spectrographic analyses of the pattern of distribution of alloying elements in structure components of the deposited metal, were conducted. Distribution of the alloying elements was examined on the «Cameca» micro-X-ray spectrographic analyzer (probe locality was below  $2 \mu m$ ,  $I = 20 \text{ nA}$ ,  $U = 20 \text{ kW}$ , probe advance speed was  $2.5 \text{ cm/min}$ ). The test specimen had austenitic-ferritic microstructure (Figure 3). Calculation according to the Schaeffler's diagram showed that proportion of the ferritic phase was less than 5 %. Polythermal sections of constitutional diagrams for steel at  $1200 \text{ }^\circ\text{N}$  show that addition of more than 20 % chromium, molybdenum and sulfur can result in formation of the  $\sigma$ -phase complicating the phase composition of steel. Molybdenum is dissolved predominantly in  $\gamma$ -solid solution and  $\sigma$ -phase, thus expanding the  $\gamma + \sigma$  range. The  $\sigma$ -phase in the metal of a sample from steel 08Kh23N18I 5 has microhardness of  $HV 11000\text{--}12900 \text{ MPa}$ . Lower microhardness of  $HV 6810\text{--}8090 \text{ MPa}$  is explained by the fact that it was impossible to register monolithic phases in view of their small dimensions, therefore the fine precipitates in the austenitic matrix were measured. Microhardness of the latter varies within the  $2130\text{--}2840 \text{ MPa}$  range, which is due to difference in affinity of some alloying elements to carbon. In the presence of carbide-forming elements, such as chromium and molybdenum, at

 $J$ , rel. un

**Figure 4.** Distribution of elements throughout solid phase in samples from steel 08Kh23N18I 5

higher magnifications, fine precipitates of complex carbides are observed in steel (Figure 3, b). Simultaneously were recorded radiation intensities of molybdenum, nickel, chromium, manganese, silicon and iron (Figure 4). X-ray spectrographic analysis was conducted by scanning of the surfaces of samples along the probe  $\gamma$ - $\alpha$ - $\gamma$  travel paths.

Microhardness measurements show that the solid phase is enriched with chromium and molybdenum, while the content of nickel and iron is a bit lower than in the matrix. Presence of the solid phase enriched with chromium and molybdenum, as well as fine carbides on their basis, promotes improvement of cavitation-corrosion resistance of steel 08Kh23N18I 5. The solid phase is non-uniform; it may contain portions of the matrix or the other phase. Diversity of structures and difference in properties of individual structural components ( $\alpha$ -phase, carbides) promotes hardening of steels or alloys and occurrence of failures. Addition of molybdenum results in hardening of steel, reduction of chromium carbides precipitation along the grain boundaries and propensity of the deposited metal to intercrystalline corrosion [6].

Contamination of steel with nonmetallic inclusions was determined by metallographic method in accordance with GOST 1778-70 by calculation of the amount and volume per cent of impurities. The criterion in estimating the degree of contamination was mean

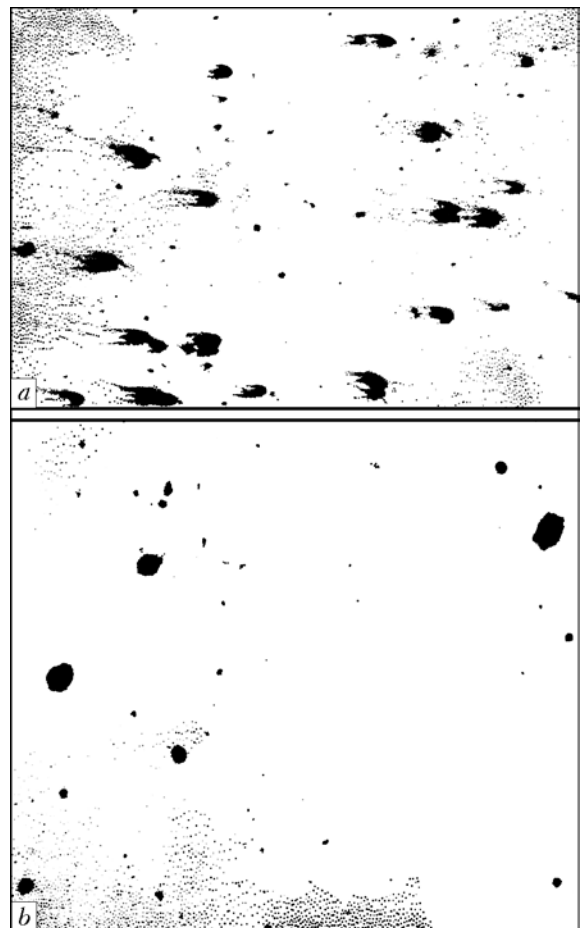


**Figure 5.** Contamination of reference sample from steel 12Kh18N10O (a) and from test steel 08Kh23N18I 5 (b)

arithmetic value of volume per cent of each microsection and the amount of impurities of specific groups of particles on 100 mm<sup>2</sup> areas, counted at  $\times 280$  magnification. The general level of contamination with nonmetallic inclusions in metal deposited using tested electrodes, is lower in comparison with steel 12Kh18N10O (Figure 5), their dimensions being much smaller (below 2-4  $\mu$ m). The content of inclusions in steel 08Kh23N18I 5, vol.%: globules --- 0.016; oxides --- 0.072; oxysulphides --- 0.0005; sulphides --- 0.01. Thus in steel 08Kh23N18I 5 are prevailing globules, oxide and sulphide inclusions. Contamination of the latter with nonmetallic inclusions is much lower than with steel 12Kh18N10O (see Figure 5), which also improves metal resistance.

## CONCLUSIONS

1. Steel 08Kh23N18I 5 has improved cavitation-corrosion resistance in 92-98 % solution of H<sub>2</sub>SO<sub>4</sub>, close to that of alloy 06Kh23N28I 3D30. This is due to the presence of the superfluous phase enriched with chromium and molybdenum, as well as carbides of these elements. This phase has non-uniform structure and hardens steel 08Kh23N18I 5. Molybdenum in its affinity to carbon surpasses chromium, therefore formation of molybdenum carbides along the grain boundaries in steel is more preferable. This factor reduces propensity of metal to intercrystalline corrosion.



2. For manufacturing and restoration of parts of chlorine compressors (cones, rotors, covers of the casing, etc.) subject to cavitation-corrosive attack while in service, preferable is steel 08Kh23N18I 5 or welding consumables providing deposited layers of the required chemical composition.

1. Ivanov, A.I. (1962) *Electrolysis production of magnesium*. Moscow: Metallurgizdat.
2. Khlumsky, V. (1971) *Rotary compressors*. Moscow: Metallurgizdat.

3. Sukhotin, A.M., Zotikov, V.S. (1975) *Chemical resistance of materials: Refer. Book*. Leningrad: Khimiya.
4. Patyupkin, A.V. (2004) Effect of corrosion factor on cavitation-corrosion wear kinetics of stainless steels and alloys. *Novi Materialy i Tekhnologii v Metallurgii ta Mashynobuduvanni*, **1**, 143–145.
5. Patyupkin, A.V., Antonyuk, D.A. (2005) Effect of alloying on cavitation-corrosion resistance of stainless steels and alloys. *The Paton Welding J.*, **4**, 14–16.
6. Ulianin, E.A., Svistunova, T.V., Levin, F.L. (1987) *Corrosion-resistant high alloys*. Moscow: Metallurgiya.

## STRUCTURE AND PROPERTIES OF POWDERS OF Al–Cu–Fe SYSTEM ALLOY FOR THERMAL SPRAYING OF QUASI-CRYSTALLINE COATINGS

A.L. BORISOVA, A.Yu. TUNIK and L.I. ADEEVA  
E.O. Paton Electric Welding Institute, NASU, Kiev, Ukraine

Given are the results of investigation of structure, phase composition and technological properties of powders of an Al–Cu–Fe system alloy produced by different atomisation methods (argon, high-pressure water, compressed air), as well as by ingot crushing. Behaviour of the powders in heating is studied under conditions of differential thermal analysis.

*Keywords:* thermal spraying, coatings, quasi-crystalline phase, Al–Cu–Fe system alloy, powders, production methods, structure, properties

New class of coatings from the quasi-crystalline phase containing materials, taking an intermediate position between amorphous and metal alloys, is characterised by a combination of such properties as low thermal and electrical conductivity, high hardness and wear resistance, as well as low friction and adhesion coefficients [1].

One of the key factors affecting properties of thermal spray coatings is structure and properties of a spraying material, i.e. powder or wire. In particular, flowability and apparent density of a powder are determined by its transport characteristics, such as the possibility of a stable and controllable feed into the high-temperature gas jet. The shape of particles is related to their specific surface area, which influences the processes of heat exchange, gas dynamics and interaction between the phases in the gas jet during spraying of coatings.

The quality of thermal spray coatings and their quasi-crystalline phase content depend upon the composition, structure, size and shape of particles, as well as other characteristics of a spraying powder, which, in turn, are determined by the method used to produce this powder.

These factors acquire special importance in thermal spraying of coatings using the quasi-crystalline  $\psi$ -phase containing powders of an Al–Cu–Fe system alloy, which is attributable to a very small size of the region occupied by this phase in the constitutional diagram of the Al–Cu–Fe system [2–5]. Even insignificant

deviations in the initial composition of the  $\text{Al}_{63}\text{Cu}_{25}\text{Fe}_{12}$  alloy powder and differences in conditions of heating of its particles associated with size and shape of the particles, as well as stability of feeding them into the jet, determine to a considerable degree the probability of formation of the  $\psi$ -phase in a sprayed layer. For this reason, investigations of structure and properties of such powders depending upon the method used to produce them allow technologists to choose a right initial material [6, 7].

Additional characteristic of thermal spraying powders is their behaviour under conditions of differential thermal analysis (DTA), which makes it possible to predict the phase transformation processes.

**Methods for production of powders of an Al–Cu–Fe system alloy.** Powders of the quasi-crystalline phase containing alloys are produced by the methods considered below.

*Compressed gas or air atomisation of melt* consists in dispersion of the melt jet with compressed gases [6–10]. The melt of the Al–Cu–Fe system heated to 100–300 °C above the liquidus line is atomised with a compressed air or high-pressure inert gas. The rate of cooling of the melt in this case reaches  $1 \cdot 10^5$  K/s. Powders produced by compressed air atomisation have particles of a globular or rounded shape, while in the case of using inert gases the shape of the powder particles is close to spherical. The main commercial method for producing aluminium and aluminium alloy powders is atomisation of the melt in argon [11].

*Water atomisation of melt* is based on dispersion of the melt with high-pressure water [12, 13]. The



problem of explosion safety of this process and prevention of oxidation of aluminium alloy powders is solved through dispersing the melt with a water containing inhibitor additions, controlling its temperature and pH value, hydraulic classification of powders in size, and drying them in vacuum. With this method used to produce the  $\text{Al}_{63}\text{Cu}_{25}\text{Fe}_{12}$  alloy powder [10] by atomising the melt with high-pressure water, the free flowing melt jet is split by separate water jets located circumferentially around the melt jet. In this case, the resulting powder particles are of an irregular shape. The powder is subjected to drying at  $200\text{ }^{\circ}\text{C}$  for 4 h.

*Crushing of ingots* to produce powders is performed in two stages: the first stage consists in melting of ingots of a preset composition, and the second stage consists in mechanical crushing. The ingots are melted in a water-cooled copper crucible of the high-frequency furnace in argon atmosphere [14–17]. The ingots are milled in a tumbling mill with steel balls. The resulting wires contain, as a rule, several crystalline phases, in addition to the quasi-crystalline one. To increase the  $\psi$ -phase content, it is necessary to perform annealing for 24 h at 1084 K [15]. The powders produced by crushing have particles of a fragmented shape.

*Method for spontaneous disintegration of jet with water cooling and crushing of granules* consists in the fact that the jet of the  $\text{Al}_{63}\text{Cu}_{25}\text{Fe}_{12}$  melt is passed through a round orifice [11]. Under the effect of minor disturbances according to the Rayleigh law, it disintegrates into separate fragments to form droplets under the effect of surface tension. The water-cooled melt droplets 10–15 mm in size have both rounded and irregular dump-bell shape. After drying at  $200\text{ }^{\circ}\text{C}$  for 4 h, they are subjected to mechanical crushing to sizes below 3 mm and milling in a ball mill for 30 min to produce particles less than  $350\text{ }\mu\text{m}$  in size.

*Method for centrifugal dispersion of melt* described in [18] consists in the following. An ingot preliminarily melted in the induction furnace in argon atmosphere is again melted in a crucible located at the centre of an atomisation chamber in helium atmosphere. Upon reaching the temperature of pouring, which is higher than the melting temperature by about  $200\text{ }^{\circ}\text{C}$ , the hole at the crucible bottom is opened, and the melt flows out onto a disk rotated at a speed of 30,000 rpm. The melt spreads over the disk, and splits into droplets at its end. The droplets solidify during their movement to the chamber walls. The powder particles have a rounded and flattened shape. To provide a homogeneous chemical composition of the powder, heating from  $800\text{ }^{\circ}\text{C}$  to the pouring temperature is performed at a rate of  $5\text{ K/min}$ . The rate of cooling of the melt in centrifugal dispersion is not in excess of  $1\cdot 10^4\text{ K/s}$ , and the  $\psi$ -phase content of the powder is comparatively low. It is impossible to provide a single-phase composition of the powder by annealing [13]. This method for production of powders from

alloys takes an intermediate position between the laboratory and commercial ones.

*Method of evaporation and condensation* for production of powders containing the quasi-crystalline phase is based on a high-rate evaporation of ingots of an Al–Cu–Fe system alloy in vacuum. Laser with wavelength  $\lambda = 248\text{ nm}$  is used as an energy source in this case [19]. The powder particles have a flaky shape, size of 10–20  $\mu\text{m}$ , and ultra-fine granular structure. This method allows producing only a small amount of a powder. Therefore, its application in industry is problematic.

*Mechanical alloying* consists in processing of a mechanical mixture of powders of the alloy components in a high-energy planetary-type ball mill (triboreactor) [20, 21]. A mixture of pure components is used as a raw material. An important role in formation of the quasi-crystalline phase is played by a ratio of atomic concentrations of aluminium and copper + iron. The powder particles have an irregular shape. The drawback of this method is that a high-energy milling cannot provide a sufficient amount of the quasi-crystalline phase without additional annealing at a temperature of  $500\text{--}600\text{ }^{\circ}\text{C}$ .

Phase composition, shape and structure of the powder particles, as well as technological properties (apparent density and flowability) depend upon the method used to produce the quasi-crystalline powders. The above methods for producing powders have substantial differences, which determine their properties.

Firstly, this is a difference in the rate of solidification of the melt. In the case of gas atomisation of the melt, the rate of solidification of droplets is several orders of magnitude higher than that of solidification of an ingot in cooled moulds. The powder produced by atomisation has a homogeneous fine structure. If a powder is produced by solidification of the melt in a cooled mould, followed by crushing of a resulting ingot, this powder will be characterised by an inhomogeneous structure, variable composition (because of liquation) and a lower content of the  $\psi$ -phase.

Secondly, a difference lies in the methods used to split the melt. With gas atomisation, the melt jet is split by a gas flow into droplets, which acquire a spherical shape in the inert gas atmosphere, and after that they solidify. The resulting powder with particles of a spherical shape are characterised by a good flowability. With high-pressure water atomisation, the powder particles take on an intricate irregular shape and have a large number of internal pores. Particles of the powders produced by vapour phase condensation have a flaky shape, and those of the powders produced by crushing of a solidified ingot have an irregular fragmented shape and low flowability.

Properties of a material are substantially affected by an environment in which it was produced. Powders produced by compressed air or high-pressure water atomisation of the melt contain a large amount of oxygen, which leads to deterioration of their proper-

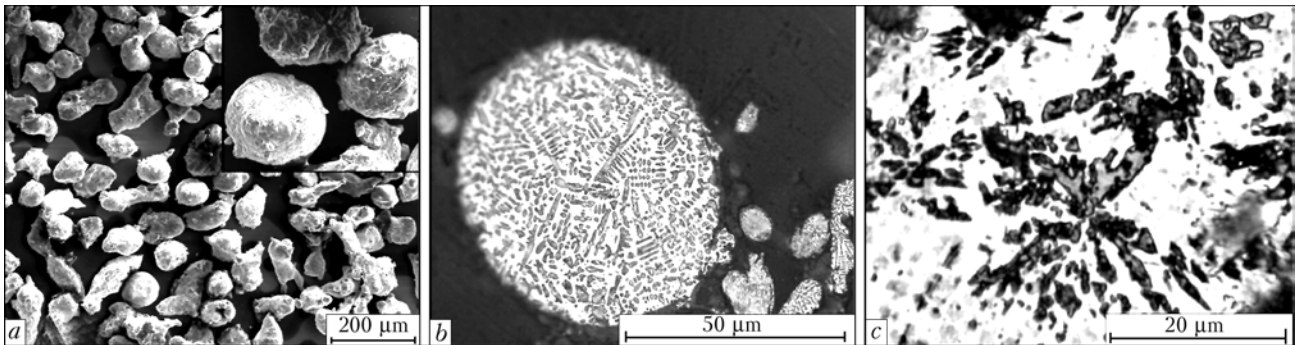


**Figure 1.** Appearance (a) and microstructure (b, c — etched) of the Al-Cu-Fe system alloy powders produced by argon atomisation of the melt: a, b — particle size 63–80 μm; c — less than 40 μm

ties. Inert gas atomisation prevents oxidation of the surface of the particles.

The purpose of this study was to investigate the effect of the methods used to produce powders of alloy  $Al_{63}Cu_{25}Fe_{12}$  on their structure, phase composition, and technological and mechanical properties.

**Methods for experimental studies.** The powders were made by the following methods: argon atomisation of the melt, high-pressure water atomisation of the melt, and crushing of ingots. The investigations were conducted by an integrated procedure, including metallography using optical microscope «Neophot-32» with a digital photography attachment, scanning electron microscopy using scanning electron microscope JSM-840, and X-ray microanalysis using microanalyser «Camebax SX-50». The oxygen content was determined with the LECO gas analyser RO-316 by the method of reduction melting in a carrier gas flow (nitrogen).

X-ray phase analysis (XPA) was conducted using diffractometer «DRON-UM1» in monochromatic radiation  $CuK_{\alpha}$ . The content of the  $\psi$ -phase was determined by the Sordelet's procedure [22]. With this procedure, the X-ray patterns were fixed in an angular range of reflection of the strongest diffraction maxima of the basic phases, i.e.  $40^{\circ} < 2\theta < 50^{\circ}$ .

In addition, phase transformations during heating in the helium atmosphere to a temperature of 1500 °C, as well as the effect of isothermal annealing on phase composition of powders, were investigated by the DTA method.

Technological properties of the powders (flowability and apparent density) were evaluated according to GOST 20899–75 and GOST 19440–74.

Prior to the investigations, the powders were classified in particle sizes using vibrosieves (GOST 18318–73), and each size of the powder particles was investigated separately.

**Morphology and microstructure of particles of Al-Cu-Fe system alloy.** The shape of particles is an important characteristic of a powder, as it determines such technological properties as flowability and apparent density. As noted above, the shape of the particles is related also to the specific surface area, which affects the processes of heat exchange, gas dynamics and interaction between the phases in the gas jet during spraying of coatings.

To ensure a uniform feed of the powder into the gas jet during spraying, it is desirable that the particles have a spherical and spheroidal shape, homogeneous chemical composition and insignificant porosity. The method of atomisation, i.e. dispersion, of the jet of molten metal or alloy with a neutral gas, compressed air or high-pressure water meets the above requirements to the highest degree.

However, as shown by the investigations, the powders with particles of a spheroidal shape can be produced only by atomisation of the melt with argon, and if the particles are less than 25 μm in size, in this case they will have an ideal spherical shape (Figure 1, a, b).

The powders produced by high-pressure water atomisation (Figure 2, a) consist mostly of particles of an elongated shape with sharp or molten edges. The particles have a rough surface with depressions and cavities. Particles of the powder produced by compressed air atomisation are characterised by a variable

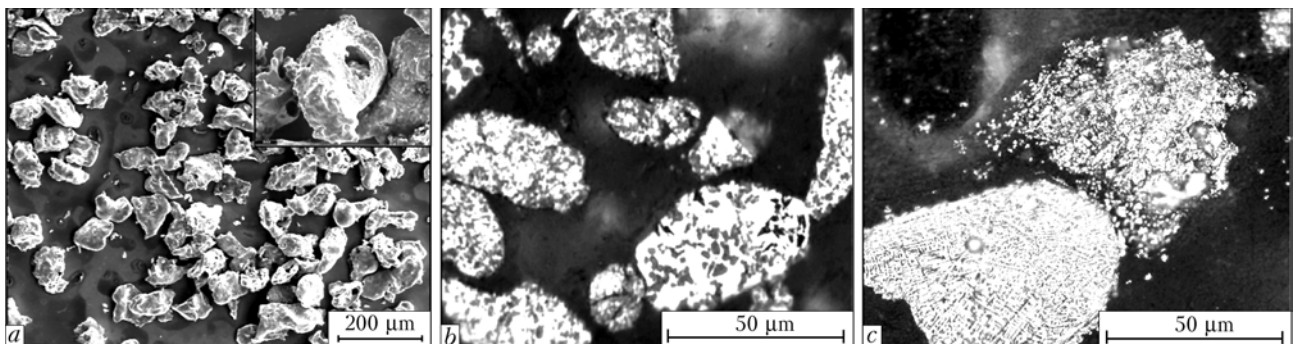


**Figure 2.** Appearance (a) and microstructure (b, c — etched) of the Al-Cu-Fe system alloy powders produced by high-pressure water atomisation of the melt (particle size 40–63 μm)

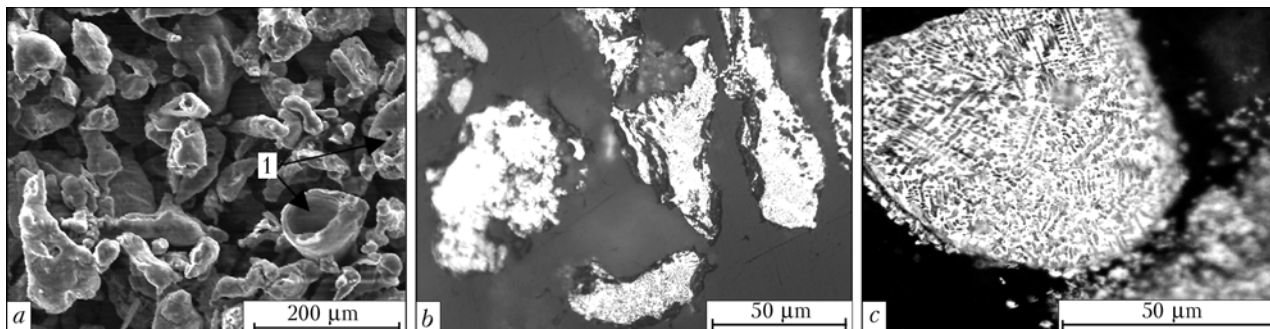


**Figure 3.** Appearance (a) and microstructure (b, c — etched) of powders of Al-Cu-Fe system alloy produced by compressed air atomisation of the melt: a, b — particle size 80–100 µm; c — less than 50 µm

(irregular) shape with the developed surface and substantial amount of internal cavities (Figure 3, a, b).

In all the cases the shape of the particles depends upon their size: the larger the diameter of the particles, the larger the deviation of their shape from the spherical one (the shape factor increases).

The process of spheroidisation of droplets formed in dispersion of the jet is more stable for the melts with high surface tension and low viscosity. With the compressed air or water used as an energy carrier, the melt absorbs oxygen and nitrogen, and interacts with the water vapours contained in the atomisation chamber. This results in growth of viscosity of the melt, which hampers the spheroidisation process. Being an inert gas, argon does not interact with the melt, and does not affect the spheroidisation process. Other conditions being equal, the probability of spheroidisation depends upon the size of a droplet, i.e. stability of the droplet determined by the Laplace forces ( $L_p = \sigma/r$ , where  $\sigma$  is the surface tension, and  $r$  is the particle diameter [23]) decreases with increase in its size. This attributes to the deviation of the shape of coarse particles from the ideal spherical one even in powders produced by argon atomisation.

The powders produced by crushing of granules (Figure 4, a) have particles with a fragmented shape, which is typical of this atomisation method. As a rule, the particles have sharp edges and a smooth surface of the facets, which is indicative of a brittle character of fracture.

As seen from microstructure of the particles revealed by etching, they have a heterogeneous and multi-phase composition. The powders produced by argon atomisation have the most homogeneous and

fine-crystalline structure. Polyhedral crystals of the  $\psi$ -phase in the form of dendrites (see Figure 1, b) or rosettes (see Figure 1, c) precipitate in a light crystalline matrix ( $\beta$ -phase). In coarse particles of the powders produced by water or compressed air atomisation, regions of the grey  $\psi$ -phase are bordered with the light  $\beta$ -phase (see Figures 2, b and 3, b), and particles less than 40 µm in size have a similar but more fine-crystalline structure (see Figures 2, c and 3, c), the powder particles more than 100 µm in size being characterised by a considerable porosity.

The powders produced by crushing of granules (Figure 4) have a coarser and less homogeneous structure, compared with the above three methods.

**Chemical composition of powders of Al-Cu-Fe system alloy.** As shown by chemical analysis (Table 1), the powders with particles of different sizes, produced by atomisation of the melt using argon, compressed air or high-pressure water as an energy carrier, have approximately identical content of the main chemical elements. In the powders produced by crushing of granules, the size of which prior to milling was 10–15 mm, the effect of liquation is unavoidable, which leads to heterogeneous chemical composition across an ingot.

The composition of atmosphere in the atomisation chamber and type of an energy carrier affect the oxygen content of an atomised powder. The powders produced by argon atomisation have a minimal (0.05–0.14 wt.%) content of oxygen, and the water atomised powders have an oxygen content of 1.35–1.95 wt.%. The effect of particle size composition of the powders on their oxygen content is ambiguous. Analysis of the data in Table 1 allows a conclusion that deviation of

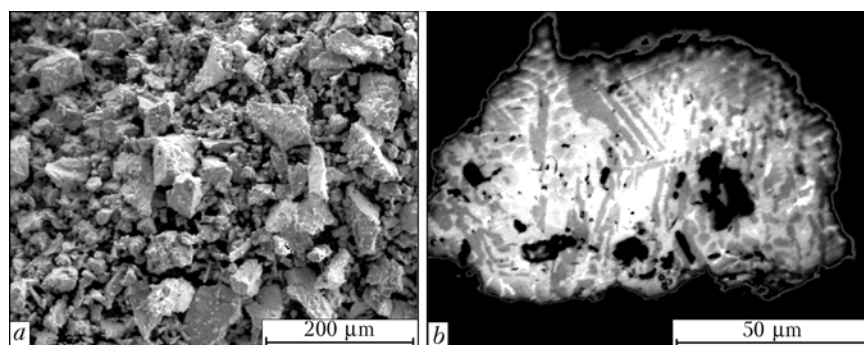


**Figure 4.** Appearance (a) and microstructure (b — etched) of the Al-Cu-Fe system alloy powders produced by crushing of granules (particle size 80–100 µm)



**Table 1.** Chemical composition (wt.%) of Al<sub>63</sub>Cu<sub>25</sub>Fe<sub>12</sub> alloy powders produced by different methods

Powder production method	Particle size, μm	Al	Cu	Fe	[O]
Argon atomisation of melt	120-160	41.80	39.4	18.40	0.13
	63-80	41.60	39.2	18.30	0.12
	40-63	--	--	--	0.05
	25-40	--	--	--	0.14
	< 25	41.90	38.6	18.40	0.14
High-pressure water atomisation of melt	100-125	42.12	38.5	18.70	1.60
	80-100	41.20	39.4	17.87	1.35
	50-80	41.62	39.5	18.98	1.75
	< 50	41.50	37.9	18.98	1.95
Compressed air atomisation of melt	100-160	40.50	37.9	19.50	0.63
	80-100	39.20	37.9	19.00	0.38
	50-80	--	--	--	--
	< 50	--	--	--	1.50
Mechanical crushing of granules	160	39.70	37.6	18.60	0.65
	100-160	48.00	34.5	17.50	0.91
	80-100	--	--	--	0.73
	50-80	--	--	--	--
	< 50	--	--	--	0.77

the oxygen content from a mean value towards growing is characteristic of powders with a particle size of less than 50 and more than 100 μm, which are produced by atomisation. Increase in the oxygen content of fine powders is associated with increase in the specific surface area of solidifying droplets, and in coarse powders --- with formation of closed pores (gas cavities), which are detected by structural microanalysis of particles.

The similar mechanism of the effect exerted by the composition of an energy carrier and particle size com-

position of a powder on its gas content was established for self-fluxing nickel alloys [24].

It should be noted that no such relationship between the oxygen content and particle size composition is seen in the powders produced by crushing of granules.

**Phase composition of powders of Al-Cu-Fe system alloys.** The X-ray phase analysis data (Table 2, Figures 5 and 6) are indicative of the fact that powders with a particle size of up to 120 μm, produced by atomisation, consist of a mixture of ψ- and β-phases

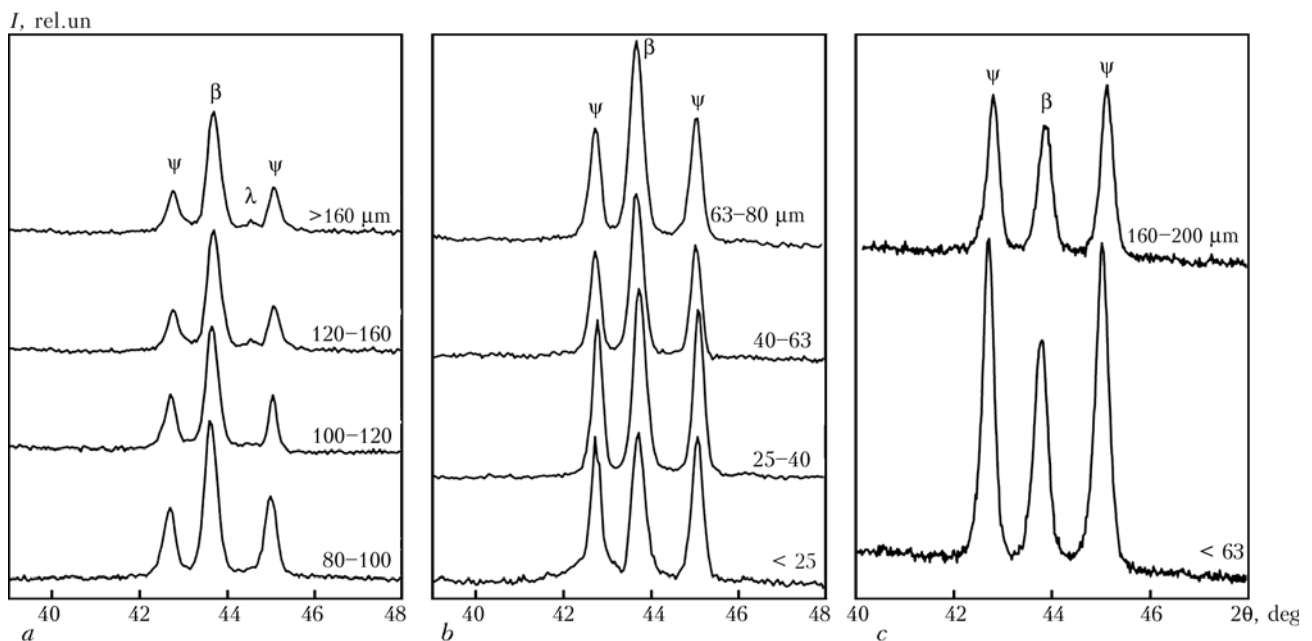


**Figure 5.** X-ray patterns of powders with particles of different sizes produced by argon (a, b) and high-pressure water (c) atomisation: I --- X-ray radiation intensity; θ --- angle of reflection of diffraction maxima



**Table 2.** Characteristics of Al-Cu-Fe system alloy powders

Powder production method	Particle size, $\mu\text{m}$	Phase composition*	Content of $\psi$ -phase, wt. %	Flowability, s/50 g	Apparent density, $\text{g}/\text{cm}^3$
Argon atomisation of melt	> 160	$\beta, \psi, \lambda$	20	--	--
	120-160	$\beta, \psi, \lambda$	25	59	1.78
	100-120	$\beta, \psi$	32	50	1.88
	80-100	$\beta, \psi$	38	47	1.97
	63-80	$\beta, \psi$	42	44	2.06
	40-63	$\beta, \psi$	45	35	2.15
	25-40	$\psi, \beta$	50	38	2.20
High-pressure water atomisation of melt	< 25	$\psi, \beta$	58	56	2.32
	80-100	$\beta, \psi$ , traces of $\lambda$	47	63	1.38
	63-80	$\beta, \psi$	48	No flow	1.33
	40-63	$\psi, \beta$	53	Same	1.36
	25-40	$\psi, \beta$	55	»	1.30
Compressed air atomisation of melt	< 25	$\psi, \beta$	59	»	--
	100-160	$\psi, \beta$	--	--	--
	80-100	$\psi, \beta$	50	65	1.50
	50-80	$\psi, \beta$	52	58	1.65
Mechanical crushing of granules	< 50	$\psi, \beta$	54	80	1.88
	100-160	$\beta, \psi, \lambda, \theta$	22	No flow	--
	80-100	$\beta, \psi, \lambda, \theta$	30	Same	--
	50-80	$\beta, \psi, \lambda, \theta$	22	»	--
	< 50	$\beta, \psi, \lambda, \theta$	29	»	1.50

\*Phases are arranged in an order of decrease in the intensity of reflection of X-rays.

(cubic lattice), and an impurity of the monoclinic  $\lambda$ -phase (alloy  $\text{Al}_{72}\text{Cu}_5\text{Fe}_{23}$ ) was detected only in coarser powders. The powders produced by milling of granules have a more complex phase composition. In addition to the  $\beta$ - and  $\lambda$ -phases, with which the  $\psi$ -phase is in equilibrium at a temperature of 800 °C, they contain also the tetragonal  $\theta$ -phase ( $\text{Al}_2\text{Cu}$ )

formed at a temperature below 680 °C as a result of complex phase transformations. As solidification of granules occurs at a comparatively low rate of cooling of the melt, this creates conditions for formation of the  $\lambda$ - and  $\theta$ -phases in them.

The content of the quasi-crystalline  $\psi$ -phase in the powders is in direct relationship with the rate of cool-

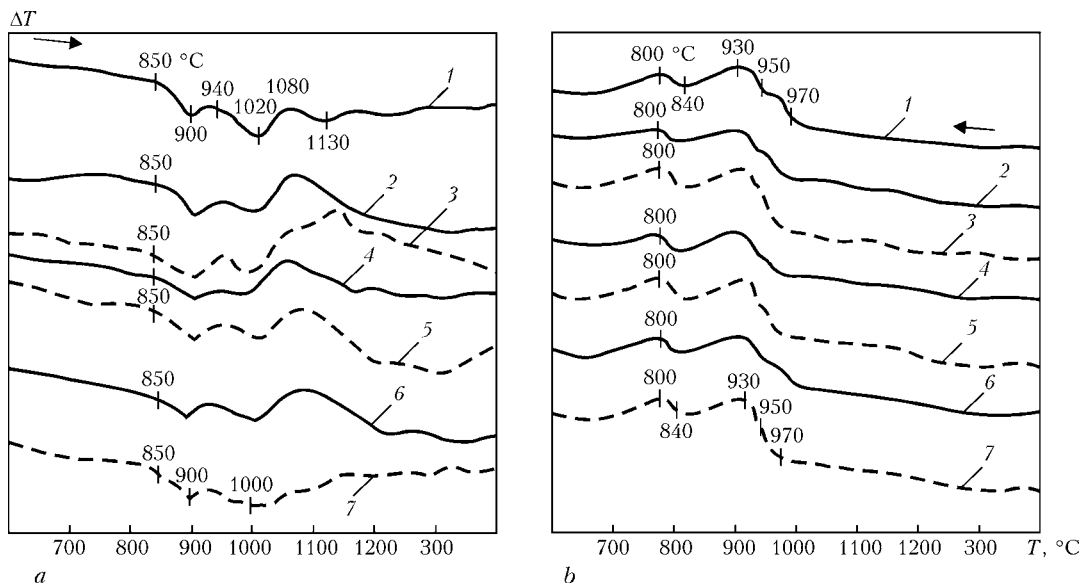


**Figure 6.** Differential thermal curves of heating (a) and cooling (b) of powders atomised in argon (solid curves) and high-pressure water (dashed curves) with particle more than 160 (1), 80-100 (2, 3), 63-80 (4), 40-63 (5) and less than 25 (6, 7)  $\mu\text{m}$  in size

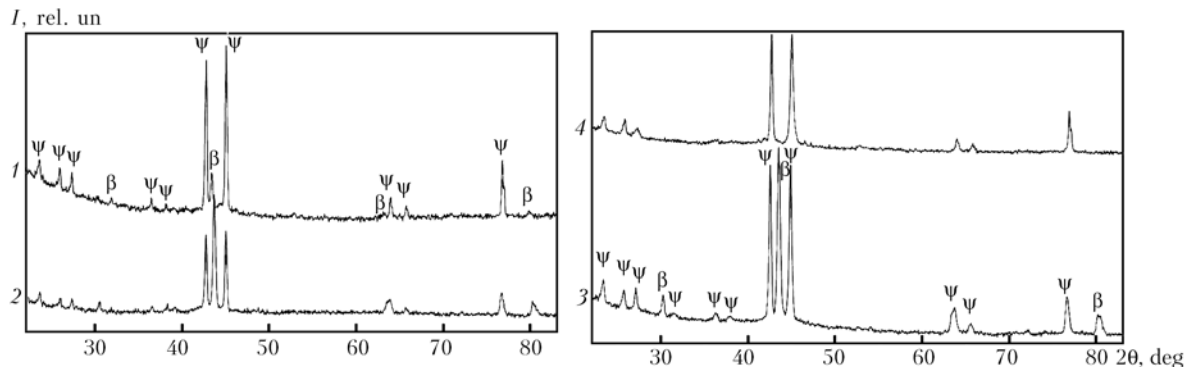


**Figure 7.** X-ray patterns of  $\text{Al}_{63}\text{Cu}_{25}\text{Fe}_{12}$  alloy powder with a particle size of 40–63  $\mu\text{m}$  produced by argon atomisation (1, 2) and high-pressure water atomisation (3, 4) before (1, 3) and after (2, 4) annealing in vacuum at 700 °C for 2 h

ing of the melt during solidification, which depends upon the type of an energy carrier and particle size composition. As to the order of decrease in the  $\psi$ -phase content of the powders of the same particle size, the methods used to produce them can be arranged as follows: high-pressure water atomisation --- compressed air atomisation --- argon atomisation --- granulation of the melt with free splitting of the jet followed by crushing of granules. With this arrangement, the rate of cooling of the droplets decreases from  $(0.5\text{--}5.0)\cdot 10^4$  (water atomisation) to 100 K/s (spontaneous disintegration of the jet) [10].

Because of decrease in the cooling rate, increase in size of the droplets results in a minimal content of the  $\psi$ -phase in atomised coarse powders. The content of this phase in the powders produced by crushing of granules is no more than 30 wt.%, and it does not depend upon the particle size composition.

**Behaviour of powders under DTA conditions.** DTA (heating and cooling at a rate of 80 K/min in helium) was carried out to reveal the sequence of phase transformations in heating of the powders. Investigations were conducted for the powders of different particle size composition produced by argon and high-pressure water atomisation. Analysis of thermograms (Figure 6) showed no fundamental differences in character of the differential thermal curves for the powders under investigations.

The heating curves (Figure 6, a) comprise two (for two-phase powders) or three (for three-phase coarse powders) endothermic effects, which are likely to be caused by melting of the  $\psi$ -phase at a temperature of 850–900 °C and a mixture of the  $\psi$ - and  $\beta$ -phases at 940–1020 °C. The third, weak endothermic effect (at 1080–1130 °C) is related to melting of the  $\lambda$ -phase. The process of solidification of alloys begins particularly from this effect [11]. The same sequence of phase transformations can be seen from the cooling curves (Figure 6, b), if we take into account that no full coincidence of temperature ranges for separate transformation stages occurs because of an inevitable overcooling of the melt during solidification.

**Effect of heat treatment on phase composition of Al–Cu–Fe system alloy powders.** It is a known fact that heat treatment can cause a change in phase composition of the Al–Cu–Fe system alloy powder to

increase its quasi-crystalline  $\psi$ -phase content. For example, as reported in study [10], to provide a single-phase (quasi-crystalline) composition of the powder produced by argon atomisation, it was subjected to annealing in vacuum at 700 °C for 2 h.

In this study the argon and high-pressure water atomised powders with a particle size of 40–63  $\mu\text{m}$  were treated by annealing at 700 °C for 2 h. In the first case (Figure 7, curves 1 and 2) the content of the  $\psi$ -phase increased from 45 to 87 wt.%, and in the second case the powders with a 53 wt.% of the  $\psi$ -phase transformed practically to the single-phase state (Figure 7, curves 3 and 4).

**Technological properties of Al–Cu–Fe system alloy powders.** Technological properties of argon and water atomised powders are given in Table 2. Flowability of the argon atomised powders improves with transition from coarse to fine particle sizes, and at a particle size of 40–63  $\mu\text{m}$  it reaches its maximal value. With finer particle sizes the flowability deteriorated because of the adhesion forces. Apparent density of the argon atomised powder continuously increased as the particles became finer. An irregular shape of particles of the powders produced by water atomisation results in their low flowability: powders with a particle size of 63–80  $\mu\text{m}$  and finer do not flow. Apparent density of the powders with particles of this shape is lower compared with that of the powders with particles of a spherical shape. A powder produced by crushing of granules does not flow when tested according to GOST 20899–75.

As shown by using the pycnometric method to measure density of a powder, the water atomised powders have the highest (about 19 %) internal porosity, internal porosity of the argon atomised powders is 2–6 %, depending upon the particle size, and that of the crushed powders is approximately 8.5 %.

## CONCLUSIONS

1. Methods used to produce powders of the Al–Cu–Fe system alloy have a substantial effect on shape of their particles, phase composition and technological properties. Moreover, in powders produced by atomisation of the melt the shape of the particles depends upon their size: the larger the diameter of a particle, the



larger the deviation of their shape from the spherical one (shape factor increases).

2. The content of the quasi-crystalline  $\psi$ -phase in powders is in direct relationship with the rate of cooling of the Al-Cu-Fe system melt in solidification, which depends upon the type of an energy carrier and particle size. Powders produced from the melts consist mostly of a mixture of two phases, i.e. quasi-crystalline  $\psi$ -phase and crystalline  $\beta$ -phase. Coarse particles contain the monoclinic  $\lambda$ -phase. Powders produced by high-pressure water atomisation have an increased content of the  $\psi$ -phase, compared with those atomised in gas (due to an increased solidification rate). Powders produced by crushing of ingots have mostly the four-phase composition ( $\lambda$ ,  $\beta$ ,  $\psi$ ,  $\theta$ ). Decrease in the  $\psi$ -phase content with increase in size of the particles holds true for all atomised powders.

3. Technological properties of the powders (flowability and apparent density) depend upon the size, shape and specific surface area of their particles. Particles of the powders produced by argon atomisation have the most perfect shape, close to the spherical one. They are characterised by higher values of flowability and apparent density, which grow with decrease in size of the particles.

4. Heat treatment of the Al<sub>63</sub>Cu<sub>25</sub>Fe<sub>12</sub> alloy powders, independently of the method used to produce them, leads to increase in their quasi-crystalline  $\psi$ -phase content. Annealing of the powders produced by atomisation and containing more than 53 wt.% of the  $\psi$ -phase at 700 °C for 2 h makes it possible to transform them into a single-phase quasi-crystalline structure.

*The authors are thankful for co-operation in manufacture of powders investigated in this study to Dr. O.D. Nejkov and leading engineer V.L. Rupchev. The authors are grateful to the Science and Technology Center in Ukraine for the financial support it rendered to Project 1630, under which the present study was performed.*

1. Adeeva, L.I., Borisova, A.L. (2002) Quasi-crystalline alloys as a new promising material for protective coatings. *Fizyka i Khimiya Tv. Tila*, 3(3), 454–465.
2. Prevarsky, A.P. (1971) Study of Fe-Cu-Al system. *Izvestiya AN SSSR*, 4, 220–222.
3. Gratias, D., Calvayrac, Y., Devand-Rzepski, J. et al. (1993) The phase diagram and structures of ternary Al-Cu-Fe system in vicinity of the icosahedral region. *J. Non-Crystalline Solids*, 153/154, 482–488.
4. Noskova, N.I., Ponomareva, V.G., Yartsev, S.V. et al. (1995) Quasi-crystalline phases in Al-Mn and Al-Cu-Fe alloys. *Fizika Metallov i Metallovedenie*, 79(2), 80–86.
5. Dubois, J.-M. (2000) New prospects for potential applications of quasicrystalline materials. *J. Mater. Sci. and Eng.*, 294–296, 4–9.
6. Sordelet, D.J., Kramer, M.J., Unai, O. (1995) Effect of starting powders on the control of microstructural development of Al-Cu-Fe quasicrystalline plasma-sprayed coatings. *J. Thermal Spray Technol.*, 4(3), 235–244.
7. Sordelet, D.J., Besser, M.F., Anderson, I.E. (1996) Particle size effects on chemistry and structure of Al-Cu-Fe quasicrystalline coatings. *Ibid.*, 5(2), 161–174.
8. Sordelet, D.J., Kim, J.S., Besser, M.F. (1999) Dry sliding of polygrained quasicrystalline and crystalline Al-Cu-Fe alloys. In: *Proc. of the Mater. Res. Soc. Symp. on Quasicrystals* (Warrendale), 553, 459–471.
9. Shield, J.E., Goldman, A.I., Anderson, I.E. et al. *Method of making quasicrystal alloy powder, protective coatings and articles*. Pat. 5433978 USA. Int. Cl. B 22 F 9/08. Publ. 18.07.95.
10. Borisov, Yu.S., Panko, M.T., Adeeva, L.I. et al. (2001) Technologies for production and properties of powders of the Al-Cu-Fe system for thermal spraying of coatings with quasi-crystalline structure. *The Paton Welding J.*, 1, 45–50.
11. Nabojchenko, S.S., Nichiporenko, O.S., Murashova, I.B. (1997) *Powders of non-ferrous metals*: Refer. Book. Moscow: Metallurgiya.
12. Neikov, O.D., Vasilieva, G.I., Kalinkin, V.G. et al. *Method for production of aluminium and aluminium alloy powders*. Pat. 9505 USA. Publ. 30.09.96.
13. Neikov, O.D., Krajnikov, A.V., Sameljuk, A.V. et al. (2002) An experimental study of water atomization of aluminium alloys. In: *Proc. of World Congress Compiled by Metal Powder Industrial Federation* (Princeton, USA, 2002), 7, 15–27.
14. Dubois, J.-M., Piranelli, A. *Aluminum alloys, substrates coated with these alloys and their applications*. Pat. 5652877 USA. Int. Cl. B 22 F 7/04. Publ. 11.07.95.
15. Giacometti, E., Guyot, P., Baluc, N. et al. (2001) Plastic behavior of icosahedral Al-Cu-Fe quasicrystals: experiment and modeling. *J. Mater. Sci. and Eng.*, 312–332, 429–433.
16. Kang, S.S., Dubois, J.-M. (1992) Compression testing of quasicrystalline materials. *Philosophical Mag.*, 1, 151–163.
17. Sanchez, A., Garcia de Blas, F.J., Algaba, J.M. et al. (1999) Application of quasicrystalline materials as thermal barriers in aeronautics and future perspectives of use for these materials. In: *Proc. of the Mater. Res. Soc. Symp. on Quasicrystals* (Warrendale), 553, 447–458.
18. Michot, G. (1996) Production of icosahedral Al-Cu-Fe powders by centrifugal atomization method. In: *Proc. of 5th Int. Conf. on Quasicrystals* (Singapore, May 22–26, 1995). Singapore: World Scientific, 794–797.
19. Nicula, R., Jianu, A., Grigoriu, C. et al. (2000) Laser ablation synthesis of Al-based icosahedral powders. *J. Mater. Sci. and Eng.*, 294–296, 86–89.
20. Barua, P., Murty, B., Srinivas, V. (2001) Mechanical alloying of Al-Cu-Fe elemental powders. *Ibid.*, 304–306, 863–866.
21. Salimon, A.I., Korsunsky, A.M., Shelekhov, E.V. et al. (2001) Crystallochemical aspects of solid state reactions in mechanically alloyed Al-Cu-Fe quasicrystalline powders. *Acta Mater.*, 49, 1821–1833.
22. Sordelet, D.J., Besser, M.F., Kramer, M.J. (1998) Thermal spray quasicrystalline coatings among processing, phase structure and splot morphology. In: *Proc. of 15th Int. Conf. on Thermal Spray Technol.* (Nice, France, May 25–29, 1998), 1, 467–472.
23. Nichiporenko, O.S., Najda, Yu.I., Medvedovsky, A.B. (1980) *Atomised metal powders*. Kiev: Naukova Dumka.
24. Grigorenko, G.M., Borisova, A.L., Kalinyuk, N.N. et al. (1990) Study of gas content of powders and sprayed coatings of nickel self-fluxing alloys. *Avtomatich. Svarka*, 2, 40–44.

# TECHNOLOGY OF EBW OF THE STAINLESS STEEL--ALUMINIUM ALLOY WELDED JOINTS

A.A. BONDAREV and A.Ya. ISHCENKO

E.O. Paton Electric Welding Institute, NASU, Kiev, Ukraine

A fundamentally new technology of electron beam welding of dissimilar joints of stainless steel–aluminium alloy in the form of tubular elements has been developed. The technology allows eliminating the application of interlayers of pure aluminium between the metals, which prevents formation of intermetallics in the joints and provides a high level of mechanical properties of the joints.

*Keywords:* electron beam welding, nanostructured materials, welding, aluminium alloys, dissimilar materials, vapour phase condensation

Over the recent years a lot of attention has been given to studying the weldability of new promising materials, in particular, nanostructured materials. A large number of nanotechnologies (for instance, deposition of ultradisperse metal coatings from the vapour phase) have now been developed and are used to produce such materials.

It is known that in welding of metals with limited mutual solubility, to which aluminium and stainless steel belong, it is practically impossible to prevent formation of intermetallic new phases, which are characterized by a high hardness and brittleness on their interface. In addition, the surface of stainless steel and aluminium is covered by stable oxides, which also prevent wetting or mixing of the materials being welded during welding.

The problem of reliable joining of such two materials as aluminium or aluminium alloy and stainless steel, can be successfully solved, if it is possible to avoid formation of brittle intermetallic interlayers, provide good wetting of the stainless steel surface by liquid aluminium, on the interface of these metals, and achieve joint strength on the level of mechanical properties of aluminium alloy welded joints.

It should be noted that a great number of processes of welding aluminium to steel have already been developed, which are based on the following engineering solution: joining of these materials occurs in the solid phase as, for instance, in pressure welding, having several varieties. The main of them are diffusion, friction, wedge-press and magnetic-pulse welding, etc. With all these processes welding is performed on a limited surface of part contact, and the billets are of a specific shape. Fusion welding is mainly used for joining tubular elements. To ensure normal wetting of steel by aluminium, a film of aluminium or zinc-aluminium is applied on the surface of item edges.

As a rule, the interlayer is applied at the temperature above 660 °C, when aluminium is in the liquid state. Only pure aluminium is used, and this means that the mechanical properties of the joints of any

aluminium alloy will be on the level of those of pure aluminium --- 60–90 MPa. However, it is not possible to avoid formation of intermetallic interlayers, if the aluminizing process runs for several seconds and is repeated already during welding. Figure 1 gives the temperature-time dependence of intermetallics formation in the bimetal. As in surface melting of an item from aluminium alloy the pool temperature is by 100–150 °C higher than that of melting of the alloys,  $T_{melt}$ , formation of brittle interlayers cannot be avoided.

To solve this problem a number of studies were conducted, which were aimed at selection of materials, in which intermetallics would not form at contact with liquid aluminium, and if they do form, they would go into the solid solution at contact with liquid aluminium.

In this case the main attention was focused on application of stainless steel interlayers with such elements, which can go into the solid solution at contact with the aluminium melt. To ensure a fast running of this process, interlayers from modifiers in the nanostructured condition were used, which were applied onto the stainless steel surface by vacuum deposition from the vapour phase.

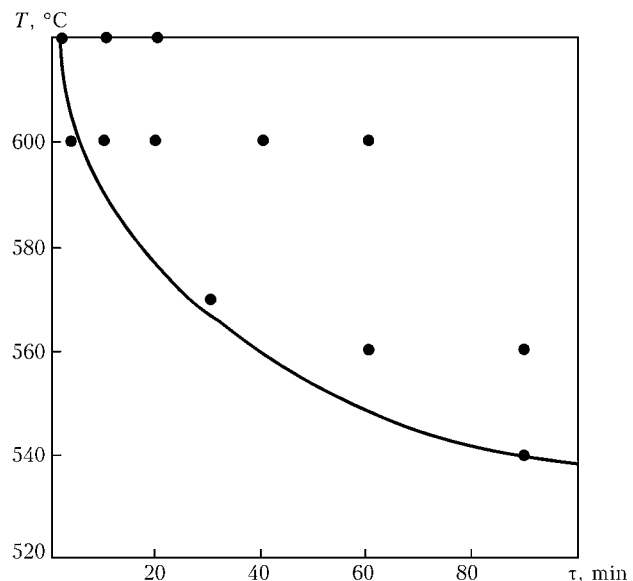
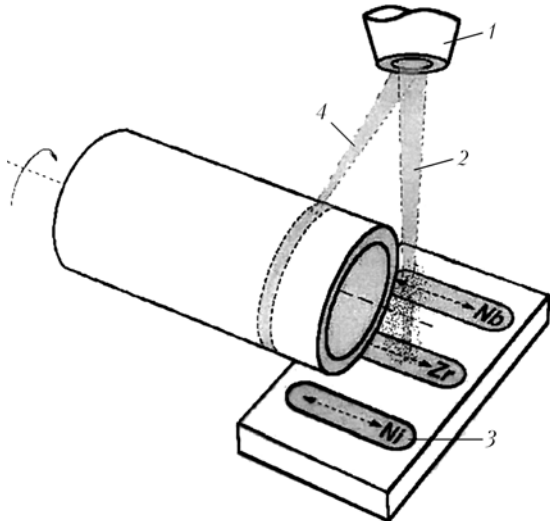


Figure 1. Temperature-time dependence of formation of intermetallics (dots) in the Armco-iron-AD0 aluminium bimetal



**Figure 2.** Technological sequence of applying on the surface of a stainless steel pipe intermediate interlayers of modifiers from the vapour phase in vacuum: 1 — electron beam gun; 2 — melting and evaporation of deposited metals; 3 — pool for metal melting and evaporation; 4 — pipe preheating

Investigation results showed that some of the elements of groups IV and V react with aluminium by an eutectic reaction. And although the solubility of the other material in aluminium is low (for instance, zirconium — 0.28 wt.%; nickel — 0.05 wt.%),  $NiAl_3$  and  $ZrAl_3$  compounds are in equilibrium with aluminium, and the metals proper, acting as modifiers, strengthen the solid solution. In view of the above, the authors developed the technology of application of interlayers of these elements on the surface of stainless steel items. It was taken into account that the temperature of the nonvariant transformations of  $NiAl_3$  and  $ZrAl_3$  phases is equal to 640 and 660 °C, which corresponds to aluminium melting temperature.

Electron beam technology of metal evaporation in vacuum with subsequent condensation opens up wide possibilities for producing super thin interlayers with a high level of physico-mechanical properties. It is established that the main parameter influencing the

mechanical properties of the joints, is the thickness of the interlayer, which should be equal to 1–3  $\mu m$ . Interlayers of such a thickness are the most suitable for welding by the new technology, as the time of producing them in a welding unit is equal to 3–5 min. Technique and technology of evaporation of the above metals are developed so that during melting the billet of the stainless steel branchpipe was above the pool of the molten metal and was simultaneously rotating for uniform deposition of the condensate both on the inner and outer surface of the edge to be welded (Figure 2).

To ensure a reliable adhesion of the condensates to the matrix material of the target, it is necessary for its temperature during condensation to be not less than  $0.5 T_{melt}$  of condensed metal.

In this connection, the process of producing interlayers from stainless steel was performed as the following sequence. First the tubular sample fastened with thermally-insulated transition pieces in a chuck was preheated by a defocused beam up to a temperature not lower than 850 °C. After achievement of the required temperature, the electron beam was guided to the surface of graphite pool, which contained one of the evaporation metals. The nickel and zirconium melting rate rose with increase of the electron beam power. The liquid metal pool was kept under the preheated branchpipe for 3–5 min. The rarefaction in the chamber was equal to  $1.33 \cdot 10^{-2}$  Pa, which ensured the necessary vapour flow and its condensation on the steel surface in 3–5  $\mu m$  thick layer.

Tubular stainless steel billets of 40 and 55 mm diameter and of AMg6 alloys of 45 and 58 mm diameter were prepared for welding in keeping with the developed technique and technology of welding dissimilar materials. Figure 3 gives two types of the studied butt joints of tubular transition pieces from dissimilar materials. In both the cases, the tube from AMg6 alloy was moved over the stainless steel tube. This is required so that melting of the aluminium, and not the steel tube, occurred in welding. Before the start of the process of butt welding (Figure 4), preheating of the stainless steel billet by a defocused beam up to the temperature of 500–550 °C should be performed. The liquid melt of the aluminium alloy wets the surface of the stainless steel tube, on the edges of which the nickel and zirconium interlayer has been applied.

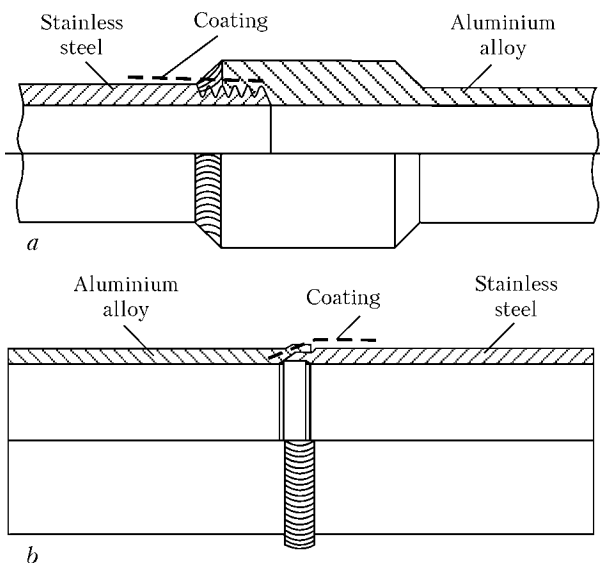


**Figure 3.** Types of welded joints of tubular transition pieces from dissimilar materials of stainless steel–aluminium alloy

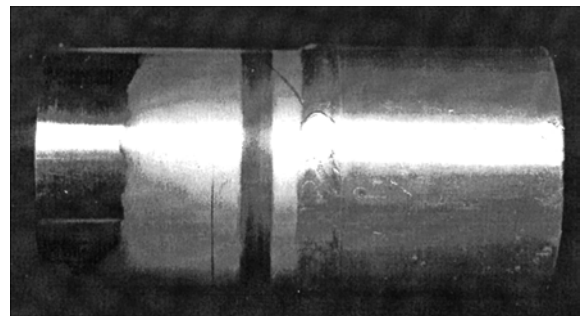


**Figure 4.** Appearance of a welded tubular transition piece of 60 mm diameter of stainless steel–aluminium alloy



**Figure 5.** Macrosection of welded joints from dissimilar materials of stainless steel-aluminium alloy AMg6 produced by the schematic given in Figure 3: *a* — billet assembled with an overlap; *b* — billet before welding assembled using thread

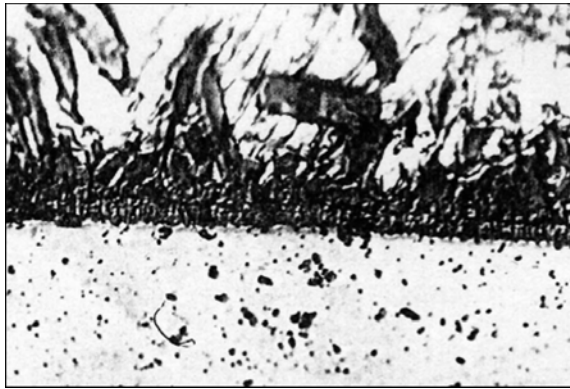


**Figure 6.** Microstructure of a welded joint of steel 10Kh18N10T and aluminium alloy AK5 produced by electron beam welding ( $\times 500$ )

Transverse sections were prepared for metallographic examination (Figure 5), from which it is seen that a good wetting of the stainless steel item with liquid aluminium has been achieved in welding.

Figure 6 gives the microstructure of the joint of stainless steel with aluminium alloy AK5 made by EBW in vacuum. In the presence of a nickel and zirconium interlayer 5  $\mu\text{m}$  thick on the interphase, the intermetallics are absent. A stronger etching out of the interlayer, which is an aluminium and nickel eutectic, is observed. No defects are found in the joint. A metal bond without defects is found between the stainless steel and applied interlayer, as well as formation of the crystalline structure with the dendrite cell size of up to 1–3  $\mu\text{m}$ .

Element distribution in the joint can be another confirmation of the results of microstructural analysis (Figure 7). The interlayer contains up to 20 wt.% Ni, this lowering the brittleness of the transition zone metal, and giving it the necessary ductility and strength.

Mechanical testing confirmed the reliability of the new technology, which ensures the strength of specimens from dissimilar materials of stainless steel-aluminium alloys AMg6 and 1201 on the strength level of aluminium joints of 290–330 MPa. Fracture of dis-

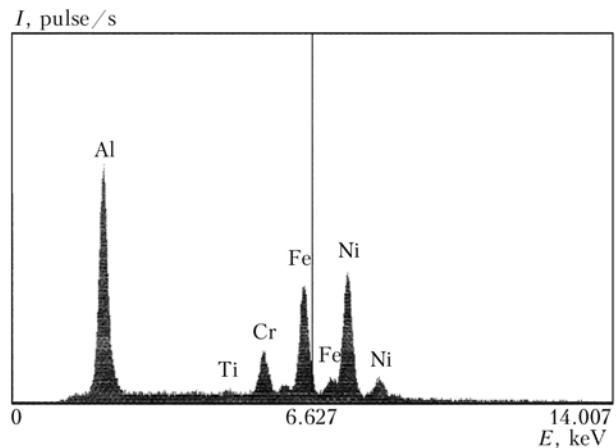


**Figure 7.** Distribution of alloying elements in the metal of the joint of dissimilar materials of stainless steel-aluminium and qualitative pattern of the composition of the welded joint transition zone (see Figure 6): *I* — intensity; *E* — accelerating voltage

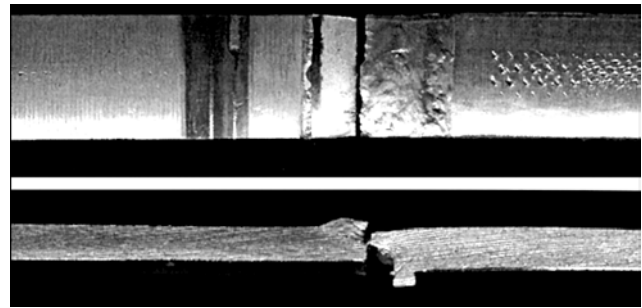


**Figure 8.** Appearance of samples of joints of dissimilar materials of stainless steel-aluminium alloy AMg6 after mechanical rupture testing

similar material samples (Figure 8) always ran in the weld metal without delamination from stainless steel.

Conducted research enabled optimization of the process parameters, and elaboration of recommendations for industrial production of items from dissimilar materials. The Table gives the main parameters of the process of EBW of transition pieces of two typesizes.

Proceeding from the results of metallographic examinations and mechanical testing of joints of dissimilar materials of stainless steel-aluminium alloy, a fundamentally new technology of joining the above materials has been developed, the application of which prevents formation of brittle intermetallic interlayers between them, impairing the mechanical and ductile properties of the produced joints.

Proceeding from the above, it is possible to define the main technological requirements to manufacture of tubular transition pieces applied in cryogenic systems. The main operations are performed in such a sequence: preparation of the item surface before depo-

Parameters of welding tubular transition pieces (stainless steel-aluminium alloys AMg6)

Billet diameter, mm	Edge thickness, mm	Accelerating voltage, kV	Welding current, mA	Welding speed, m/h	Scanned diameter, mm	Ratio of beam dwell time
58	5	30	60	30	5	8 (Al):1 (SS)
45	4	30	40	30	5	8 (Al):1 (SS)

Note. Temperature of preheating the stainless steel (SS) billet is 450–500 °C.



sition of intermediate interlayers of modifiers (degreasing and mechanical removal of oxides on the welded edges; application of intermediate interlayers from nickel and zirconium on the stainless steel surface from the vapour phase at metal evaporation by the electron beam in vacuum); temperature of stainless steel preheating should be not less than  $0.5T_{\text{melt}}$ ; assembly of the elements of the transition piece into one component and its mounting in the manipulator of the welding machine vacuum chamber; preheating of the stainless steel billet by a defocused beam up to the temperature of 450–550 °C; guiding the electron beam to the aluminium alloy edges and its melting using a beam scanner (direct hitting of stainless steel by the electron beam is inadmissible); item cooling

after welding in vacuum and its removal from the manipulator; performance of control operations to determine the welded joint quality and tightness.

Thus, based on the use of nanotechnologies and materials, a fundamentally new method was developed for welding dissimilar materials of stainless steel–aluminium alloys, which does not have any analogs in the world and allows producing welded joints with the strength on the level of mechanical properties of joints of aluminium alloys. Their application in production will offer significant advantages over the traditional structural materials both in terms of improvement of mechanical and technological properties, and provision of the reliability and performance of items from these materials in service.

## ANTICORROSION PROTECTION OF BASE METAL STRUCTURES BY METALLISED COATINGS (REVIEW)

A.P. MURASHOV, I.A. DEMIANOV, Yu.S. BORISOV, M.L. ZHADKEVICH and V.F. GOLNIK  
E.O. Paton Electric Welding Institute, NASU, Kiev, Ukraine

The review considers the advantages and objects of application of metallised coatings of zinc, aluminium and their alloys. Selection of coating material should be based on service conditions of metal structures and electrochemical mechanism of their protection. Improvement of protective properties of the facilities is provided through application of composite metal polymeric coatings.

*Keywords:* thermal spraying, metal structures, aggressive medium, corrosion, corrosion potential, thermal metallised coatings, painting

Metal corrosion is one of the most widely spread kinds of structure failure. Large-sized items can have considerable corrosion damage, the development of which is promoted by presence of different welded joints, rivets, pockets, etc. Periodical renewal and restoration of anticorrosion protection of metal-polymer coatings is required to avoid the risk of failure of facilities in long-term service as a result of corrosion damage.

Due to their high reliability and fatigue life thermal metallisation coatings take up a special place among the currently existing methods of anticorrosion

protection. These coatings are used for corrosion protection of metal structures in high-speed motorways, bridges, tanks and other facilities of different purpose under the impact of production environment, sea water or mist, alkaline and acid medium, etc. Anticorrosion protection using metallised coatings is widely used in the USA, Japan, UK, Norway and other countries (Figure 1 and 2) [1]. This type of coatings not only protect the surface by creating a barrier to penetration and action of the aggressive medium, but also provide electrochemical protection of the base due to negative electrochemical potential of the coating material relative to that of the structure material.



**Figure 1.** Overpass in Japan with aluminium metallised coating painted with acryl paint in two layers (coating service life is more than 25 years)



**Figure 2.** Bridge across a strait in Japan with zinc metallised coating 90 µm thick with applied four paint coats (service life is more than 25 years)

**Table 1.** Corrosion rate (g/(m<sup>2</sup>·h)) of steel without coating and with metallised coatings in different corroding media

Corroding medium	Steel grade	Uncoated	Coating material		
			Zn	Al-7 % Zn	Al
Synthetic sea water	12KhN3MA	0.0630	0.0079	0.0068	0.0021
	45G17Yu3	0.0573	0.0092	0.0078	0.0026
	10KhSND	0.0652	0.0082	0.0074	0.0028
Salt mist	12KhN3MA	0.2963	0.0117	0.0097	0.0032
	45G17Yu3	0.4826	0.0124	0.0112	0.0035
	10KhSND	0.4474	0.0123	0.0115	0.0037

Cost of metallised coatings is 2–3 times higher than that of painting. Under the conditions of operation of large-sized facilities, however, the operating costs for lacquer-paint coatings, in view of their low reliability and short service life, are much higher than those for spray-deposited coatings. By the data of the American Welding Society, the cost of metallization coatings after 5–10 years of service is lower than that of the lacquer-paint coatings due to the high fatigue life of metallised coating and lower operating costs [1].

Arc metallization and flame spraying of coatings are widely used for deposition of anticorrosion coatings. This is associated with their relative simplicity, mobility of the processes and high efficiency, as well as the ability to produce coatings with high strength properties and density.

The most widely spread materials for anticorrosion coatings are zinc, aluminium and their alloys. Selection of coating material depends on the degree of aggressiveness of the operating medium. Coating effectiveness is determined by the difference between the electrochemical potentials of the coating and base materials in the operating medium, properties of corrosion products and the associated rate of the corrosion process.

The data of a number of foreign companies, as well as results of investigations conducted at the E.O. Paton Electric Welding Institute, demonstrated the high corrosion resistance of the coatings in a production environment, as well as in the medium of chlorine,

**Table 2.** Coating influence on structural steel resistance (time to fracture, h) to cracking in different aggressive media

Sample	Steel grade (corroding medium)		
	12KhN3MA (synthetic sea water at $T = 35\text{ }^{\circ}\text{C}$ )	45G17Yu3 (salt mist at $T = 27\text{ }^{\circ}\text{C}$ )	Kh18N10T (partial immersion in NaCl solution at $T = 150\text{ }^{\circ}\text{C}$ )
Uncoated	817	796	57
With aluminium coating	10750	7200	500

Note. Samples with aluminium coating did not fail.

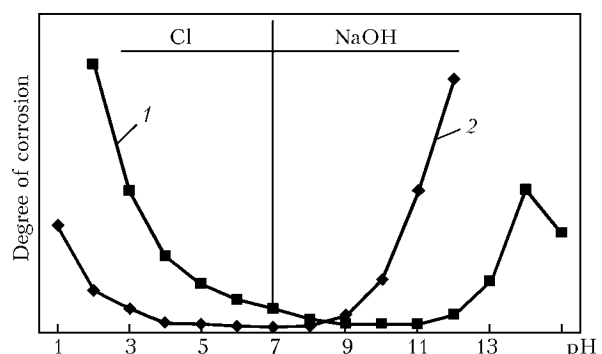
SO<sub>2</sub>, alkali and acid, in salt mist, sea and fresh water, etc.

Figure 3 shows the change of the degree of corrosion damage of zinc and aluminium coatings, depending on the medium acidity pH [2].

Zinc coatings on steel have rather high resistance at pH 5–12, but fail quickly at pH 1.0–3.5 or 13–14. Their corrosion resistance is determined by formation of thin dense films of zinc oxide and its insoluble salts on the coating surface in air. In fresh and sea water corrosion also leads to formation of insoluble compounds of ZnO, Zn<sub>5</sub>(CO<sub>3</sub>)<sub>2</sub>(OH)<sub>6</sub>, 4ZnO·CO<sub>2</sub>·4H<sub>2</sub>O, which results in the corrosion process running at a low constant rate, and the coating life can be assessed with sufficient accuracy.

Aluminium coatings are resistant in a medium with pH 2–10, but fail quickly at pH > 10. Corrosion results in formation of a dense oxide film on the coating surface, which protects it, and filling the pores, makes the coating denser, thus preventing the penetration of the aggressive medium inside. Presence of aluminium oxide in the coating lowers the negative values of aluminium corrosion potential. This to a certain extent impairs the anticorrosion properties of aluminium, which is the anode relative to steel. However, the protective properties of the coating are improved due to reduction of its porosity and corrosion rate. Unlike zinc coating, the process of aluminium coating corrosion runs nonuniformly.

Testing coatings from Zn–13 % Al, Al–(7, 11 %)Zn, Al–(5–6, 10–11 %)Si, Al–5 % Mg alloys in different media showed that their electrochemical potential and anticorrosion properties change due to the second component. Presence of a small amount of

**Figure 3.** Dependence of the degree of corrosion damage of zinc (1) and aluminium (2) coatings on acidity of the corroding medium

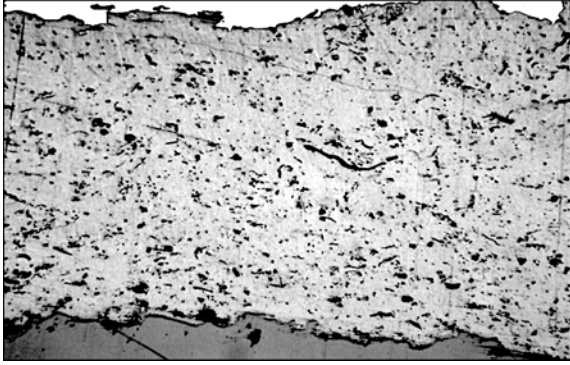


**Figure 4.** Microstructure of AK5 aluminium alloy coating made by arc metallisation at particle velocity of 59 m/s ( $\times 200$ )

aluminium in a zinc-based coating improves its resistance to acid medium and sea water [3].

Given below are the values of corrosion potential of coatings from different materials in 3.5 % water solution of NaCl [3]:

Al .....	-1.2000
Zn-13 % Al .....	-1.0504
Zn .....	-1.0457
Al-1 % Si .....	-0.8740
Al-11 % Si .....	-0.8220
Al-3 % Mg .....	-0.8657
Al-5 % Mg .....	-0.8740
Al-7 % Mg .....	-0.8846
Steel .....	-0.5830

Coating from Al-7 % Zn alloy has higher protective properties in the salt mist than a pure zinc coating, being, however, inferior to pure aluminium coating (Table 1) [4].

Application of metallised coatings for protection of welded metal structures lowers the hazardous corrosion cracking of welds. Corrosion cracking testing of loop samples in synthetic sea water, as well as salt mist, showed that aluminium metallisation increases the time to fracture of samples in the first case by 13 times, and in the second --- more than 8 times compared to uncoated samples (Table 2) [4].

Testing Al-5 % Mg alloy coating in sea mist showed that its corrosion resistance is higher than that of the aluminium coating. Results of coating analysis indicate that corrosion products in the form of aluminium and magnesium oxides formed on its surface, strongly adhering to it [5].

When anticorrosion coatings are used, the degree of protection of their surface is determined not only by the sprayed material, but also by its thickness, as well as spraying process. This is attributed to the structure of spray-deposited coating, in particular, presence of pores in it, including through-thickness pores, thus allowing the aggressive medium to penetrate to the coating-base interface.

Analysis conducted at the E.O. Paton Electric Welding Institute showed that they are characterized by a higher density compared to flame coatings produced from powders. This is related to the fact that metallised coatings are made up by completely melted particles, formed at wire melting and spraying (Figure 4). In flame powder spraying, coatings form from particles heated to different degrees, including partially melted ones. In this connection, impenetrability of metallised coatings made from wires, is achieved at their thickness smaller than that of powder coatings. This difference is approximately equal to 30-50 % and is determined by the conditions of coating deposition. Porosity of coatings from aluminium alloy AK5 deposited by arc or flame (using wires) and flame (using powders) processes differed on average by approximately 3-4 %.

The above features determine selection of the protective coating thickness, depending on the operating conditions of the facilities. According to standards of several countries, the thickness of zinc coating should be 70-160  $\mu\text{m}$ , and that of aluminium --- 200-250  $\mu\text{m}$  (SNiP 2.03.11-85, GOST 9.304-87, GOST 28302-89; European standards EN 1461/14713 and EN 22063, British standard BS EN 2206 ISO 2063, international

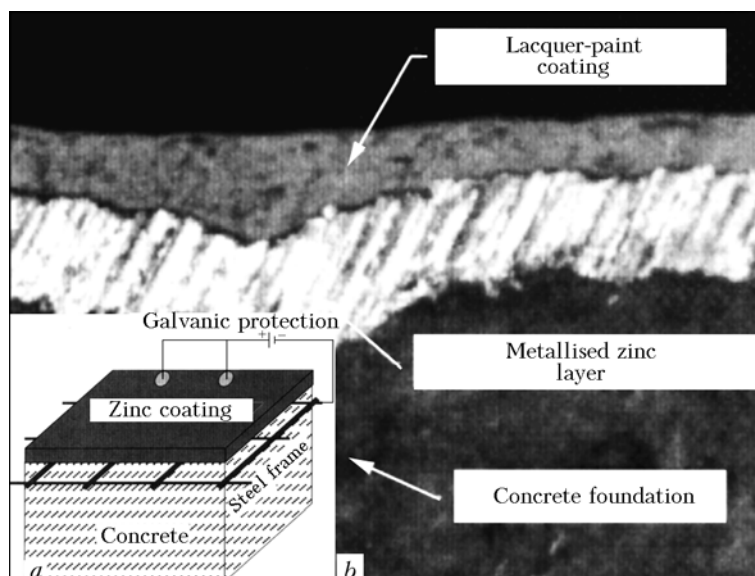


**Figure 5.** Microstructure of metallised zinc coating on concrete (a) and system of galvanic protection using this coating (b) ( $\times 200$ )



standard ISO 2063, etc.), and a smaller thickness is specified for arc coatings.

Surface roughness characteristic for metallised coatings, is equal to  $R_z = 10\text{--}40\ \mu\text{m}$ , this allowing deposition of any lacquer-paint coatings on it. Two purposes are achieved in this case: a decorative colour is obtained and coating is made more compact due to its impregnation. In such a combined coating due to the impregnation material filling the unevenness of its surface, as well as pores and microcracks, a significant increase of anticorrosion properties is observed, which is preserved for 30–50 years. This is achieved due to a combined action of coating elements: metallised coating provides corrosion protection and strong adhesion to the base, and the impregnation corrosion-resistant material, being inside and outside the coating, creates a barrier for this corrosion medium and thus further increases the protective properties. The above effect changes the ideology of application of anticorrosion coatings. For a number of facilities (bridges through sea straits, overpasses, etc.) thin coatings are used with success (for instance, from zinc  $70\ \mu\text{m}$  instead of  $150\text{--}160\ \mu\text{m}$  thick) with subsequent painting by lacquer-paint materials in several layers [6, 7], this allowing high-quality coatings to be produced at lower cost of anticorrosion layer application.

It is noted [6, 7] that the adhesion of impregnation material to coating surface and its resistance are much higher than these parameters for the same material, but which was just painted without the coating. This is achieved due to a strong bond of the painting material with the developed surface of metallised coating and absence of macro- or microdefects in it. Materials based on silicon-organic lacquers, epoxy compositions, polyurethane, acryl paints, etc. are widely used for impregnation.

Investigations of composite metal-polymer coatings conducted in several countries showed a 2–5 times increase of their protective properties, compared to metallised coatings without impregnation [6, 8]. For structures with aluminium-based coatings, used in fresh or sea water, it is recommended to perform painting based on silicon-polymer or polyurethane compositions.

Producing a metallised zinc coating on concrete or reinforced concrete structures is effective (Figure 5, b) [7]. Such a coating is characterized by high anti-corrosion properties under the conditions of increased humidity and prevents moisture penetration into con-

crete, thus reducing the risk of electrochemical processes initiation in concrete pores, and r-bars, and increasing the concrete resistance to temperature gradients. In addition, presence of a zinc coating on reinforced concrete allows applying a system of galvanic protection of the facility by creating an electrically closed circuit and applying negative voltage to it (Figure 5, a).

## CONCLUSIONS

1. For long-term protection of steel metal structures it is rational to apply metallised coatings from zinc, aluminium or their alloys.

2. Thermal or metallisation anticorrosion coatings provide protection of the metal structure surface due to electrochemical mechanism, as well as creating a barrier to penetration and impact of the aggressive medium.

3. Application of composite metal-polymer coatings provides a more reliable protection of facilities, the effectiveness of which increases several times compared to that of metallised coatings, thus allowing thinner coatings to be made.

1. Wixson, M.S. (1993) Arc sprayed zinc coatings for cathodic protection of steel rebar in concrete. In: *Proc. of National Thermal Spray Conf.* (Anaheim, USA, June 7–11, 1993), 673–678.
2. Hasui, A. (1969) *Procedure of spraying*. Moscow: Mashinostroenie.
3. Ueno, G., Nawa, Y.L. (1998) Coating protection against atmospheric corrosion for iron and steel structural components. Status of metallization in Japan. In: *Proc. of 1st United Thermal Spray Conf. on Scientific and Technological Advances* (Indianapolis, USA, Sept. 15–18, 1977). Material Park: ASM Int., 191–197.
4. Orlov, L.P., Katkov, I.N. (1987) Metallised and combined coatings as an effective means of steel product protection from corrosion damages. In: *Protective coatings in machine-building*. Kiev: Naukova Dumka.
5. Ishikawa, K., Seki, M., Tobe, S. (1993) Application of thermal spray coatings to prevent corrosion of construction in Japan. In: *Proc. of National Thermal Spray Conf.* (Anaheim, USA, June 7–11, 1993), 679–684.
6. Tobe, S. (1998) A review on protection from corrosion, oxidation and hot corrosion by thermal spray coatings. In: *Proc. of 15th Int. Thermal Spray Conf. on Challenges of the 21st Century* (Nice, France, May 25–29, 1998). Material Park: ASM Int., 3–11.
7. Knepper, M., Melzer, A. (2002) Wire arc spraying of zinc as effective method to produce anodes for the corrosion protection of reinforced concrete structures. In: *Proc. of Int. Thermal Spray Conf.* (Essen, Germany, March 4–6, 2002), 27–31.
8. Grasme, D. (1993) Thermal sprayed aluminium coatings made of galvanic effective aluminium alloys for corrosion protection of steel and aluminium materials and maritime atmosphere. In: *Proc. of Thermal Spraying Conf.* (Aachen, Germany, 1993). Duesseldorf, 188–191.



## PROBLEMS OF WELDERS' LABOUR SAFETY

O.G. LEVCHENKO and A.O. PAVLYK

E.O. Paton Electric Welding Institute, NASU, Kiev, Ukraine

It is shown that the cause of occupational morbidity of welders is the unsatisfactory condition of ambient air in welding workshops. It is noted that the inefficient protection of respiratory organs of welders is caused by an incorrect choice and utilization of the means for protection of respiratory organs. Ways are outlined for formation of the information system to make an optimal decision on selection of the ventilation and individual protection means to match the actual labour conditions.

*Keywords: welding, labour protection, occupational morbidity, harmful substances, ventilation systems, individual protection means for respiratory organs, information systems*

By the data of «Goskomstat» of Ukraine, each fourth welder works under the conditions that do not correspond to sanitary standards and regulations. More than UAH 900 mln are paid annually to the workers as benefits and compensations for the work in harmful conditions that essentially influences the cost and competitive ability of the commodity output.

Profession of a welder still remains to be one of the most professionally dangerous. Combined influence of harmful industrial factors of chemical (welding aerosols, gases) and physical (arc radiation, thermal and physical loads and so on) nature promote development of occupational and production-conditioned pathology.

Systems of general ventilation by dilution that are available in industrial workshops as a rule do not supply the air of required purity. Welders who perform manual and mechanized welding, surfacing and cutting at non-stationary work places that are not equipped with local ventilation (the latter is typical for construction, shipbuilding and other branches) are in the most unfavorable conditions. Concentrations of harmful substances in the welder's breathing zone in these cases are much higher than the TLVs. The levels of the worker exposure to harmful substances can be even higher when highly productive flux-cored wires are used, as well as when welding high alloy steels and cast iron by electrodes containing chromium, nickel and copper. The concentration of toxic agents is by an order of magnitude higher in the case when welding is done in insufficiently well-ventilated vessels, chambers, tanks and so on. Workers of welding professions also suffer from considerable static loads, they are subjected to the influence of optic radiation (ultraviolet, visible and heat), sparks and spatter of metal and slag.

Considering the great diversity of welding consumables and types of welding technologies, the task of correct selection of protection means takes on special significance as, in accordance with the physicians' information, the number of professional diseases of respiratory organs has considerably increased lately. Concern over this issue has grown into a problem on the international level. In this connection, great attention is paid to the matters of impact of harmful industrial factors on the state of welders' health, as well as on the means that reduce their impact.

The state of labour protection leaves much to be desired in the majority of industrial enterprises of small and medium businesses, that is associated with the following main factors: performing of the work with gross violation of rules, norms and instructions on labour safety; discrepancy between the labour conditions, technologies, equipment, mechanisms and the demands of standards, sanitary norms and rules; malfunction or disuse of individual protection means by workers.

State policy in the sphere of labour safety is directed to securing the citizens' constitutional right to safe and healthy labour conditions. In the Decree of the President of Ukraine dated July 13, 2001 No. 515/2001 «About Urgent Measures on Prevention of Occupational Traumatism and Professional Diseases» it is stated that ensuring safe and harmless labour conditions at the enterprises, in organizations regardless of the forms of property and types of activity, in order to avoid occupational traumatism and professional diseases, is one of the most important directions of realization of the state social policy, which should take the following demands into account: the priority of life and health preservation of workers in the process of production activity; complete responsibility of employers for creation of safe and harmless working conditions.

At present labour safety becomes one of the priority directions, and this refers primarily to welding production. Creation of favorable and safe labour conditions is associated with providing to the working people different methods of protection that allow considerably decreasing the level of influence of unfavorable production factors. Their effective use provides complex protection of workers from all types of harmful impact of the production factors. Correct selection of protection means should be conducted taking into account the features of the performed work by predicting the occupational morbidity risk and its consequences in the case of imperfection or disuse of these means.

**Means of protection from welding aerosols.** One of the most dangerous factors in the majority of Ukrainian enterprises are welding aerosols (WA) from which a welder is insufficiently protected even today (that particularly refers to the electric arc welding processes). The main and compulsory measure of welders' protection from WA is ventilation that provides not only collective protection but also individual one. At the same time, modern means of local ventilation also solve ecological problems: they provide cleaning from harmful substances of the air released into the atmosphere. In addition to sanitary and ecological effects, it also gives a cost effect connected with the



reduction of electric and heat energy consumption as a result of replacement of general ventilation by dilution by local ventilation or their combined use.

*Systems of ventilation.* Ventilation of premises is achieved through open windows and doors in case of natural ventilation. This system is cost-effective, although it does not completely solve the problem of harmful substances removal from the industrial area. In addition, it is characterized by great heat losses [1].

General mechanical ventilation by dilution is based on air removal from the premises by axial fans and air return through the windows. This type does not require big capital investment, although at its application the WA spread along the entire production area penetrating into respiratory organs of the workers [2]. It is not effective for welding operations, and can be used only in addition to local ventilation.

Local exhaust ventilation (particularly with wall-mounted flexible local suction) is based on WA removal directly from the place of their formation. In such a way, WA spreading through the whole premises and its penetration into the breathing zone of workers are prevented [3]. The main condition for providing effective WA collection by local exhaust ventilation is that the flow rate of air passing through air inlet funnels of 125–160 mm diameter should be 600–1000 m<sup>3</sup>/h [4]. The advantage of this method is a high efficiency of harmful substance collection at a comparatively small volume of the removed air so that such a decision is justified also in economic terms. General ventilation by dilution requires much bigger expenditures connected with ventilation and in the cold season also with heating of considerable volumes of air [5, 6], in order to obtain the same results.

Economic efficiency of exhaust ventilation local means, equipped with filtering elements, increases as a result of cleaned air recirculation and respective reduction of ventilated air volume, as well as its heating [7]. Moreover, its application allows increasing the labour productivity by 10–12 % [4], lowering the morbidity level and the associated expenses in the public health and social sphere. For effective collection of harmful substances, it is necessary to place the devices for local suction at the distance of 25–50 cm from the place of welding, that is why such ventilation is not always applicable, taking into account the types of welded constructions. More over, this system is difficult to install in large premises, when welding stations are placed at a considerable distance from the walls. At present different means for local ventilation are produced. The following basic systems became widely accepted [8, 9]: turnover devices of local suction connected to the centralized system through which the contaminated air is removed from the premises by the fan; turnover devices of local suction that return cleaned air into the premises; bracket-swing devices of local suction connected by the general air conduit to the filter with return of cleaned air into the premises; portable ventilators with flexible hoses; traveling (mobile) filter-ventilating units (FVU); portable transferable FVU; suction devices built into the welding equipment.

Mobile FVU allow removing the polluted air from the welding sites, its cleaning and returning. They do not require performance of assembly work, can be

moved to any spot in the workshop, feature a high level of harmful particle collection, save power as a result of air recirculation. Inconvenience of their application consists in the need to periodically clean, wash or replace the filter elements by new ones [8].

Certain progress in this area is also observed in Ukraine. Serial production of local ventilation means, developed with PWI participation, is being mastered now: mobile and stationary FVU of «Temp 2000», «Temp-NT» series [10, 11], FVU «Shmel-1500» [12], portable ventilation units of «Temp-NV» [13] and «Shmel-2500» [14] series designed for working under different conditions.

*Means of individual protection for respiratory organs.* Means of individual protection for respiratory organs (MIPRO) are used in cases when ventilation is not effective or not used at all (when carrying out welding works in closed premises, hard-to-reach places and so on). At present two types of MIPRO are used for protection of respiratory organs from WA: dust-fighting respirators; protective masks with forced supply of cleaned air into the breathing zone.

Dust-fighting respirators of «Snezhok» type [15] for different purposes are widely used in Ukraine, system of air cleaning and supply to the breathing zone of the welder is becoming popular [16]. The choice of MIPRO depends on the type of welding and welding consumable, and labour conditions. Necessary filtering materials are determined by WA physico-chemical properties (dispersed and chemical composition, content of harmful substances in the air).

**Information systems for selection of protection means.** Selection of the removed air volume, local suction design, air cleaning method, as well as optimum cost of equipment depend on the welding process, type and grade of welding consumables, shape of welded product, workshop space, number of welding stations and a number of other factors [17]. The efficiency of ventilation systems greatly depends on their correct selection. For this purpose it is necessary to take into account the features of the production process, nature and intensity of harmful factors impact on a worker that determine the time of providing the necessary level of protection, features of physical activity, as well as his individual features. Experience showed that the correct selection of appropriate safety means is impossible without application of special information systems. Computer information retrieval system ECO-WELD designed at PWI [18] can be considered as the first practical development for selection of protection means for welders' respiratory organs. It allows obtaining information on WA for different arc welding processes, mode parameters and welding consumables, as well as calculating the necessary productivity of welder's work place ventilation, and choosing ventilation equipment and means for individual protection of respiratory organs. Information about the composition and quantity of WA formed when using different welding technologies and welding consumables, is gathered and systematized in the given system. The result of the search is an output document containing indices of welding consumable hygienic characteristics at the specified welding process parameters:



chemical composition and level of WA precipitation, as well as design data on the required efficiency of general ventilation by dilution. In addition, the database contains information about the means of local ventilation and individual protection for respiratory organs, as well as information about practically all welding consumables manufactured in Ukraine and Russia. It is used at PWI and many enterprises of Ukraine for designing measures for protection of welders and environment, as well as a device for treatment of experimental data by hygienic evaluation of new welding consumables with proper labour safety recommendations [19]. Another similar development is information-analytical system for welders' protection (IASWP) [20], suggested by the specialists of National SRI of Labour Safety. In spite of a lack of such broad data and knowledge base, as the one described in work [18], the system permits planning measures on labour safety in welding production, based on evaluation of risk of professional diseases and, based on that, developing economically justified and rational measures for their prevention. They include selection of the rational proportion of the types of means for collective and individual protection of respiratory organs that should be applied in welding. The index of limit doses of production environment influence on the human body, i.e. the time of welder's working in aerosol-polluted zone at a certain concentration of WA, was used.

Estimation of limit doses of production environment was performed by mathematical modeling of the composition and level of precipitation of harmful substances in WA composition, depending on welding conditions, based on PWI data [21, 22], as well as by studying the data on the state of workers' health, depending on labour conditions [23, 24]. Joint consideration of these two factors allows finding the optimum solutions for definition of aerosol load on the respiratory organs and corresponding selection of planned preventive measures. Disadvantage of IASWP system [20] is its limited application: it was compiled on the basis of published literature data on welding with certain grades of welding electrodes.

**Trends of information systems development.** Experience of application of modern means for protection of welders' respiratory organs shows that in spite of their sufficient efficiency, they do not yield the proper safety effect in most cases. It is obvious that without using computer information systems of the new generation, it is impossible, first, to take an optimum decision on selection of protection means, proper welding technology, and, second, to use these means correctly, taking into account the availability of the existing general ventilation by dilution and labour conditions (parameters of microclimate, labour intensity, duration and frequency of welding works) in the production premises. The following welding-technological factors should be also taken into consideration in the new information system obtained on the basis of system integration [18, 20]: welding process, type and grade of welding consumable (type of coating for coated electrodes); chemical class WA [25]; welding conditions (type and intensity of welding current, arc voltage, polarity).

Such information will permit solving the tasks of providing the necessary level of welders' safety, predicting the risk of occupational disease and, eventually, lowering its level. It will provide the enterprise managers, specialists on labour safety and other interested persons with systematized information about protection means for welders, allow making their adequate selection, predicting the consequences of the use of collective and individual protection means, and can be used for designing the welder work places.

1. Pisarenko, V.L., Roginsky, M.L. (1981) *Ventilation of work places in welding production*. Moscow: Mashinostroenie.
2. Gritimlin, M.I. (1990) Means of further improvement of ventilation efficiency and ecological safety of welding production. In: *Proc. of Sci.-Techn. Seminar on Current Problems of Ventilation and Ecological Safety in Welding Production* (Leningrad, July 5-6, 1990). Leningrad: LDNTP.
3. Gritimlin, M.I., Kondrashov, S.Yu., Alekseeva, I.S. et al. (1987) Improvement of air in assembly-welding shops. In: *Labor safety under the conditions of production intensification*. Leningrad: Znanie.
4. Plimut, J. (1988) *Pure fresh air*: Catalogue. Malme, Sweden.
5. Kundiev, Yu.I., Gorban, L.N., Mazur, A.A. et al. (1986) Economic efficiency of application of filter-ventilation units in electric welding production. In: *Proc. of All-Union Sci.-Techn. Conf. on New Processes of Welding, Surfacing and Thermal Spray Coatings in Machine-Building* (Taganrog, Oct. 5-8, 1986). Taganrog: Dom Tekhniki.
6. Kundiev, Yu.I., Mazur, A.A., Gorban, L.N. (1987) Hygienic and ecological aspects of problems of welding aerosol control. *Svarochn. Proizvodstvo*, **3**, 1-3.
7. Mazur, A.A., Gorban, L.N., Ennan, A.A. (1992) Economics of air purification in welding. In: *Proc. of 1st Int. Seminar on Ecological Problems of Welding Production* (Gliwice, Poland, Oct. 13-15, 1992). Gliwice: MAS.
8. Levchenko, O.G., Metlitsky, V.A. (1995) Modern means of ventilation in welding. Review. *Avtomatich. Svarka*, **3**, 40-48.
9. (1991) *Pure fresh air*: Pricelist. Leningrad: Sovplim.
10. Levchenko, O.G., Metlitsky, V.A. (2001) *Current means of welder's protection*. Kiev: Ekotekhnologiya.
11. Levchenko, O.G., Agasian, N.Yu. (2006) Filter-ventilation units of «Temp» model for welding production. In: *Proc. of 14th Int. Sci.-Pract. Conf. on Ecology and Man's Health, Safety of Environment and Water Basins, Waste Recovery* (Shchelkino, June 5-9, 2006). Vol. 2. Kharkov: Rejder.
12. Iliinsky, N.I., Levchenko, O.G. (2000) Filter-ventilation unit «Shmel-1500». *Svarshchik*, **6**, 37.
13. Levchenko, O.G., Agasian, N.Yu. (2003) Low-voltage portable ventilation unit «Temp-NV». *Ibid.*, **1**, 32-33.
14. Levchenko, O.G., Iliinsky, N.I. (2005) Portable ventilation unit «Shmel-2500». In: *Proc. of Sci.-Techn. Sem. on Service Reliability Control of Pipeline Transport Systems* (Kiev, April 25-27, 2005). Kiev: Ekotekhnologiya.
15. Ennan, A.A., Bolshakov, D.A., Gorban, L.N. (1999) Light-weight respirators of type «Snezhok». *Svarshchik*, **1**, 32-33.
16. Iliinsky, N.I., Levchenko, O.G. (2004) New modification of device for air purification and supply into the welder's breathing zone. *Ibid.*, **3**, 42.
17. Levchenko, O.G. (2004) *Occupational hygiene and industrial sanitation in welding production*: Manual. Kiev: Osnova.
18. Demchenko, V.F., Levchenko, O.G., Metlitsky, V.A. et al. (2001) Information retrieval system of hygienic characteristics of welding aerosols. *Svarochn. Proizvodstvo*, **8**, 41-45.
19. Levchenko, O.G., Metlitsky, V.A., Ryabtsev, I.A. et al. (2003) Sanitary-hygienic evaluation of flux-cored wires for electric arc surfacing. *The Paton Welding J.*, **8**, 41-45.
20. Polukarov, O.I., Kruzhilko, O.E., Polukarov, Yu.O. (2006) Application of information-analytical system in planning of labour safety measures in welding production. *Svarshchik*, **2**, 42-44.
21. Podgaetsky, V.V., Golovatyuk, A.P., Levchenko, O.G. (1989) About mechanism of welding aerosol formation and prediction of its composition in CO<sub>2</sub> welding. *Avtomatich. Svarka*, **8**, 9-12.
22. Levchenko, O.G. (2001) Mathematical modeling of chemical composition and level of welding aerosol emission. *Svarochn. Proizvodstvo*, **7**, 25-28.
23. Asanok, I.S. (1992) *Scientific grounding and development of a modern control system for morbidity prevention of industrial workers*: Synopsis of Thesis for Cand. of Med. Sci. Kiev.
24. Initskaya, A.V., Syromyatnikov, Yu.P. (1994) Prediction of health and prevention of occupational diseases in plasma technology. *Svarochn. Proizvodstvo*, **8**, 15-17.
25. Levchenko, O.G. (1999) Classification of welding aerosols and selection of their neutralizing methods. *Avtomatich. Svarka*, **6**, 38-41.



## STRUCTURE AND PROPERTIES OF A JOINT OF 10Kh13G18D + 09G2S STEELS

A.I. GEDROVICH<sup>1</sup>, A.N. TKACHENKO<sup>2</sup> and S.A. TKACHENKO<sup>2</sup>

<sup>1</sup>V. Dal East-Ukrainian University, Lugansk, Ukraine

<sup>2</sup>HC «Luganskteplovoyz», Lugansk, Ukraine

Experimental data on evaluation of the structure and microhardness of different regions of dissimilar welded joints of steels 10Kh13G18DU + 09G2S are presented. Recommendations are given for application of Sv-08Kh20N9G7T wire for gas-arc welding of joints.

*Keywords:* arc welding, dissimilar joints, filler wire, shielding medium, structure, microhardness

Low-carbon, low-alloyed, medium-carbon and medium-alloyed steels of pearlitic class 1–8 mm thick are traditionally used in Ukraine and other countries for manufacture of bodies of diesel- and electric trains. Plating of the roofs and walls, flooring of the main frames and other welded components are made from sheet metal 2–3 mm thick. Profiled or sheet metal 3–5 mm thick is used for frame elements. Car components are made from purchased special profiled or sheet metal, and their individual elements require repair or replacement already after five or six years, because of susceptibility to considerable atmospheric corrosion.

Current operating conditions of the rolling stock elements (bodies, main frames, walls, roofs and other components) necessitate applying more stringent requirements to welded joints to provide a longer service life. This is related to considerable alternating and dynamic loads in operation, due to high velocities of locomotive movement, aggressive environment and other factors. In this connection, new approaches are required to design of welded metal structures, which make up the assemblies and subassemblies of the rolling stock.

Current tendencies in design and manufacture of structures of cars for diesel- and electric trains are associated, in particular, with their weight reduction with simultaneous provision of the specified strength, fatigue life, corrosion resistance and other parameters [1]. To extend the service life and ensure the corrosion resistance of the car plating, there is experience of application of stainless chromium-nickel steels of austenitic class in the world practice. In CIS countries chromium-nickel steel 12Kh18N10T was used only in Russia in manufacture of test samples of electric trains ED6 at OJSC BMZ.

Over the last years the I.P. Bardin TsNIChermet (Moscow) developed and recommended chromium-manganese steel 10Kh13G18D, in particular for car manufacture. This steel belongs to the austenitic class, and in as-heat-treated condition (austenitizing from 1050 °C in water) it is characterized by a set of high

mechanical properties ( $\sigma_t = 670$  MPa,  $\sigma_{0.2} = 345$  MPa,  $\delta = 48$  %) and corrosion resistance, and also has a lower cost compared to chromium-nickel steel. In as-cold rolled condition to a thin sheet (1.5 mm) it has the following mechanical properties:  $\sigma_t = 870$  MPa,  $\sigma_{0.2} = 450$  MPa,  $\delta = 29$  %.

HC «Luganskteplovoyz» has extensive experience of application of this steel in similar joints in fabrication of body elements [2]. Mastering the technology of mechanized welding of structures of 10Kh13G18D steel involved overcoming certain difficulties, due to susceptibility of the HAZ metal to cold cracking. Technology of mechanized arc welding with the above-mentioned cooling turned out to be effective in this case. At present use of steel 10Kh13G18D in dissimilar joints with 09G2S steel is an urgent issue. Application of low-alloyed 09G2S steel for frame elements of the body allows reducing their thickness from 3.0 to 2.5 mm, and use of stainless steel 10Kh13G18D in the cold-rolled condition allows reducing the plating thickness from 2.5 to 1.5 mm.

Conducting bench testing of a test car made of a combination of these steels confirmed the correctness of their selection. Considering the design features of welded components of bodies of the motor-car rolling stock (overall dimensions, thicknesses of welded items, extent and need to make welds in different positions), it is rational to apply the automatic or mechanized welding in shielding gases or their mixtures. Flash-butt welding can also be used, when individual elements of metal structures are manufactured.

The purpose of this work is optimization of the structure and properties of metal of dissimilar joints of steels 10Kh13G18D + 09G2S, made by gas-arc welding.

During experimental studies the influence of the conditions of welding zone shielding from the environment (carbon dioxide gas and argon) was evaluated, and the structure and properties were compared in joints made following the technical recommendations of [2], using welding wires Sv-08Kh20N9G7T (wt. %: 0.08C; 0.6Si; 6.8Mn; 19.5Cr; 8.5Ni; 0.45Ti; 0.018S; 0.025P) and 09Kh18N8G7S, Sweden (wt. %: 0.02C; 1.05Si; 6.5Mn; 18.5Cr; 8.6Ni) capable of pro-



**Table 1.** Microstructure of metal of overlap welds made by mechanized process in welding dissimilar 10Kh13G18D + 09G2S steels

Sample type	Welding consumables, shielding medium	Structure of weld and HAZ metal
1	Sv-08Kh20N9G7T, Ar	Austenitic base, presence of acicular structure of deformation martensite (HAZ), $\delta$ -ferrite precipitates along cell boundaries (WM)
2	Sv-08Kh20N9G7T, CO <sub>2</sub>	Austenitic base, cellular structure with precipitation of thin $\delta$ -ferrite streaks along grain boundaries (WM). No martensite component (HAZ)
3	02Kh18N8G7S, Ar	Same
4	02Kh18N8G7S, CO <sub>2</sub>	»
5	VL-2, Ar	HAZ from the side of 09G2S steel: pearlitic structure with precipitation of pre-eutectoid ferrite along austenite grain boundaries. Austenite grain point is 6 acc. to GOST 5039-82. From the side of 10Kh13G18D steel: matrix of austenite with acicular precipitates of deformation martensite, as well as round-shaped structural inclusions of $\delta$ -ferrite

**Table 2.** Microhardness of joint zones in steel 10Kh13G18D + 09G2S

Sample type	Wire grade	Shielding medium	Microhardness, MPa, in the zone of		
			09G2S HAZ	WM	10Kh13G18D HAZ
1	Sv-08Kh20N9G7T	Ar	1850–2180	2200–3300	2660–2700
2	Sv-08Kh20N9G7T	CO <sub>2</sub>	1800–2800	2200–2860	2300–2680
3	02Kh18N8G7S	Ar	1950–2460	2380–3380	2700–2720
4		CO <sub>2</sub>	1900–2100	2020–3000	2620–2700
5	Without filler wire	Ar	1900–2700	2460–4040	2430–2780

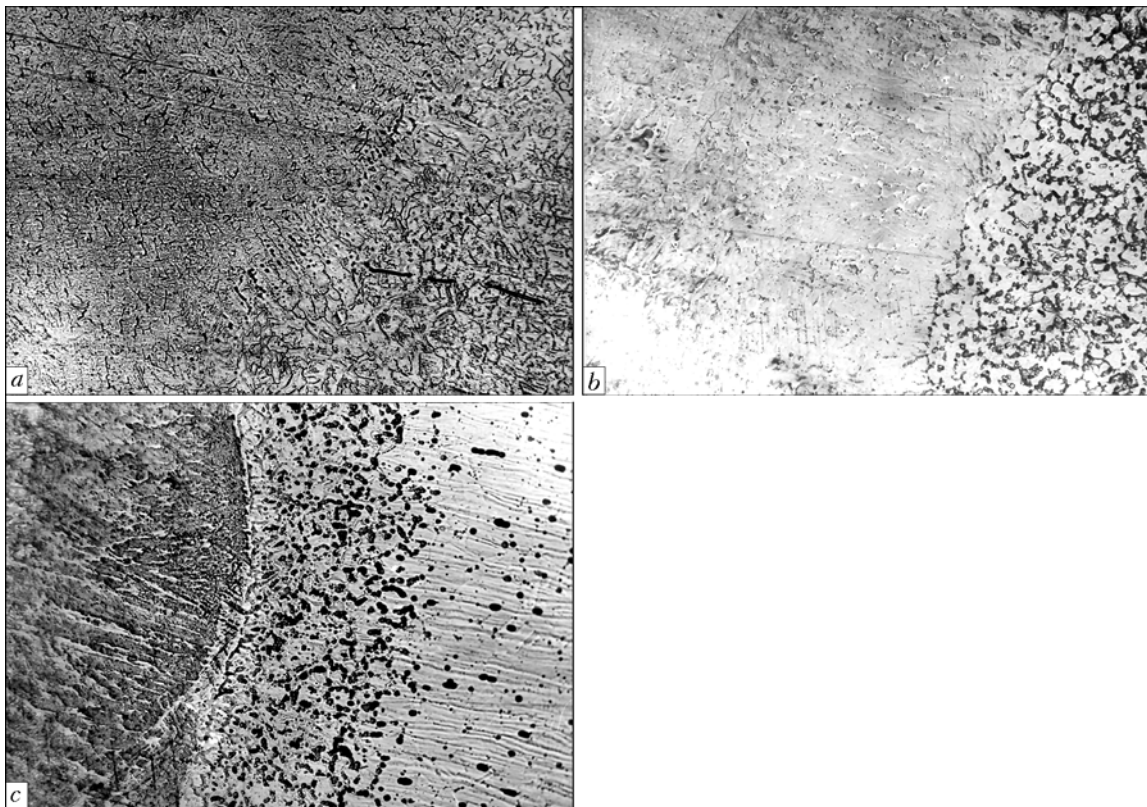


**Figure 1.** Microstructures of weld and HAZ metal from the side of 10Kh13G18D steel in dissimilar joints of 09G2S + 10Kh13G18D made with welding wire Sv-08Kh20N9G7T in Ar (a), 02Kh18N8G7S in CO<sub>2</sub> (b) and nonconsumable electrode without filler wire in Ar (c) (×400)



viding the austenitic structure of weld metal in dissimilar joints.

Four types of samples (Table 1) assembled with an overlap were welded by the mechanized process with semi-automatic machine A-547U3 with BS-300B source in the following modes:  $I_w = 130\text{--}140$  A;  $U_a = 18\text{--}19$  V;  $v_f = 178$  m/h;  $d_{el} = 1.2$  mm. For comparison samples (type 5) were also welded by manual argon-arc welding with tungsten electrode of 2 mm diameter (UD-GU-301 AC/DC power source) at DCSP ( $I_w = 60\text{--}100$  A) in argon. Macro- and microsections were prepared for evaluation of microstructure and determination of metal microhardness in different sections of the welded joints, and separate etching was used to reveal the microstructure of sample metal. Carbon metal was etched in 4 % alcohol solution (ethyl alcohol) and nitric acid  $\text{HNO}_3$ . Microstructure of chromium-manganese steel was revealed by electrolytic method in 10 % water solution of chromium acid (chromium anhydride  $\text{CrO}_3$ ) in the following mode:  $U = 20$  V;  $I = 0.20\text{--}0.25$  A; etching time of 5–20 s. Sample microstructure was studied in «Neophot-32» optical microscope. After the appropriate preparation of the sections, the microhardness of welded joint metal was measured in the LECO hardness meter of model M-400 at 50 g load with  $n = 0.5$  mm increment.

Structural components were identified at filming with magnification of  $\times 200$ , 320, 400 and 1000. Microstructure of weld metal on samples from steels 10Kh13G18D + 09G2S is systematized (Table 1) and given in Figure 1.

It is established that the microstructure of weld metal of the joints made with welding wire Sv-08Kh20N9G7T in  $\text{CO}_2$  and with welding wire 02Kh18N8G7S in  $\text{CO}_2$  and Ar, is austenitic with small inclusions of  $\delta$ -ferrite. The HAZ metal has no martensite component.

Microhardness was determined on polished and etched samples in the transverse sections of welded joints. Schematic of sample hardness measurement is given in Figure 2. Table 2 gives the results of microhardness measurements of the studied samples. The data of microhardness measurement correlate quite

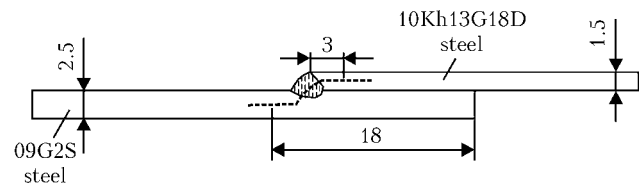


Figure 2. Schematic of microhardness measurement in a welded joint of samples

well with the results of metallographic studies. Zones of higher microhardness are found in the first group of samples where precipitation of deformation martensite was observed in the weld metal structure.

In the sample made with a tungsten electrode without filler wire in argon microhardness of 09G2S steel, HAZ metal from the side of the same steel rises from 190 to 270 MPa, and an abrupt change of microhardness from 246 to 404 MPa is also observed across the weld metal section with subsequent lowering to 278 MPa closer to the HAZ metal of 10Kh13G18D steel. Analysis of microhardness distribution in joints of 10Kh13G18D + 09G2S steel leads to the conclusion that the greatest scatter in microhardness values is observed across the section of welded joints in samples welded by nonconsumable tungsten electrodes in argon, and this index changes more smoothly in semi-automatic welding of samples of the above dissimilar steels using wire Sv-02Kh18N8G2S in Ar and  $\text{CO}_2$ , while the indices of microhardness across the section of samples welded with Sv-08Kh20N9G7T wire in  $\text{CO}_2$  are practically identical.

It is established that application of Sv-08Kh20N9G7T wire in  $\text{CO}_2$  in gas-arc welding of dissimilar joints of steels 10Kh13G18D + 09G2S provides the most favourable structure of weld metal and hardness distribution in the joint.

1. Basov, G.G., Golubenko, A.L., Mishchenko, K.P. (2003) Concept for development of prototype of current motor-car rolling stock for Ukrainian railways. In: *Transact. on Problems of Implementation and Development of Manufacturing in Ukraine of Motor-Car Rolling Stock on the Base of Unified Trailer Car*. Leningrad: Mashinostroenie.
2. Tkachenko, A.N., Gedrovich, A.I., Galtsov, I.A. (2002) Application of metastable corrosion-resistant steel 10Kh13G18D for plating of electric and diesel train cars. In: *Proc. of Int. Conf. on Welding and Related Technologies* (Kiev, April 22–26, 2002). Kiev: PWI.



## THESIS FOR SCIENTIFIC DEGREE



### E.O. Paton Electric Welding Institute of NASU.

On October 28, 2006 **Maksimov Yu.S.** (PWI) defended Doctor's thesis on «Physico-Metallurgical Features and Technology of Arc Welding of Low-Alloyed Steels in Water».

The thesis is devoted to investigation of the features of the influence of water environment on physico-metallurgical regularities of the arc welding process and development of theoretical fundamentals and scientifically-based complex of metallurgical and technological measures to ensure the quality of welded joints of low-carbon and low-alloyed steels with up to 600 MPa strength point.

It was established experimentally with simulation in a hydraulic pressure chamber of the conditions of consumable-electrode wet arc welding at down to 200 m depth that the main factor for manifestation of the adverse influence of hydrostatic pressure of the water environment on arcing stability is an abrupt increase of the number of short-circuits with the immersion depth. An explanation of this fact is provided, which is based on the inevitability of the arc column contraction and increase of its electric field intensity predominantly in the hydrogen environment at increased pressure.

Rational and effective methods of solving the problem of stabilization of an arc running in water are shown and experimentally confirmed: at small depths (down to 20 m) --- by increasing the arc power by 10--15 % and adding to electrode materials a substance with a capability of an increased gas evolution at dissociation to increase the vapour-gas bubble volume; at great depths (down to 200 m) --- use of substances with a low ionization potential (alkali metal salts) to increase the electrical conductivity of the peripheral «cold» regions of the arc column and extend the arc length.

Features of metal interaction with gases in underwater wet welding process have been studied. Thermodynamic analysis showed that in view of the high

thermal resistance of water molecules up to temperatures of 2000--2500 K the atmosphere of the vapour gas bubble, in which the arc runs, consists predominantly of water vapours and molecular hydrogen. At direct contact of water vapour with molten metal, its intensive oxidation takes place, and the atmosphere of the vapour gas bubble is additionally enriched in hydrogen. This results in weld metal oversaturation with hydrogen, increased oxygen concentration, practically complete loss of carbon, silicon and manganese, lowering of the effectiveness of microalloying with titanium and boron and increase of the quantity and size of nonmetallic inclusions.

The concept of the regularities of pore formation process in welding in the water environment is developed. The hydrogen-related nature of their origin is established experimentally by studying the gas composition in weld pores. Numerical methods are used to study the evolution of the gas bubble formed on the solidification front, and it is established that the probability of pore formation, determined mainly by three factors, namely solidification rate, hydrogen content and hydrostatic pressure, rises with increase of each of them in the depth range down to 100 m. With greater depth, because of lowering of the rate of increase of hydrogen solubility in the weld pool metal, the intensity of the critical radius decreases, and after 100 m has been reached, the nature of pressure influence is reversed, namely the critical radius increases, and the pressure factor loses its determinant role.

The cause for an abrupt lowering of the resistance of welded joints in low-alloyed steels to HAZ crack formation under the conditions of increased heat sink, stringent thermal cycle and weld metal oversaturation by hydrogen characteristic for welding in water, is established. It is shown that compared to the conditions of welding in air, simultaneous action of the structural and hydrogen factors is enhanced, being manifested in the martensite ridge, which inevitably forms in the HAZ near the fusion line, accumulating 2--3 times larger quantity of hydrogen at a simultaneous narrowing of the HAZ section, where tensile stresses increasing at a high rate are localized during cooling.

It is shown that alloying of the ferrite-type weld metal by nickel, having a low affinity to oxygen, allows achieving a simultaneous increase of its strength and ductility characteristics to the level required for solving the problem of welding low-alloyed steels with the tensile strength up to 540 MPa, due to formation of a structure with an increased fraction of acicular ferrite. The problem of welding low-alloyed steels of a higher strength ( $\sigma_t$  of up to 600 MPa), prone to formation of hardening structures in the HAZ, is



solved through application of electrode materials of austenitic class. The level of alloying the weld metal of Cr–Ni–Mn–Mo system is determined, which guarantees the welded joints properties meeting the requirements of class A «Specification on Underwater Welding» ANSI/AWS D3.6.

The principles of development of new generation electrode consumables for arc welding of higher strength low-alloyed steels directly in water are proposed and implemented. Flux-cored wires and stick electrodes (of ferritic and austenitic types) were developed, which ensure the required level of properties of the welded joints and form the basis of the technology of wet underwater welding of low-alloyed steels with up to 600 MPa tensile strength. Pilot production trials of the developments were conducted to solve the practical problems of repair of pipelines, port facilities and ships afloat. Technical documentation was developed for manufacture and application of new electrode consumables, technological instructions were developed on repair of underwater metal structures, including pipelines in operation with guaranteed safe welding modes.



#### **E.O. Paton Electric Welding Institute of NASU.**

On November 1, 2006, **Pustovojt S.V.** (PWI) defended the thesis of Candidate of Sci (Eng.) on «Scientific Fundamentals and Technical Means of Increasing the Efficiency of Manual Pulsed-Arc Welding».

The thesis contains system analysis of the theoretical and experimental investigations of the magnetic field impact on the welding arc penetrability, as well as the results of hydro- and magnetohydrodynamic processes in the weld pool, affecting the formation of its crater and liquid metal flows in it, which are gen-

eralized in the form of a dynamic model of the weld pool in immersed arc welding.

The nature of arc power distribution in the pool crater shows that the active spot and the heated spot surrounding it, are erring continuously over the front wall and only seldom are located on the crater bottom. It is shown that the arc column axis does not coincide with the electrode axis, and its direction is determined chiefly by the electric field between the electrodes, the impact of which on the motion of electrons in the column is by an order of magnitude stronger than the Lorentz force. Therefore, the active spot on the item being welded is located in the zones closest to the electrode.

The main force causing the motion of the liquid metal from the crater front wall to its tail part, is the electromagnetic force arising from interaction of the current spreading in front of the arc with the inherent magnetic field. This force is always directed to the crater bottom, and its magnitude depends on the arc current and angle of inclination of the electrode to the item. It is shown that the plasma flow of the conic arc creates a velocity head on all the elements on its surface, the crater depth being determined not only by the base metal penetration depth, but also by the change of the amount of plasma motion in its base.

The thesis gives a description of an instrument for recording the weld pool oscillations. The operating principle of the instrument is based on conversion of mechanical oscillations of the melt into electrical oscillations, using piezo effect. The developed instrument allows deriving the oscillograms of pool oscillations at a pulsed action of the arc on it, and quickly finding the «resonance» conditions. A method of upgrading VDU type rectifier has been developed. Its mounting into the electric circuit of the modulator block allows obtaining an additional pulsed arcing mode and widening its technological capabilities, respectively. The algorithm given in the work for calculation of the main elements of modulator block will allow the interested enterprises to perform such an upgrading through their own efforts, in order to introduce into production the pulsed-arc welding process, which has a number of advantages compared to stationary arc welding. The thesis contains the results of experimental investigations of pulsed electromagnetic impact on penetration depth in manual arc welding. It is established that the arc penetrability essentially depends on the frequency of current pulse repetition. The maximum effect is observed at current pulse frequencies close to that of free oscillations of the weld pool, i.e. so called resonance. Pulsed arc application in manual arc welding allows increasing the penetration depth by 20–25 % without increasing the heat input.

# INDEX OF ARTICLES FOR TPWJ'2006, Nos. 1-12

## Alloying

Effect of phosphorus on crack resistance of low-carbon deposited metal (Ryabtsev I.I., Kuskov Yu.M. and Novikova D.P.)

5

Effect of scandium additions on fine structure of weld metal in aluminium alloy 1460 welded joints (Markashova L.I., Grigorenko G.M., Ishchenko A.Ya., Lozovskaya A.V. and Kushnaryova O.S.)

2

Effect of silicon on properties of low-alloy carbon deposited metal (Zhudra A.P., Krivchikov S.Yu. and Petrov V.V.)

8

Effect of the degree of alloying of heat-resistant chromium steels on hardness of metal within the welded joint zone (Skulsky V.Yu.)

9

Improvement of weld strength in arc welding of Al-Cu alloys with application of Sc-containing fillers (Poklyatsky A.G., Lozovskaya A.V., Grinyuk A.A., Yavorskaya M.R. and Chajka A.A.)

2

Influence of alloying of filler material and welded steel on fusion zone structure (Skulsky V.Yu.)

2

Influence of oxygen potential of welding fluxes on solid solution alloying in weld metal (Golovko V.V.)

10

Laser-microplasma alloying and coating of steel (Shelyagin V.D., Khaskin V.Yu. and Pereverzev Yu.N.)

2

Selection of steel for critical building welded structures (Kovtunenka V.A., Gerasimenko A.M. and Gotsulyak A.A.)

11

Study of sulfur effect on properties of deposited metal of Kh51 FS type (Osin V.V., Ryabtsev I.A. and Kondratiev I.A.)

12

## Alloys

### Aluminium alloys

Application of high-power fibre lasers in laser and laser-MIG hybrid welding (Thomy C., Kohn H. and Vollertsen F.)

7

Basics and applications of laser-GMA hybrid welding (Thomy C. and Seefeld T.)

6

Effect of scandium additions on fine structure of weld metal in aluminium alloy 1460 welded joints (Markashova L.I., Grigorenko G.M., Ishchenko A.Ya., Lozovskaya A.V. and Kushnaryova O.S.)

2

Effect of scandium additions on structure-phase condition of weld metal produced by welding aluminium alloy 1460 (Markashova L.I., Grigorenko G.M., Ishchenko A.Ya., Lozovskaya A.V., Kushnaryova O.S., Alekseenko T.A. and Chajka A.A.)

1

Effect of scandium additions on structure-phase state of weld metal in aluminium alloy joints after heat treatment (Markashova L.I., Grigorenko G.M., Lozovskaya A.V., Kushnaryova O.S. and Fedorchuk V.E.)

6

High power diode laser welding of aluminum alloy ENAW-1050A (Klimpel A., Lisiecki A., Janicki D. and Stano S.)

9

Improvement of fatigue resistance of welded joints in metal structures by high-frequency mechanical peening (Review) (Lobanov L.M., Kirian V.I., Knyshev V.V. and Prokopenko G.I.)

9

Improvement of quality of deposited metal in plasma-MIG cladding of aluminium alloys (Chigarev V.V., Kondrashov K.A. and Granovsky N.A.)

6

Influence of structural transformations in welding of aluminium alloy B96 on fracture resistance parameters (Labur T.M., Taranova T.G., Kostin V.A., Ishchenko A.Ya., Grigorenko G.M. and Fedorchuk V.E.)

11

Residual stresses in butt joints of thin sheets from alloy AMg6 after arc and laser-arc welding (Shonin V.A., Mashin V.S., Khaskin V.Yu. and Nedej T.N.)

9

### Aluminium-copper alloys

Improvement of weld strength in arc welding of Al-Cu alloys with application of Sc-containing fillers (Poklyatsky A.G., Lozovskaya A.V., Grinyuk A.A., Yavorskaya M.R. and Chajka A.A.)

2

### Aluminium-lithium alloys

Mechanical properties of plasma welded joints on aluminium-lithium alloys (Labur T.M., Grinyuk A.A. and Poklyatsky A.G.)

6

### Magnesium alloys

Properties of CO<sub>2</sub>-laser welded joints of dissimilar magnesium alloys (Kalita W., Kolodziejczak P., Kwiatkowski L., Grobelny M. and Hoffman J.)

7

### Nickel alloys

Application of nano-structured materials for diffusion bonding of heat-resistant nickel alloys (Yushchenko K.A., Zadery B.A., Zvyagitseva A.V., Kushnaryova T.N., Nesmikh V.S., Polishchuk E.P. and Savchenko V.S.)

11

### Shape-memory alloys

Weldability of shape-memory alloys of Ni-Ti system (Paton B.E., Kaleko D.M., Shevchenko V.P., Koval Yu.N., Slipchenko V.N., Neganov L.M. and Musienko R.Ya.)

5

### Titanium alloys

Repair welding of titanium blades of gas turbine engine compressors (Zamkov V.N., Vrzhezhevsky E.L., Topolsky V.F. and Petrchenko I.K.)

1

### Brazing

Application of reconditioning technologies to extend the life of gas turbine engines (analysis of state-of-the-art and development) (Zhadkevich A.M.)

5

### Calculation

Calculation of induction of controlling longitudinal magnetic field with consideration for magnetic properties of core, wire and work-piece as applied to arc surfacing (Razmyshlyayev A.D., Deli A.A. and Mironova M.V.)

8

Calculation of the kinetics of diffusion phase transformations in low-alloyed steels in beam welding (Dilthey U., Gumenyuk A.V. and Turichin G.A.)

2

Calculation technique for defining parameters of soldered seam solidification (Denisevich E.A.)

9

Characteristics of pulsed plasma flow in plasma-detonation generator at different flow rates of fuel mixture (Zhadkevich M.L., Tyurin Yu.N., Kolisnichenko O.V. and Mazunin V.M.)

11

Design and features of fabrication technology of a large-sized transformable shell structure (Paton B.E., Lobanov L.M., Samilov V.N., Pilishenko I.S., Makhnenko O.V., Pashchin N.A., Gorinov V.A. and Shiyan K.V.)

7

Design-experimental assessment of the features of electrode melting and transfer process (Chigarev V.V., Belik A.G. and Sergienko Yu.V.)

8

Dynamics of movement and heating of powder in detonation spraying of coatings (Ulshin V.A., Kharlamov M.Yu., Borisov Yu.S. and Astakhov E.A.)

9

Effect of parameters of plasma detonation unit discharge circuit on gas-dynamic characteristics of pulsed plasma flows (Zhadkevich M.L., Tyurin Yu.N., Kolisnichenko O.V. and Mazunin V.M.)

8

Influence of oxygen potential of welding fluxes on solid solution alloying in weld metal (Golovko V.V.)

10

Methods to lower the hydrogen content in metal of welded joints of low-alloyed steels in submerged-arc welding (Golovko V.V.)

2

On heating and acceleration of disperse particles with pulse plasma (Zhadkevich M.L., Tyurin Yu.N., Kolisnichenko O.V. and Mazunin V.M.)

7

Optimization of transformer with developed transverse magnetic leakage fluxes and magnetic shunt (Rymar S.V.)

5

Peculiarities of the process of microplasma wire spraying (Borisov Yu.S., Kisilitsa A.N. and Vojnarovich S.G.)

4

Procedure for determination of residual stresses in welded joints and structural elements using electron speckle-interferometry (Lo-banov L.M., Pivtorak V.A., Savitsky V.V. and Tkachuk G.I.)

Regularities of the impact of item shape on electromagnetic field of welding current (Chigarev V.V., Shchetinina V.I., Shchetinin S.V. and Fedun V.I.)

### Cast iron

Main aspects of weldability of structural cast irons (Gretsky Yu.Ya.)

### Cladding

Economic effectiveness of railway wheel profile restoration (Matveev V.V.)

Effect of graphite on kinetics of transfer of carbon to weld pool in flux-cored wire cladding (Zhudra A.P., Krivchikov S.Yu. and Petrov V.V.)

Effect of phosphorus on crack resistance of low-carbon deposited metal (Ryabtsev I.I., Kuskov Yu.M. and Novikova D.P.)

Effect of silicon on properties of low-alloy carbon deposited metal (Zhudra A.P., Krivchikov S.Yu. and Petrov V.V.)

Energy characteristics of low-amperage arcs (Yushchenko K.A., Chervyakov N.O. and Kalina P.P.)

Extension of service life of column equipment at oil refineries (Chekotilo L.V., Bulat A.V., Lebedevich Ya.B., Zvyagintseva A.V., Danilov Yu.B., Kachanov V.A., Kabashny A.I., Ivanuna S.M., Shepel T.E., Gvozdkova E.K. and Kozin Yu.V.)

Improvement of quality of deposited metal in plasma-MIG cladding of aluminium alloys (Chigarev V.V., Kondrashov K.A. and Granovsky N.A.)

Influence of ESC parameters on the quality of reconditioned gear teeth (Kozulin S.M., Sushchuk-Slyusarenko I.I. and Lychko I.I.)

Laser-microplasma alloying and coating of steel (Shelyagin V.D., Khaskin V.Yu. and Pereverzev Yu.N.)

Sensitivity of  $\delta$ -ferrite formation to FCAW process parameters in stainless steel claddings (Palani P.K. and Murugan N.)

### Coatings

Aluminoceramic plasma coatings (Borisov Yu.S., Golnik V.F., Ipatova Z.G., Mits I.V., Saakov A.G. and Saakov V.A.)

Anticorrosion protection of base metal structures by metallised coatings (Review) (Murashov A.P., Demianov I.A., Borisov Yu.S., Zhadkevich M.L. and Golnik V.F.)

Dynamics of movement and heating of powder in detonation spraying of coatings (Ulshin V.A., Kharlamov M.Yu., Borisov Yu.S. and Astakhov E.A.)

Effect of heat treatment on structure of amorphised detonation Fe-B coatings (Astakhov E.A., Borisov Yu.S., Kaplina G.S., Kokerina N.N., Ipatova Z.G. and Chernyakov O.F.)

Features of welding products with protective enamel coatings (Savitsky A.M., Vashchenko V.N. and Bobrov I.V.)

Initiation and re-distribution of internal stresses in electric arc coatings during their formation (Pokhmursky V.I., Student M.M., Dovgunyk V.M., Sidorak I.I., Dzioba Yu.V. and Ryabtsev I.A.)

Laser-microplasma alloying and coating of steel (Shelyagin V.D., Khaskin V.Yu. and Pereverzev Yu.N.)

Magnetic control of low-temperature plasma flows in the processes of thermal spraying of coatings (Pashchenko V.N. and Solodky S.P.)

Structure and properties of powders of Al-Cu-Fe system alloy for thermal spraying of quasi-crystalline coatings (Borisova A.L., Tunik A.Yu. and Adeeva L.I.)

Thermal spray screen coatings for personal computers (Murashov A.P., Demianov I.A., Demianov A.I., Provozin A.P. and Soldatenko G.T.)

### Consumables

Comparative analysis of application of covered electrodes for major repairs at main oil pipelines (Zavalinich D.A., Dzyuba V.M., Lozovoj V.G. and Storozhik D.L.)

Content of acicular ferrite in weld metal in wet welding (Maksimov S.Yu. and Krazhanovsky D.V.)

Design-experimental assessment of the features of electrode melting and transfer process (Chigarev V.V., Belik A.G. and Sergienko Yu.V.)

Effect of graphite on kinetics of transfer of carbon to weld pool in flux-cored wire cladding (Zhudra A.P., Krivchikov S.Yu. and Petrov V.V.)

Flux-cored wire for electric-arc metallizing of the surface of working rolls of the cold rolling mill tempering stand (Royanov V.A., Matvienko V.N., Stepnov K.K., Semyonov V.P., Zavarika N.G., Zakharova I.V. and Klimanchuk V.V.)

Flux-cored wire for strengthening the necks and fillets of mill rolls (Matvienko V.N.)

Flux-cored wire for surfacing of maraging steel layer (Kondratiev I.A., Ryabtsev I.A. and Chernyak Ya.P.)

Improvement of weld strength in arc welding of Al-Cu alloys with application of Sc-containing fillers (Poklyatsky A.G., Lozovskaya A.V., Grinyuk A.A., Yavorskaya M.R. and Chajka A.A.)

Improvement of welding consumables and technologies for increased safety and life of NPS with WWER reactors (Gorynin I.V., Karzov G.P., Timofeev B.T. and Galyatkin S.N.)

Influence of alloying of filler material and welded steel on fusion zone structure (Skulsky V.Yu.)

Influence of electric arc metallizing modes and compositions of applied flux-cored wires on structure and abrasive wear resistance of coatings (Pokhmursky V.I., Student M.M., Ryabtsev I.A., Sidorak I.I., Dzioba Yu.V., Dovgunyk V.M. and Formanek B.)

Influence of oxygen potential of welding fluxes on solid solution alloying in weld metal (Golovko V.V.)

Main aspects of weldability of structural cast irons (Gretsky Yu.Ya.)

Methods to lower the hydrogen content in metal of welded joints of low-alloyed steels in submerged-arc welding (Golovko V.V.)

Peculiarities of the process of microplasma wire spraying (Borisov Yu.S., Kislitsa A.N. and Vojnarovich S.G.)

Production and application of flux-cored wire in Ukraine (Rosert R. and Alimov A.)

Production of welding consumables in 2005 in the CIS countries

Reactivity of ferroalloys in liquid glass (Skorina N.V. and Marchenko A.E.)

Sanitarian-hygienic characteristics of welding fluxes with locally changed chemical composition of grains (Kuzmenko V.G. and Guzej V.I.)

Single-pass arc welding of thick metal using embedded electrode (Kuzmenko G.V., Kuzmenko V.G., Galinich V.I., Otrokov V.V. and Laktionov M.A.)

Sparsely alloyed consumables providing in the deposited metal deformation hardening in operation (Malinov V.L.)

Structure and cold resistance of welded joints in steel 09G2S after repair welding (Poznyakov V.D., Kasatkin S.B. and Dovzhenko V.A.)

Structure and properties of a joint of 10Kh13G18D + 09G2S steels (Gedrovich A.I., Tkachenko A.N. and Tkachenko S.A.)

Structure and properties of powders of Al-Cu-Fe system alloy for thermal spraying of quasi-crystalline coatings (Borisova A.L., Tunik A.Yu. and Adeeva L.I.)

Surfacing consumables for hardening of parts operating under impact-abrasive wear conditions (Balin A.N., Berezovsky A.V., Vishnevsky A.A. and Kulishenko B.A.)

The Chair of Welding Equipment and Technology is 60 years (Royanov V.A.)

Welded freight bogie bolster project (Makhnenko V.I., Garf E.F., Rimsky S.T., Galinich V.I., Makhnenko O.V., Yukhimets P.S., Bubnov V.M., Tusikov E.K. and Varenchuk P.A.)

## Control systems

Application of object-oriented design in development of welding TPACS (Kisilevsky F.N., Dolinenko V.V. and Nikiforov A.Yu.)

4

Calculation of induction of controlling longitudinal magnetic field with consideration for magnetic properties of core, wire and work-piece as applied to arc surfacing (Razmyshlyayev A.D., Deli A.A. and Mironova M.V.)

8

Magnetic control of low-temperature plasma flows in the processes of thermal spraying of coatings (Pashchenko V.N. and Solodky S.P.)

6

On neural network application for welded joint quality control in underwater welding (Skachkov I.O., Pirumov A.E., Maksimov S.Yu. and Prilipko E.A.)

6

Power sources with improved performance for AC arc welding (Zaruba I.I., Dymenko V.V., Andreev V.V. and Shatan A.F.)

7

Schematic for control of welding machine drives (Lankin Yu.N., Masalov Yu.A. and Bajshtruk E.N.)

7

## Controlling electromagnetic field

Calculation of induction of controlling longitudinal magnetic field with consideration for magnetic properties of core, wire and work-piece as applied to arc surfacing (Razmyshlyayev A.D., Deli A.A. and Mironova M.V.)

8

External electromagnetic effects in the processes of arc welding and surfacing (Review) (Ryzhov R.N. and Kuznetsov V.D.)

10

Regularities of the impact of item shape on electromagnetic field of welding current (Chigarev V.V., Shchetinina V.I., Shchetinin S.V. and Fedun V.I.)

8

## Corrosion resistance

Aluminoceramic plasma coatings (Borisov Yu.S., Golnik V.F., Ipatova Z.G., Mits I.V., Saakov A.G. and Saakov V.A.)

7

Anticorrosion protection of base metal structures by metallised coatings (Review) (Murashov A.P., Demianov I.A., Borisov Yu.S., Zhadkevich M.L. and Golnik V.F.)

12

Cavitation-corrosion resistance of surfaced parts of compressors of titanium-and-magnesium production process (Patyupkin A.V. and Bykovsky O.G.)

12

Extension of service life of a pipeline with defects on the inner surface (Yukhimets P.S., Kobelsky S.V., Kravchenko V.I., Klimenko I.A. and Lesovets V.P.)

3

Forecasting cavitation-corrosion resistance of deposited metal of Fe-Cr-Ni-(Mo) alloying systems in 92 % solution of sulfuric acid (Patyupkin A.V. and Antonyuk D.A.)

11

## Crack resistance

Effect of phosphorus on crack resistance of low-carbon deposited metal (Ryabtsev I.I., Kuskov Yu.M. and Novikova D.P.)

5

Effect of silicon on properties of low-alloy carbon deposited metal (Zhudra A.P., Krivchikov S.Yu. and Petrov V.V.)

8

Evaluation of crack resistance of welded joint metal based on the results of standard mechanical tests with regard for the dimensions of structural elements (Girenko V.S., Rabkina M.D. and Girenko S.V.)

6

Main aspects of weldability of structural cast irons (Gretsky Yu.Ya.)

9

Modelling of the shock wave process in local pulsed treatment of plane samples using ring charges (Palamarchuk B.I., Pashchin N.A., Malakhov A.T., Cherkashin A.V., Manchenko A.N. and Chajka A.A.)

3

Role of peak stresses in formation of cold cracks in welded joints of hardenable steels (Sterenbogen Yu.A., Vasiliev D.V., Demchenko E.L. and Novikova D.P.)

4

Welded freight bogie bolster project (Makhnenko V.I., Garf E.F., Rimsky S.T., Galinich V.I., Makhnenko O.V., Yukhimets P.S., Bubnov V.M., Tusikov E.K. and Varenchuk P.A.)

4

## Developed at PWI

1-12

## Dissimilar joints

Influence of alloying of filler material and welded steel on fusion zone structure (Skulsky V.Yu.)

1

Properties of CO<sub>2</sub>-laser welded joints of dissimilar magnesium alloys (Kalita W., Kolodziejczak P., Kwiatkowski L., Grobelny M. and Hoffman J.)

7

Resistance welding of aluminium-steel transition pieces using deformable composite interlayers (Kuchuk-Yatsenko V.S., Lozovskaya A.V., Nakonechny A.A. and Sakhatsky A.G.)

8

Structure and properties of a joint of 10Kh13G18D + 09G2S steels (Gedrovich A.I., Tkachenko A.N. and Tkachenko S.A.)

12

Technology of EBW of the stainless steel-aluminium alloy welded joints (Bondarev A.A. and Ishchenko A.Ya.)

12

## Electron speckle-interferometry

Procedure for determination of residual stresses in welded joints and structural elements using electron speckle-interferometry (Lobanov L.M., Pivtorak V.A., Savitsky V.V. and Tkachuk G.I.)

1

## Equipment

Algorithm of automatic orientation of manipulation robot relative to tested surfaces (Tsybulkin G.A.)

3

Calculation of induction of controlling longitudinal magnetic field with consideration for magnetic properties of core, wire and work-piece as applied to arc surfacing (Razmyshlyayev A.D., Deli A.A. and Mironova M.V.)

8

Characteristics of pulsed plasma flow in plasma-detonation generator at different flow rates of fuel mixture (Zhadkevich M.L., Tyurin Yu.N., Kolisnichenko O.V. and Mazunin V.M.)

11

Computer system of electron beam and laser welding modeling (Lopota V.A., Turichin G.A., Valdajtseva E.A., Malkin P.E. and Gumenyuk A.V.)

4

Current trends in development of technological lasers (Garashchuk V.P. and Shelyagin V.D.)

2

Effect of parameters of plasma detonation unit discharge circuit on gas-dynamic characteristics of pulsed plasma flows (Zhadkevich M.L., Tyurin Yu.N., Kolisnichenko O.V. and Mazunin V.M.)

8

Ensuring safe operation of equipment for flame treatment of metal (Sergienko V.A. and Yumatova V.I.)

10

Improvement of quality of deposited metal in plasma-MIG cladding of aluminium alloys (Chigarev V.V., Kondrashov K.A. and Granovsky N.A.)

6

Lowering of material content of power sources and power consumption in welding (Paton B.E., Zaruba I.I., Dymenko V.V. and Shatan A.F.)

10

Modern mechanisms of electrode wire feed in machines for mechanized welding, surfacing and cutting (Lebedev V.A. and Pritula S.I.)

4

New machine for studding of heating surfaces (Zhuk G.V., Lukianets B.M. and Mazur S.V.)

3

Optimization of transformer with developed transverse magnetic leakage fluxes and magnetic shunt (Rymar S.V.)

5

Peculiarities of the process of microplasma wire spraying (Borisov Yu.S., Kislitsa A.N. and Vojnarovich S.G.)

4

Power sources with improved performance for AC arc welding (Zaruba I.I., Dymenko V.V., Andreev V.V. and Shatan A.F.)

7

Schematic for control of welding machine drives (Lankin Yu.N., Masalov Yu.A. and Bajshtruk E.N.)

7

Simferopol Electric Machine-Building Plant SELMA mastered production of low voltage universal welding converters KSU-320

3

System of laser following of weld reinforcement (Kiselevsky F.N., Shapovalov E.V. and Kolyada V.A.)

1

The Chair of Welding Equipment and Technology is 60 years (Royanov V.A.)

8

## Fatigue resistance

Improvement of fatigue resistance of welded joints in metal structures by high-frequency mechanical peening (Review) (Lobanov L.M., Kirian V.I., Knysh V.V. and Prokopenko G.I.)

9

Increasing fatigue resistance of welded joints by high-frequency mechanical peening (Knysh V.V., Kuzmenko A.Z. and Vojtenko O.V.)

1

Modelling of the shock wave process in local pulsed treatment of plane samples using ring charges (Palamarchuk B.I., Pashchin N.A., Malakhov A.T., Cherkashin A.V., Manchenko A.N. and Chajka A.A.)

Welded freight bogie bolster project (Makhnenko V.I., Garf E.F., Rimsky S.T., Galinich V.I., Makhnenko O.V., Yukhimets P.S., Bubnov V.M., Tusikov E.K. and Varenchuk P.A.)

### Fracture resistance

Influence of structural transformations in welding of aluminium alloy B96 on fracture resistance parameters (Labur T.M., Taranova T.G., Kostin V.A., Ishchenko A.Ya., Grigorenko G.M. and Fedorchuk V.E.)

Role of peak stresses in formation of cold cracks in welded joints of hardenable steels (Stereobogen Yu.A., Vasiliev D.V., Demchenko E.L. and Novikova D.P.)

### Gas turbine blades

Application of reconditioning technologies to extend the life of gas turbine engines (analysis of state-of-the-art and development) (Zhadkevich A.M.)

Repair welding of titanium blades of gas turbine engine compressors (Zamkov V.N., Vrzhezhevsky E.L., Topolsky V.F. and Petrichenko I.K.)

### Hybrid technologies

Application of high-power fibre lasers in laser and laser-MIG hybrid welding (Thomy C., Kohn H. and Vollertsen F.)

Basics and applications of laser-GMA hybrid welding (Thomy C. and Seefeld T.)

Laser-microplasma alloying and coating of steel (Shelyagin V.D., Khaskin V.Yu. and Pereverzev Yu.N.)

Residual stresses in butt joints of thin sheets from alloy AMg6 after arc and laser-arc welding (Shonin V.A., Mashin V.S., Khaskin V.Yu. and Nedej T.N.)

Structural heredity in the initial materials-metal melt-solid metal system (Review) (Ryabtsev I.A.)

### In memory of Dr. Sossenheimer

### Laser technologies

Application of high-power fibre lasers in laser and laser-MIG hybrid welding (Thomy C., Kohn H. and Vollertsen F.)

Current trends in development of technological lasers (Garashchuk V.P. and Shelyagin V.D.)

Glass joining technologies and examples of their application (Koebler G., Mueller G., Basler U., Dahms St., Luhn R., Kasch S. and Waechter S.)

High power diode laser welding of aluminum alloy ENAW-1050A (Klimpel A., Lisecki A., Janicki D. and Stano S.)

Laser-microplasma alloying and coating of steel (Shelyagin V.D., Khaskin V.Yu. and Pereverzev Yu.N.)

Laser welding and formability study of tailor-welded blanks of different thickness combinations and welding orientations (Cheng C.H., Chan L.D., Chow C.L. and Lee D.C.)

Technological characteristics of laser beam for cutting and welding (Garashchuk V.P.)

### Metallizing

Anticorrosion protection of base metal structures by metallized coatings (Review) (Murashov A.P., Demianov I.A., Borisov Yu.S., Zhadkevich M.L. and Golnik V.F.)

Flux-cored wire for electric-arc metallizing of the surface of working rolls of the cold rolling mill tempering stand (Royanov V.A., Matvienko V.N., Stepanov K.K., Semyonov V.P., Zavarika N.G., Zakharova I.V. and Klimanchuk V.V.)

Influence of electric arc metallizing modes and compositions of applied flux-cored wires on structure and abrasive wear resistance of coatings (Pokhmursky V.I., Student M.M., Ryabtsev I.A., Sidorak I.I., Dzioba Yu.V., Dovgunyk V.M. and Formanek B.)

### Modelling

Calculation of the kinetics of diffusion phase transformations in low-alloyed steels in beam welding (Dilthey U., Gumenyuk A.V. and Turichin G.A.)

Computer system of electron beam and laser welding modeling (Lopota V.A., Turichin G.A., Valdajtseva E.A., Malkin P.E. and Gumenyuk A.V.)

Effect of parameters of plasma detonation unit discharge circuit on gas-dynamic characteristics of pulsed plasma flows (Zhadkevich M.L., Tyurin Yu.N., Kolisnichenko O.V. and Mazunin V.M.)

Energy characteristics of low-amperage arcs (Yushchenko K.A., Chervyakov N.O. and Kalina P.P.)

Dynamics of movement and heating of powder in detonation spraying of coatings (Ulshin V.A., Kharlamov M.Yu., Borisov Yu.S. and Astakhov E.A.)

Features of  $\delta$ -ferrite formation on the fusion boundary in welding heat-resistant chromium martensitic steel (Skulsky V.Yu.)

Forecasting cavitation-corrosion resistance of deposited metal of Fe-Cr-Ni-(Mo) alloying systems in 92 % solution of sulfuric acid (Patyupkin A.V. and Antonyuk D.A.)

Influence of structural transformations in welding of aluminium alloy B96 on fracture resistance parameters (Labur T.M., Taranova T.G., Kostin V.A., Ishchenko A.Ya., Grigorenko G.M. and Fedorchuk V.E.)

Mathematical model for MAG welding in a manufacturing environment (Ohji T., Miyasaka F., Yamamoto T. and Tsuji Y.)

Modelling of the shock wave process in local pulsed treatment of plane samples using ring charges (Palamarchuk B.I., Pashchin N.A., Malakhov A.T., Cherkashin A.V., Manchenko A.N. and Chajka A.A.)

Numerical modelling of absorption of gases by deposited metal in wet underwater welding (Portnov O.M. and Maksimov S.Yu.)

Optimization of transformer with developed transverse magnetic leakage fluxes and magnetic shunt (Rymar S.V.)

### Nano-structured materials

Application of nano-structured materials for diffusion bonding of heat-resistant nickel alloys (Yushchenko K.A., Zadery B.A., Zvyagintseva A.V., Kushnaryova T.N., Nesmikh V.S., Polishchuk E.P. and Savchenko V.S.)

Effect of heat treatment on structure of amorphised detonation Fe-B coatings (Astakhov E.A., Borisov Yu.S., Kaplina G.S., Kokorina N.N., Ipatova Z.G. and Chernyakov O.F.)

Technology of EBW of the stainless steel-aluminium alloy welded joints (Bondarev A.A. and Ishchenko A.Ya.)

### NDT

Procedure for determination of residual stresses in welded joints and structural elements using electron speckle-interferometry (Lobanov L.M., Pivtorak V.A., Savitsky V.V. and Tkachuk G.I.)

Structure of welded joints in tungsten single crystals (Yushchenko K.A., Zadery B.A., Kotenko S.S., Polishchuk E.P. and Karasevskaya O.P.)

System of laser following of weld reinforcement (Kiselevsky F.N., Shapovalov E.V. and Kolyada V.A.)

### News

Congratulation of jubilee persons

59th Annual assembly of the International Institute of Welding

### Patents in the field of welding production

### Pipelines

Comparative analysis of application of covered electrodes for major repairs at main oil pipelines (Zavalinich D.A., Dzyuba V.M., Lozovoj V.G. and Storozhik D.L.)

Development and certification of automatic narrow-gap argon-arc welding technology of MCP Dn850 elements at NPP (Tsaryuk A.K., Skulsky V.Yu., Kasperovich I.L., Byvalkevich A.I., Ostashko T.V., Zhukov V.V., Dudkin S.N., Ivanov N.A., Miroshnichenko A.P., Nemlej N.V. and Bazhukov A.V.)

Evaluation of remaining life of welded joints of pipelines for thermal power plants (Dmitrik V.V., Tsaryuk A.K., Bugaets A.A. and Grinchenko E.D.)	2	Personnel training at the PSTU Welding Department (Razmyshlyayev A.D. and Shaferovsky V.A.)	8
Extension of service life of a pipeline with defects on the inner surface (Yukhimets P.S., Kobelsky S.V., Kravchenko V.I., Klimenko I.A. and Lesovets V.P.)	3	The Chair of Welding Equipment and Technology is 60 years (Royanov V.A.)	8
Methodology for control of fitness for purpose of flash butt welded joints in pipelines (Kuchuk-Yatsenko S.I., Kirian V.I., Kazymov B.I. and Khomenko V.I.)	10	<b>Spraying</b>	
<b>Power plant units</b>		Aluminoceramic plasma coatings (Borisov Yu.S., Golnik V.F., Ipatova Z.G., Mits I.V., Saakov A.G. and Saakov V.A.)	7
Development and certification of automatic narrow-gap argon-arc welding technology of MCP Dn850 elements at NPP (Tsaryuk A.K., Skulsky V.Yu., Kasperovich I.L., Byvalkevich A.I., Ostashko T.V., Zhukov V.V., Dudkin S.N., Ivanov N.A., Miroshnichenko A.P., Nemlej N.V. and Bazhukov A.V.)	5	Anticorrosion protection of base metal structures by metallised coatings (Review) (Murashov A.P., Demianov I.A., Borisov Yu.S., Zhadkevich M.L. and Golnik V.F.)	12
Evaluation of remaining life of welded joints of pipelines for thermal power plants (Dmitrik V.V., Tsaryuk A.K., Bugaets A.A. and Grinchenko E.D.)	2	Characteristics of pulsed plasma flow in plasma-detonation generator at different flow rates of fuel mixture (Zhadkevich M.L., Tyurin Yu.N., Kolisnichenko O.V. and Mazunin V.M.)	11
Improvement of welding consumables and technologies for increased safety and life of NPS with WWER reactors (Gorynin I.V., Karzov G.P., Timofeev B.T. and Galyatkin S.N.)	3	Dynamics of movement and heating of powder in detonation spraying of coatings (Ulshin V.A., Kharlamov M.Yu., Borisov Yu.S. and Astakhov E.A.)	9
New machine for studding of heating surfaces (Zhuk G.V., Lukianets B.M. and Mazur S.V.)	3	Effect of heat treatment on structure of amorphised detonation Fe-B coatings (Astakhov E.A., Borisov Yu.S., Kaplina G.S., Kokorina N.N., Ipatova Z.G. and Chernyakov O.F.)	11
<b>PWI activity</b>		Gas-abrasive wear resistance of thermal spray coatings of Al-Cu-Fe system alloys containing quasi-crystalline phase (Borisov Yu.S., Borisova A.L., Golnik V.F. and Ipatova Z.G.)	5
Cooperation between PWI and Brazilian Welding Society	7	Initiation and re-distribution of internal stresses in electric arc coatings during their formation (Pokhmursky V.I., Student M.M., Dovgunyk V.M., Sidorak I.I., Dzioba Yu.V. and Ryabtsev I.A.)	10
Cooperation raises investigation efficiency and reduces costs	9	Laser-microplasma alloying and coating of steel (Shelyagin V.D., Khaskin V.Yu. and Pereverzev Yu.N.)	2
«Know-how» and how to use it (Sidoruk V.S.)	8	Magnetic control of low-temperature plasma flows in the processes of thermal spraying of coatings (Pashchenko V.N. and Solodky S.P.)	6
The E.O. Paton Electric Welding Institute Technological Park is 5 years (Mazur A.A.)	3	On heating and acceleration of disperse particles with pulse plasma (Zhadkevich M.L., Tyurin Yu.N., Kolisnichenko O.V. and Mazunin V.M.)	7
<b>Quality control</b>		Peculiarities of the process of microplasma wire spraying (Borisov Yu.S., Kislitsa A.N. and Vojnarovich S.G.)	4
On neural network application for welded joint quality control in underwater welding (Skachkov I.O., Pirumov A.E., Maksimov S.Yu. and Prilipko E.A.)	6	Structure and properties of powders of Al-Cu-Fe system alloy for thermal spraying of quasi-crystalline coatings (Borisova A.L., Tunik A.Yu. and Adeeva L.I.)	12
Procedure for determination of residual stresses in welded joints and structural elements using electron speckle-interferometry (Lobanov L.M., Pivtorak V.A., Savitsky V.V. and Tkachuk G.I.)	1	Thermal spray screen coatings for personal computers (Murashov A.P., Demianov I.A., Demianov A.I., Provozin A.P. and Soldatenko G.T.)	5
<b>Sanitarian-hygienic problems</b>		<b>Steels</b>	
Problems of welders' labour safety (Levchenko O.G. and Pavlyk A.O.)	12	<i>Controlled-rolled steels</i>	
Sanitarian-hygienic characteristics of welding fluxes with locally changed chemical composition of grains (Kuzmenko V.G. and Guzej V.I.)	2	Accelerated induction heat treatment of welds on pipes from controlled-rolled steels (Kuchuk-Yatsenko S.I., Pismenny A.S., Shilov M.E., Kazymov B.I. and Zagadarchuk V.F.)	3
<b>Service life</b>		<i>Hardenable steels</i>	
Extension of service life of a pipeline with defects on the inner surface (Yukhimets P.S., Kobelsky S.V., Kravchenko V.I., Klimenko I.A. and Lesovets V.P.)	3	Role of peak stresses in formation of cold cracks in welded joints of hardenable steels (Sterenbogen Yu.A., Vasiliev D.V., Demchenko E.L. and Novikova D.P.)	4
Extension of service life of column equipment at oil refineries (Cherotilo L.V., Bulat A.V., Lebedevich Ya.B., Zvyagintseva A.V., Danilov Yu.B., Kachanov V.A., Kabashny A.I., Ivanuna S.M., Shepel T.E., Gvozdkikova E.K. and Kozin Yu.V.)	10	<i>Heat-resistant steels</i>	
Improvement of welding consumables and technologies for increased safety and life of NPS with WWER reactors (Gorynin I.V., Karzov G.P., Timofeev B.T. and Galyatkin S.N.)	3	Effect of the degree of alloying of heat-resistant chromium steels on hardness of metal within the welded joint zone (Skulsky V.Yu.)	9
<b>Soldering</b>		Evaluation of remaining life of welded joints of pipelines for thermal power plants (Dmitrik V.V., Tsaryuk A.K., Bugaets A.A. and Grinchenko E.D.)	2
Calculation technique for defining parameters of soldered seam solidification (Denisevich E.A.)	9	Features of $\delta$ -ferrite formation on the fusion boundary in welding heat-resistant chromium martensitic steel (Skulsky V.Yu.)	11
Flame soldering for joining microelements to printed circuit boards (Pavlyuk S.P., Kutlin G.N., Kislitsyn V.M. and Musin A.G.)	3	Influence of electrodynamic treatment on the stress-strain state of heat-resistant steels (Lobanov L.M., Pashchin N.A., Skulsky V.Yu. and Loginov V.P.)	5
Glass joining technologies and examples of their application (Koebler G., Mueller G., Basler U., Dahms St., Luhn R., Kasch S. and Waechter S.)	7	<i>High-strength steels</i>	
<b>Specialist training</b>		Selection of steel for critical building welded structures (Kovtunen V.A., Gerasimenko A.M. and Gotsulyak A.A.)	11
Efficient organisational structures for training welding specialists for ship building (Kvasnitsky V.F., Kostin A.M., Romanchuk N.P. and Chernov S.K.)	4	Variations in structure and properties of HAZ metal in welded joints on steel 30KhGSA in arc treatment (Kulik V.M. and Vasiliev V.G.)	7

### Low alloy steels

Calculation of the kinetics of diffusion phase transformations in low-alloyed steels in beam welding (Dilthey U., Gumenyuk A.V. and Turichin G.A.)

Improvement of welding consumables and technologies for increased safety and life of NPS with WWER reactors (Gorynin I.V., Karzov G.P., Timofeev B.T. and Galyatkin S.N.)

Influence of oxygen potential of welding fluxes on solid solution alloying in weld metal (Golovko V.V.)

Methods to lower the hydrogen content in metal of welded joints of low-alloyed steels in submerged-arc welding (Golovko V.V.)

Structure and cold resistance of welded joints in steel 09G2S after repair welding (Poznyakov V.D., Kasatkin S.B. and Dovzhenko V.A.)

Structure changes in HAZ metal of steel X60 welded joints in underwater welding (Maksimov S.Yu., But V.S., Vasiliev V.G., Zakharov S.M. and Zajtseva N.V.)

### Maraging steels

Flux-cored wire for surfacing of maraging steel layer (Kondratiev I.A., Ryabtsev I.A. and Chernyak Ya.P.)

### Rail steels

Features of formation of structure of joints of rail steel M76 to steel 110G13L made by flash-butt welding (Kuchuk-Yatsenko S.I., Shvets V.I., Gordan G.N., Shvets Yu.V. and Goronkov N.D.)

### Stainless steels

Basics and applications of laser-GMA hybrid welding (Thomy C. and Seefeld T.)

Cavitation-corrosion resistance of surfaced parts of compressors of titanium-and-magnesium production process (Patyupkin A.V. and Bykovsky O.G.)

Role of keyhole in formation of deep penetration in A-TIG welding of stainless steel (Paton B.E., Yushchenko K.A., Kovalenko D.V., Krivtsov I.V., Demchenko V.F. and Kovalenko I.V.)

Sensitivity of  $\delta$ -ferrite formation to FCAW process parameters in stainless steel claddings (Palani P.K. and Murugan N.)

### Strains and stresses

Design and features of fabrication technology of a large-sized transformable shell structure (Paton B.E., Lobanov L.M., Samilov V.N., Pilishenko I.S., Makhnenko O.V., Pashchin N.A., Gorinov V.A. and Shiyani K.V.)

Improvement of fatigue resistance of welded joints in metal structures by high-frequency mechanical peening (Review) (Lobanov L.M., Kirian V.I., Knysh V.V. and Prokopenko G.I.)

Increasing fatigue resistance of welded joints by high-frequency mechanical peening (Knysh V.V., Kuzmenko A.Z. and Vojtenko O.V.)

Influence of electrodynamic treatment on the stress-strain state of heat-resistant steels (Lobanov L.M., Pashchin N.A., Skulsky V.Yu. and Loginov V.P.)

Initiation and re-distribution of internal stresses in electric arc coatings during their formation (Pokhmursky V.I., Student M.M., Dovgunyk V.M., Sidorak I.I., Dzioba Yu.V. and Ryabtsev I.A.)

Low stress no distortion welding based on thermal tensioning effects for thin materials (Guan Q., Guo D.L., Zhang C.X. and Li J.)

Modelling of the shock wave process in local pulsed treatment of plane samples using ring charges (Palamarchuk B.I., Pashchin N.A., Malakhov A.T., Cherkashin A.V., Manchenko A.N. and Chajka A.A.)

Procedure for determination of residual stresses in welded joints and structural elements using electron speckle-interferometry (Lobanov L.M., Pivtorak V.A., Savitsky V.V. and Tkachuk G.I.)

Residual stresses in butt joints of thin sheets from alloy AMg6 after arc and laser-arc welding (Shonin V.A., Mashin V.S., Khaskin V.Yu. and Nedej T.N.)

Role of peak stresses in formation of cold cracks in welded joints of hardenable steels (Stereobogen Yu.A., Vasiliev D.V., Demchenko E.L. and Novikova D.P.)

Welded freight bogie bolster project (Makhnenko V.I., Garf E.F., Rimsky S.T., Galinich V.I., Makhnenko O.V., Yuchimets P.S., Bubnov V.M., Tusikov E.K. and Varenchuk P.A.)

### Structure-phase transformations

Abrasive wear behaviour of Fe-Cr-C overlays (Shah K.B., Kumar S. and Dwivedi D.K.)

Application of nano-structured materials for diffusion bonding of heat-resistant nickel alloys (Yushchenko K.A., Zadery B.A., Zvyagintseva A.V., Kushnaryova T.N., Nesmikh V.S., Polishchuk E.P. and Savchenko V.S.)

Calculation of the kinetics of diffusion phase transformations in low-alloyed steels in beam welding (Dilthey U., Gumenyuk A.V. and Turichin G.A.)

Cavitation-corrosion resistance of surfaced parts of compressors of titanium-and-magnesium production process (Patyupkin A.V. and Bykovsky O.G.)

Content of acicular ferrite in weld metal in wet welding (Maksimov S.Yu. and Krazhanovsky D.V.)

Effect of scandium additions on fine structure of weld metal in aluminium alloy 1460 welded joints (Markashova L.I., Grigorenko G.M., Ishchenko A.Ya., Lozovskaya A.V. and Kushnaryova O.S.)

Effect of scandium additions on structure-phase condition of weld metal produced by welding aluminium alloy 1460 (Markashova L.I., Grigorenko G.M., Ishchenko A.Ya., Lozovskaya A.V., Kushnaryova O.S., Alekseenko T.A. and Chajka A.A.)

Effect of scandium additions on structure-phase state of weld metal in aluminium alloy joints after heat treatment (Markashova L.I., Grigorenko G.M., Lozovskaya A.V., Kushnaryova O.S. and Fedorchuk V.E.)

Effect of silicon on properties of low-alloy carbon deposited metal (Zhudra A.P., Krivchikov S.Yu. and Petrov V.V.)

Effect of the degree of alloying of heat-resistant chromium steels on hardness of metal within the welded joint zone (Skulsky V.Yu.)

Evaluation of remaining life of welded joints of pipelines for thermal power plants (Dmitrik V.V., Tsaryuk A.K., Bugaets A.A. and Grinchenko E.D.)

Features of formation of structure of joints of rail steel M76 to steel 110G13L made by flash-butt welding (Kuchuk-Yatsenko S.I., Shvets V.I., Gordan G.N., Shvets Yu.V. and Goronkov N.D.)

Features of  $\delta$ -ferrite formation on the fusion boundary in welding heat-resistant chromium martensitic steel (Skulsky V.Yu.)

Influence of alloying of filler material and welded steel on fusion zone structure (Skulsky V.Yu.)

Influence of electric arc metallizing modes and compositions of applied flux-cored wires on structure and abrasive wear resistance of coatings (Pokhmursky V.I., Student M.M., Ryabtsev I.A., Sidorak I.I., Dzioba Yu.V., Dovgunyk V.M. and Formanek B.)

Influence of structural transformations in welding of aluminium alloy B96 on fracture resistance parameters (Labur T.M., Taranova T.G., Kostin V.A., Ishchenko A.Ya., Grigorenko G.M. and Fedorchuk V.E.)

Sensitivity of  $\delta$ -ferrite formation to FCAW process parameters in stainless steel claddings (Palani P.K. and Murugan N.)

Structural heredity in the initial materials-metal melt-solid metal system (Review) (Ryabtsev I.A.)

Structure and cold resistance of welded joints in steel 09G2S after repair welding (Poznyakov V.D., Kasatkin S.B. and Dovzhenko V.A.)

Structure and properties of a joint of 10Kh13G18D + 09G2S steels (Gedrovich A.I., Tkachenko A.N. and Tkachenko S.A.)

Structure changes in HAZ metal of steel X60 welded joints in underwater welding (Maksimov S.Yu., But V.S., Vasiliev V.G., Zakharov S.M. and Zajtseva N.V.)

Structure of welded joints in tungsten single crystals (Yushchenko K.A., Zadery B.A., Kotenko S.S., Polishchuk E.P. and Karasevskaya O.P.)

Variations in structure and properties of HAZ metal in welded joints on steel 30KhGSA in arc treatment (Kulik V.M. and Vasiliev V.G.)

### Surfacing

Abrasive wear behaviour of Fe–Cr–C overlays (Shah K.B., Kumar S. and Dwivedi D.K.)

Application of reconditioning technologies to extend the life of gas turbine engines (analysis of state-of-the-art and development) (Zhadkevich A.M.)

Calculation of induction of controlling longitudinal magnetic field with consideration for magnetic properties of core, wire and work-piece as applied to arc surfacing (Razmyshlyayev A.D., Deli A.A. and Mironova M.V.)

Cavitation-corrosion resistance of surfaced parts of compressors of titanium-and-magnesium production process (Patyupkin A.V. and Bykovsky O.G.)

Design-experimental assessment of the features of electrode melting and transfer process (Chigarev V.V., Belik A.G. and Sergienko Yu.V.)

External electromagnetic effects in the processes of arc welding and surfacing (Review) (Ryzhov R.N. and Kuznetsov V.D.)

Flux-cored wire for strengthening the necks and fillets of mill rolls (Matvienko V.N.)

Flux-cored wire for surfacing of maraging steel layer (Kondratiev I.A., Ryabtsev I.A. and Chernyak Ya.P.)

Renovation of bodies of energy-absorbing mechanisms of freight railway cars (Snisar V.V., Demchenko E.L., Fenogenov A.I. and Vasiliev D.V.)

Sparsely alloyed consumables providing in the deposited metal deformation hardening in operation (Malinov V.L.)

Structural heredity in the initial materials–metal melt–solid metal system (Review) (Ryabtsev I.A.)

Study of sulfur effect on properties of deposited metal of Kh51 FS type (Osин V.V., Ryabtsev I.A. and Kondratiev I.A.)

Surfacing consumables for hardening of parts operating under impact-abrasive wear conditions (Balin A.N., Berezovsky A.V., Vishnevsky A.A. and Kulishenko B.A.)

Temperature and geometrical dimensions of weld pool in plasma-powder surfacing (Gladky P.V., Pavlenko A.V. and Pereplyotchikov E.F.)

### Thesis for scientific degree

1, 3–5, 7, 11, 12

### Treatment

Accelerated induction heat treatment of welds on pipes from controlled-rolled steels (Kuchuk-Yatsenko S.I., Pismenny A.S., Shinlov M.E., Kazymov B.I. and Zagadarchuk V.F.)

Effect of heat treatment on structure of amorphised detonation Fe–B coatings (Astakhov E.A., Borisov Yu.S., Kaplina G.S., Kokorina N.N., Ipatova Z.G. and Chernyakov O.F.)

Effect of scandium additions on structure-phase state of weld metal in aluminium alloy joints after heat treatment (Markashova L.I., Grigorenko G.M., Lozovskaya A.V., Kushnaryova O.S. and Fedorchuk V.E.)

Ensuring safe operation of equipment for flame treatment of metal (Sergienko V.A. and Yumatova V.I.)

Improvement of fatigue resistance of welded joints in metal structures by high-frequency mechanical peening (Review) (Lobanov L.M., Kirian V.I., Knysh V.V. and Prokopenko G.I.)

Increasing fatigue resistance of welded joints by high-frequency mechanical peening (Knysh V.V., Kuzmenko A.Z. and Vojtenko O.V.)

Influence of electrodynamic treatment on the stress-strain state of heat-resistant steels (Lobanov L.M., Pashchin N.A., Skulsky V.Yu. and Loginov V.P.)

Low stress no distortion welding based on thermal tensioning effects for thin materials (Guan Q., Guo D.L., Zhang C.X. and Li J.)

7	Modelling of the shock wave process in local pulsed treatment of plane samples using ring charges (Palamarchuk B.I., Pashchin N.A., Malakhov A.T., Cherkashin A.V., Manchenko A.N. and Chajka A.A.)	3
11	Structural heredity in the initial materials–metal melt–solid metal system (Review) (Ryabtsev I.A.)	11
5	Variations in structure and properties of HAZ metal in welded joints on steel 30KhGSA in arc treatment (Kulik V.M. and Vasiliev V.G.)	7
	<b>Wear resistance</b>	
8	Abrasive wear behaviour of Fe–Cr–C overlays (Shah K.B., Kumar S. and Dwivedi D.K.)	11
8	Aluminoceramic plasma coatings (Borisov Yu.S., Golnik V.F., Ipatova Z.G., Mits I.V., Saakov A.G. and Saakov V.A.)	7
12	Effect of heat treatment on structure of amorphised detonation Fe–B coatings (Astakhov E.A., Borisov Yu.S., Kaplina G.S., Kokorina N.N., Ipatova Z.G. and Chernyakov O.F.)	11
8	Gas-abrasive wear resistance of thermal spray coatings of Al–Cu–Fe system alloys containing quasi-crystalline phase (Borisov Yu.S., Borisova A.L., Golnik V.F. and Ipatova Z.G.)	5
10	Influence of electric arc metallizing modes and compositions of applied flux-cored wires on structure and abrasive wear resistance of coatings (Pokhmursky V.I., Student M.M., Ryabtsev I.A., Sidorak I.I., Dzioba Yu.V., Dovgunyk V.M. and Formanek B.)	7
4	Sparsely alloyed consumables providing in the deposited metal deformation hardening in operation (Malinov V.L.)	8
1	Study of sulfur effect on properties of deposited metal of Kh51 FS type (Osин V.V., Ryabtsev I.A. and Kondratiev I.A.)	12
8	Surfacing consumables for hardening of parts operating under impact-abrasive wear conditions (Balin A.N., Berezovsky A.V., Vishnevsky A.A. and Kulishenko B.A.)	2
	<b>Weld pool</b>	
11	Effect of graphite on kinetics of transfer of carbon to weld pool in flux-cored wire cladding (Zhudra A.P., Krivchikov S.Yu. and Petrov V.V.)	11
12	Energy characteristics of low-amperage arcs (Yushchenko K.A., Chervyakov N.O. and Kalina P.P.)	4
2	Mathematical model for MAG welding in a manufacturing environment (Ohji T., Miyasaka F., Yamamoto T. and Tsuji Y.)	3
6	Role of keyhole in formation of deep penetration in A-TIG welding of stainless steel (Paton B.E., Yushchenko K.A., Kovalenko D.V., Krivtsun I.V., Demchenko V.F. and Kovalenko I.V.)	6
	Temperature and geometrical dimensions of weld pool in plasma-powder surfacing (Gladky P.V., Pavlenko A.V. and Pereplyotchikov E.F.)	6
	<b>Weldability</b>	
3	Features of $\delta$ -ferrite formation on the fusion boundary in welding heat-resistant chromium martensitic steel (Skulsky V.Yu.)	11
11	Main aspects of weldability of structural cast irons (Gretsky Yu.Ya.)	9
6	Selection of steel for critical building welded structures (Kovtunen V.A., Gerasimenko A.M. and Gotsulyak A.A.)	11
10	Technology of EBW of the stainless steel–aluminium alloy welded joints (Bondarev A.A. and Ishchenko A.Ya.)	12
9	Weldability of shape-memory alloys of Ni–Ti system (Paton B.E., Kaleko D.M., Shevchenko V.P., Koval Yu.N., Slipchenko V.N., Neganov L.M. and Musienko R.Ya.)	5
	<b>Welding</b>	
	<i>A-TIG welding</i>	
1	Role of keyhole in formation of deep penetration in A-TIG welding of stainless steel (Paton B.E., Yushchenko K.A., Kovalenko D.V., Krivtsun I.V., Demchenko V.F. and Kovalenko I.V.)	6
5	<i>Beam welding</i>	
12	Calculation of the kinetics of diffusion phase transformations in low-alloyed steels in beam welding (Dilthey U., Gumenyuk A.V. and Turichin G.A.)	2

### Capacitor-type welding

Weldability of shape-memory alloys of Ni-Ti system (Paton B.E., Kaleko D.M., Shevchenko V.P., Koval Yu.N., Slipchenko V.N., Neganov L.M. and Musienko R.Ya.)

5

### Diffusion bonding

Application of nano-structured materials for diffusion bonding of heat-resistant nickel alloys (Yushchenko K.A., Zadery B.A., Zvyagintseva A.V., Kushnaryova T.N., Nesmikh V.S., Polishchuk E.P. and Savchenko V.S.)

11

Glass joining technologies and examples of their application (Koe- hler G., Mueller G., Basler U., Dahms St., Luhn R., Kasch S. and Waechter S.)

7

### EBW

Computer system of electron beam and laser welding modeling (Lopota V.A., Turichin G.A., Valdajtseva E.A., Malkin P.E. and Gumenyuk A.V.)

4

Structure of welded joints in tungsten single crystals (Yushchenko K.A., Zadery B.A., Kotenko S.S., Polishchuk E.P. and Karasevskaya O.P.)

8

Technology of EBW of the stainless steel-aluminium alloy welded joints (Bondarev A.A. and Ishchenko A.Ya.)

12

### Embedded electrode arc welding

Single-pass arc welding of thick metal using using embedded elec- trode (Kuzmenko G.V., Kuzmenko V.G., Galinich V.I., Otrokov V.V. and Laktionov M.A.)

6

### ESW

Electroslag welding of blast furnace housing (Lankin Yu.N., Moska- lenko A.A., Tyukalov V.G., Kuran R.I. and Popov S.V.)

9

### Flash-butt welding

Accelerated induction heat treatment of welds on pipes from con- trolled-rolled steels (Kuchuk-Yatsenko S.I., Pismenny A.S., Shin- lov M.E., Kazymov B.I. and Zagadarchuk V.F.)

3

Features of formation of structure of joints of rail steel M76 to steel 110G13L made by flash-butt welding (Kuchuk-Yatsenko S.I., Shvets V.I., Gordan G.N., Shvets Yu.V. and Goronkov N.D.)

1

Methodology for control of fitness for purpose of flash butt welded joints in pipelines (Kuchuk-Yatsenko S.I., Kirian V.I., Kazymov B.I. and Khomenko V.I.)

10

### GMA welding

Energy characteristics of low-amperage arcs (Yushchenko K.A., Chervyakov N.O. and Kalina P.P.)

4

Improvement of weld strength in arc welding of Al-Cu alloys with application of Sc-containing fillers (Poklyatsky A.G., Lozovskaya A.V., Grinyuk A.A., Yavorskaya M.R. and Chajka A.A.)

2

### Laser welding

Computer system of electron beam and laser welding modeling (Lopota V.A., Turichin G.A., Valdajtseva E.A., Malkin P.E. and Gumenyuk A.V.)

4

Glass joining technologies and examples of their application (Koe- hler G., Mueller G., Basler U., Dahms St., Luhn R., Kasch S. and Waechter S.)

7

High power diode laser welding of aluminum alloy ENAW-1050A (Klimpel A., Lisiecki A., Janicki D. and Stano S.)

9

Laser welding and formability study of tailor-welded blanks of different thickness combinations and welding orientations (Cheng C.H., Chan L.Ö., Chow C.L. and Lee Ö.C.)

6

Properties of CO<sub>2</sub>-laser welded joints of dissimilar magnesium alloys (Kalita W., Kolodziejczak P., Kwiatkowski L., Grobelny M. and Hoffinan J.)

7

Weldability of shape-memory alloys of Ni-Ti system (Paton B.E., Kaleko D.M., Shevchenko V.P., Koval Yu.N., Slipchenko V.N., Neganov L.M. and Musienko R.Ya.)

5

### Narrow-gap welding

Development and certification of automatic narrow-gap argon-arc welding technology of MCP Dn850 elements at NPP (Tsaryuk A.K., Skulsky V.Yu., Kasperovich I.L., Byvalkevich A.I., Ostashko T.V., Zhukov V.V., Dudkin S.N., Ivanov N.A., Miroshnichenko A.P., Nemlej N.V. and Bazhukov A.V.)

5

### Plasma welding

Mechanical properties of joints on aluminium-lithium alloys (Labur T.M., Grinyuk A.A. and Poklyatsky A.G.)

6

### Pulsed-arc welding

Features of welding products with protective enamel coatings (Savitsky A.M., Vashchenko V.N. and Bobrov I.V.)

3

### Repair welding

Comparative analysis of application of covered electrodes for major repairs at main oil pipelines (Zavalinich D.A., Dzyuba V.M., Lo- zovoj V.G. and Storozhik D.L.)

5

Development and certification of automatic narrow-gap argon-arc welding technology of MCP Dn850 elements at NPP (Tsaryuk A.K., Skulsky V.Yu., Kasperovich I.L., Byvalkevich A.I., Ostashko T.V., Zhukov V.V., Dudkin S.N., Ivanov N.A., Miroshnichenko A.P., Nemlej N.V. and Bazhukov A.V.)

5

Extension of service life of a pipeline with defects on the inner surface (Yukhimets P.S., Kobelsky S.V., Kravchenko V.I., Kli- menko I.A. and Lesovets V.P.)

3

Extension of service life of column equipment at oil refineries (Che- kotillo L.V., Bulat A.V., Lebedevich Ya.B., Zvyagintseva A.V., Danilov Yu.B., Kachanov V.A., Kabashny A.I., Ivanuna S.M., Shepel T.E., Gvozdkova E.K. and Kozin Yu.V.)

10

Renovation of bodies of energy-absorbing mechanisms of freight railway cars (Snisar V.V., Demchenko E.L., Fenogenov A.I. and Vasiliev D.V.)

1

Repair welding of titanium blades of gas turbine engine compressors (Zamkov V.N., Vrzhezhevsky E.L., Topolsky V.F. and Petrichenko I.K.)

1

Structure and cold resistance of welded joints in steel 09G2S after repair welding (Poznyakov V.D., Kasatkin S.B. and Dovzhenko V.A.)

9

### Resistance welding

Resistance welding of aluminium-steel transition pieces using de- formable composite interlayers (Kuchuk-Yatsenko V.S., Lozovskaya A.V., Nakonechny A.A. and Sakhatsky A.G.)

8

### SAW

Methods to lower the hydrogen content in metal of welded joints of low-alloyed steels in submerged-arc welding (Golovko V.V.)

2

### TIG welding

Effect of scandium additions on structure-phase condition of weld metal produced by welding aluminium alloy 1460 (Markashova L.I., Grigorenko G.M., Ishchenko A.Ya., Lozovskaya A.V., Kushnaryova O.S., Alekseenko T.A. and Chajka A.A.)

1

Improvement of weld strength in arc welding of Al-Cu alloys with application of Sc-containing fillers (Poklyatsky A.G., Lozovskaya A.V., Grinyuk A.A., Yavorskaya M.R. and Chajka A.A.)

2

### Underwater welding

Content of acicular ferrite in weld metal in wet welding (Maksimov S.Yu. and Krazhanovsky D.V.)

1

On neural network application for welded joint quality control in underwater welding (Skachkov I.O., Pirumov A.E., Maksimov S.Yu. and Prilipko E.A.)

6

Numerical modelling of absorption of gases by deposited metal in wet underwater welding (Portnov O.M. and Maksimov S.Yu.)

7

Structure changes in HAZ metal of steel X60 welded joints in underwater welding (Maksimov S.Yu., But V.S., Vasiliev V.G., Zakharov S.M. and Zajtseva N.V.)

2

### Welding abroad

Abrasive wear behaviour of Fe-Cr-C overlays (Shah K.B., Ku- mar S. and Dwivedi D.K.)

11

Application of high-power fibre lasers in laser and laser-MIG hybrid welding (Thomy C., Kohn H. and Vollertsen F.)

7

Basics and applications of laser-GMA hybrid welding (Thomy C. and Seefeld T.)

6

Calculation of the kinetics of diffusion phase transformations in low-alloyed steels in beam welding (Dilthey U., Gumenyuk A.V. and Turichin G.A.)

2

Comparative analysis of application of covered electrodes for major repairs at main oil pipelines (Zavalinich D.A., Dzyuba V.M., Lozovoj V.G. and Storozhik D.L.)	
Computer system of electron beam and laser welding modeling (Lopota V.A., Turichin G.A., Valdajtseva E.A., Malkin P.E. and Gumenyuk A.V.)	
Glass joining technologies and examples of their application (Koebler G., Mueller G., Basler U., Dahms St., Luhn R., Kasch S. and Waechter S.)	
High power diode laser welding of aluminum alloy ENAW-1050A (Klimpel A., Lisiecki A., Janicki D. and Stano S.)	
Improvement of welding consumables and technologies for increased safety and life of NPS with WWER reactors (Gorynin I.V., Karzov G.P., Timofeev B.T. and Galyatkin S.N.)	
Indian welding industry: current scenario and prospects (Gehani M.L.)	
Influence of Ramsauer effect on the parameters of cathode region of argon arc with nonconsumable electrode (Cherny O.M.)	
Laser welding and formability study of tailor-welded blanks of different thickness combinations and welding orientations (Cheng C.H., Chan L.Ö., Chow C.L. and Lee Ö.C.)	
Low stress no distortion welding based on thermal tensioning effects for thin materials (Guan Q., Guo D.L., Zhang C.X. and Li J.)	
Mathematical model for MAG welding in a manufacturing environment (Ohji T., Miyasaka F., Yamamoto T. and Tsuji Y.)	
Production of welding consumables in 2005 in the CIS countries	
Properties of CO <sub>2</sub> -laser welded joints of dissimilar magnesium alloys (Kalita W., Kolodziejczak P., Kwiatkowski L., Grobelny M. and Hoffman J.)	
Sensitivity of $\delta$ -ferrite formation to FCAW process parameters in stainless steel claddings (Palani P.K. and Murugan N.)	
Surfacing consumables for hardening of parts operating under impact-abrasive wear conditions (Balin A.N., Berezovsky A.V., Vishnevsky A.A. and Kulishenko B.A.)	

<b>Welding arc</b>	
5 Effect of graphite on kinetics of transfer of carbon to weld pool in flux-cored wire cladding (Zhudra A.P., Krivchikov S.Yu. and Petrov V.V.)	11
4 Energy characteristics of low-amperage arcs (Yushchenko K.A., Chervyakov N.O. and Kalina P.P.)	4
7 External electromagnetic effects in the processes of arc welding and surfacing (Review) (Ryzhov R.N. and Kuznetsov V.D.)	10
9 Influence of Ramsauer effect on the parameters of cathode region of argon arc with nonconsumable electrode (Cherny O.M.)	3
<b>Welding Faculty of Priazovsky State Technical University is 35</b>	<b>8</b>
3 Personnel training at the PSTU Welding Department (Razmyshlyayev A.D. and Shaferovsky V.A.)	
4 The Chair of Welding Equipment and Technology is 60 years (Royanov V.A.)	
3 Design-experimental assessment of the features of electrode melting and transfer process (Chigarev V.V., Belik A.G. and Sergienko Yu.V.)	
6 Calculation of induction of controlling longitudinal magnetic field with consideration for magnetic properties of core, wire and workpiece as applied to arc surfacing (Razmyshlyayev A.D., Deli A.A. and Mironova M.V.)	
12 Regularities of the impact of item shape on electromagnetic field of welding current (Chigarev V.V., Shchetinina V.I., Shchetinin S.V. and Fedun V.I.)	3
10 Flux-cored wire for electric-arc metallizing of the surface of working rolls of the cold rolling mill tempering stand (Royanov V.A., Matvienko V.N., Stepnov K.K., Semyonov V.P., Zavarika N.G., Zakharova I.V. and Klimanchuk V.V.)	
7 Flux-cored wire for strengthening the necks and fillets of mill rolls (Matvienko V.N.)	
3 Sparsely alloyed consumables providing in the deposited metal deformation hardening in operation (Malinov V.L.)	
<b>Index of articles for TPWJ'2006, Nos. 1-12</b>	<b>12</b>
<b>2 List of authors</b>	<b>12</b>

## LIST OF AUTHORS

**A**deeva L.I. No.12  
Aleksenko T.A. No.1  
Alimov A. No.2  
Andreev V.V. No.7  
Antonyuk D.A. No.11  
Astakhov E.A. No.9, 11

**B**ajshtruk E.N. No.7  
Balin A.N. No.2  
Basler U. No.7  
Bazhukov A.V. No.5  
Belik A.G. No.8  
Berezovsky A.V. No.2  
Bobrov I.V. No.3  
Bondarev A.A. No.12  
Borisov Yu.S. No.4, 5, 7, 9, 11, 12  
Borisova A.L. No.5, 12  
Bubnov V.M. No.4  
Bugaets A.A. No.2  
Bulat A.V. No.10  
But V.S. No.2  
Bykovsky O.G. No.12  
Byvalkevich A.I. No.5

**C**hajka A.A. No.1, 2, 3  
Chan L.Ö. No.6  
Chekotilo L.V. No.10  
Cheng C.H. No.6  
Cherkashin A.V. No.3  
Chernov S.K. No.4  
Cherny O.M. No.3  
Chernyak Ya.P. No.4  
Chernyakov O.F. No.11  
Chervyakov N.O. No.4  
Chigarev V.V. No.6, 8(2)  
Chow C.L. No.6

**D**ahms St. No.7  
Danilov Yu.B. No.10  
Deli A.A. No.8  
Demchenko E.L. No.1, 4  
Demchenko V.F. No.6  
Demianov A.I. No.5  
Demianov I.A. No.5, 12  
Denisevich E.A. No.9  
Dilthey U. No.2  
Dmitrik V.V. No.2  
Dolinenko V.V. No.4  
Dovgunyk V.M. No.7, 10  
Dovzhenko V.A. No.9  
Dudkin S.N. No.5  
Dwivedi D.K. No.11  
Dymenko V.V. No.7, 10  
Dzioba Yu.V. No.7, 10  
Dzyuba V.M. No.5

**F**edorchuk V.E. No.6, 11  
Fedun V.I. No.8  
Fenogenov A.I. No.1  
Formanek B. No.7

**G**alinich V.I. No.4, 6  
Galyatkin S.N. No.3  
Garashchuk V.P. No.2, 11  
Garf E.F. No.4  
Gedrovich A.I. No.12  
Gehani M.L. No.4  
Gerasimenko A.M. No.11  
Girenko S.V. No.6  
Girenko V.S. No.6  
Gladky P.V. No.6  
Golnik V.F. No.5, 7, 12  
Golovko V.V. No.2, 10  
Gordan G.N. No.1  
Gorinov V.A. No.7  
Goronkov N.D. No.1  
Gorynin I.V. No.3  
Gotsulyak A.A. No.11  
Granovsky N.A. No.6  
Gretsky Yu.Ya. No.9  
Grigorenko G.M. No.1, 2, 6, 11  
Grinchenko E.D. No.2  
Grinyuk A.A. No.2, 6  
Grobelny M. No.7  
Guan Q. No.12  
Gumenyuk A.V. No.2, 4  
Guo D.L. No.12  
Guzej V.I. No.2  
Gvozdkova E.K. No.10

**H**offman J. No.7

**I**patova Z.G. No.5, 7, 11  
Ishchenko A.Ya. No.1, 2, 11, 12  
Ivanov N.A. No.5  
Ivanuna S.M. No.10

**J**anicki D. No.9

Kabashny A.I. No.10  
Kachanov V.A. No.10  
Kaleko D.M. No.5  
Kalina P.P. No.4  
Kalita W. No.7  
Kaplina G.S. No.11  
Karasevskaya O.P. No.8  
Karzov G.P. No.3  
Kasatkin S.B. No.9  
Kasch S. No.7  
Kasperovich I.L. No.5  
Kazymov B.I. No.3, 10  
Kharlamov M.Yu. No.9  
Khaskin V.Yu. No.2, 9

Khomenko V.I. No.10  
Kirian V.I. No.9, 10  
Kiselevsky F.N. No.1, 4  
Kislitsa A.N. No.4  
Kislitsyn V.M. No.3  
Klimanchuk V.V. No.8  
Klimenko I.A. No.3  
Klimpel A. No.9  
Knysh V.V. No.1, 9  
Kobelsky S.V. No.3  
Koehler G. No.7  
Kohn H. No.7  
Kokorina N.N. No.11  
Kolisnichenko O.V. No.7, 8, 11  
Kolodziejczak P. No.7  
Kolyada V.A. No.1  
Kondrashov K.A. No.6  
Kondratiev I.A. No.4, 12  
Kostin A.M. No.4  
Kostin V.A. No.11  
Kotenko S.S. No.8  
Koval Yu.N. No.5  
Kovalenko D.V. No.6  
Kovalenko I.V. No.6  
Kovtunen V.A. No.11  
Kozin Yu.V. No.10  
Kozulin S.M. No.9  
Kravchenko V.I. No.3  
Krazhanovsky D.V. No.1  
Krivchikov S.Yu. No.8, 11  
Krivtsun I.V. No.6  
Kuchuk-Yatsenko S.I. No.1, 3, 10  
Kuchuk-Yatsenko V.S. No.8  
Kulik V.M. No.7  
Kulishenko B.A. No.2  
Kumar S. No.11  
Kuran R.I. No.9  
Kushnaryova O.S. No.1, 2, 6  
Kushnaryova T.N. No.11  
Kuskov Yu.M. No.5  
Kutlin G.N. No.3  
Kuzmenko A.Z. No.1  
Kuzmenko G.V. No.6  
Kuzmenko V.G. No.2, 6  
Kuznetsov V.D. No.10  
Kvasnitsky V.F. No.4  
Kwiatkowski L. No.7

**L**abur T.M. No.6, 11  
Laktionov M.A. No.6  
Lankin Yu.N. No.7, 9  
Lebedev V.A. No.4  
Lebedevich Ya.B. No.10  
Lee Ö.C. No.6  
Lesovets V.P. No.3  
Levchenko O.G. No.12

Li J. No.12  
Lisiecki A. No.9  
Lobanov L.M. No.1, 5, 7, 9  
Loginov V.P. No.5  
Lopota V.A. No.4  
Lozovoj V.G. No.5  
Lozovskaya A.V. No.1, 2(2), 6, 8  
Luhn R. No.7  
Lukianets B.M. No.3  
Lychko I.I. No.9

**M**akhnenko O.V. No.4, 7  
Makhnenko V.I. No.4  
Maksimov S.Yu. No.1, 2, 6, 7  
Malakhov A.T. No.3  
Malinov V.L. No.8  
Malkin P.E. No.4  
Manchenko A.N. No.3  
Marchenko A.E. No.2  
Markashova L.I. No.1, 2, 6  
Masalov Yu.A. No.7  
Mashin V.S. No.9  
Matveev V.V. No.4  
Matvienko V.N. No.8(2)  
Mazunin V.M. No.7, 8, 11  
Mazur A.A. No.3  
Mazur S.V. No.3  
Mironova M.V. No.8  
Miroshnichenko A.P. No.5  
Mits I.V. No.7  
Miyasaka F. No.3  
Moskalenko A.A. No.9  
Mueller G. No.7  
Murashov A.P. No.5, 12  
Murugan N. No.3  
Musienko R.Ya. No.5  
Musin A.G. No.3

**N**akonechny A.A. No.8  
Nedej T.N. No.9  
Neganov L.M. No.5  
Nemlej N.V. No.5  
Nesmikh V.S. No.11  
Nikiforov A.Yu. No.4  
Novikova D.P. No.4, 5

**O**hji T. No.3  
Osin V.V. No.12  
Ostashko T.V. No.5  
Otrokov V.V. No.6

**P**alamarchuk B.I. No.3  
Palani P.K. No.3  
Pashchenko V.N. No.6  
Pashchin N.A. No.3, 5, 7  
Paton B.E. No.5, 6, 7, 10  
Patyupkin A.V. No.11, 12  
Pavlenko A.V. No.6  
Pavlyk A.O. No.12  
Pavlyuk S.P. No.3  
Pereplyotchikov E.F. No.6  
Pereverzev Yu.N. No.2

Petrichenko I.K. No.1  
Petrov V.V. No.8, 11  
Pilishenko I.S. No.7  
Pirumov A.E. No.6  
Pismenny A.S. No.3  
Pivtorak V.A. No.1  
Pokhmursky V.I. No.7, 10  
Poklyatsky A.G. No.2, 6  
Polishchuk E.P. No.8, 11  
Ponomarev V. No.7, 9, 10  
Popov S.V. No.9  
Portnov O.M. No.7  
Poznyakov V.D. No.9  
Prilipko E.A. No.6  
Pritula S.I. No.4  
Prokopenko G.I. No.9  
Provozin A.P. No.5

**R**abkina M.D. No.6  
Razmyshlyaev A.D. No.8(2)  
Rimsky S.T. No.4  
Romanchuk N.P. No.4  
Rosert R. No.2  
Royanov V.A. No.8(2)  
Ryabtsev I.A. No.4, 7, 10, 11, 12  
Ryabtsev I.I. No.5  
Rymar S.V. No.5  
Ryzhov R.N. No.10

**S**aakov A.G. No.7  
Saakov V.A. No.7  
Sakhatsky A.G. No.8  
Samilov V.N. No.7  
Savchenko V.S. No.11  
Savitsky A.M. No.3  
Savitsky V.V. No.1  
Seefeld T. No.6  
Semyonov V.P. No.8  
Sergienko V.A. No.10  
Sergienko Yu.V. No.8  
Shaferovsky V.A. No.8  
Shah K.B. No.11  
Shapovalov E.V. No.1  
Shatan A.F. No.7, 10  
Shchetinin S.V. No.8  
Shchetinina V.I. No.8  
Shelyagin V.D. No.2(2)  
Shepel T.E. No.10  
Shevchenko V.P. No.5  
Shinlov M.E. No.3  
Shiyan K.V. No.7  
Shonin V.A. No.9  
Shvets V.I. No.1  
Shvets Yu.V. No.1  
Sidorak I.I. No.7, 10  
Sidoruk V.S. No.8  
Skachkov I.O. No.6  
Skorina N.V. No.2  
Skulsky V.Yu. No.1, 5(2), 9, 11  
Slipchenko V.N. No.5  
Snisar V.V. No.1

Soldatenko G.T. No.5  
Solodky S.P. No.6  
Stano S. No.9  
Stepnov K.K. No.8  
Sterenbogen Yu.A. No.4  
Storozhik D.L. No.5  
Student M.M. No.7, 10  
Sushchuk-Slyusarenko I.I. No.9

**T**aranova T.G. No.11  
Thomy C. No.6, 7  
Timofeev B.T. No.3  
Tkachenko A.N. No.12  
Tkachenko S.A. No.12  
Tkachuk G.I. No.1  
Topolsky V.F. No.1  
Tsaryuk A.K. No.2, 5  
Tsuji Y. No.3  
Tsybulkin G.A. No.3  
Tunik A.Yu. No.12  
Turichin G.A. No.2, 4  
Tusikov E.K. No.4  
Tyukalov V.G. No.9  
Tyurin Yu.N. No.7, 8, 11

**U**lshin V.A. No.9

**V**aldajtseva E.A. No.4  
Varenchuk P.A. No.4  
Vashchenko V.N. No.3  
Vasiliev D.V. No.1, 4  
Vasiliev V.G. No.2, 7  
Vishnevsky A.A. No.2  
Vojnarovich S.G. No.4  
Vojtenko O.V. No.1  
Vollertsen F. No.7  
Vrzhizhevsky E.L. No.1

**W**aechter S. No.7

**Y**amamoto T. No.3  
Yavorskaya M.R. No.2  
Yukhimets P.S. No.3, 4  
Yumatova V.I. No.10  
Yushchenko K.A. No.4, 6, 8, 11

**Z**adery B.A. No.8, 11  
Zagadarchuk V.F. No.3  
Zajtseva N.V. No.2  
Zakharov S.M. No.2  
Zakharova I.V. No.8  
Zamkov V.N. No.1  
Zaruba I.I. No.7, 10  
Zavalinich D.A. No.5  
Zavarika N.G. No.8  
Zhadkevich A.M. No.5  
Zhadkevich M.L. No.7, 8, 11, 12  
Zhang C.X. No.12  
Zhudra A.P. No.8, 11  
Zhuk G.V. No.3  
Zhukov V.V. No.5  
Zvyagintseva A.V. No.10, 11